DOCTORAL COURSE IN

" TRANSLATIONAL NEUROSCIENCES AND NEUROTECHNOLOGIES "

CYCLE XXXII

COORDINATOR Prof. Luciano Fadiga

Clinical and genetic characterization of neuropathic pain through the model of small fiber neuropathy: implication for diabetic neuropathy

Scientific/Disciplinary Sector (SDS) MED/26

Candidate

Dott. Daniele Cazzato

Supervisors

Prof. Ilaria Casetta

Prof. Giuseppe Lauria Pinter

Years 2016/2019

Summary

INTRODUCTION

Peripheral nervous system organization

The peripheral nervous system includes the cranial nerves, the spinal nerves with their roots, plexuses and terminal nerves, and the peripheral components of the autonomic nervous system. From a microscopic point of view, a nerve is a bundle of axons associated to Schwann cells. In myelinated nerve fibers the axons are wrapped by multiple and compact layers of Schwann cells membrane that insulate the axons except at regular gaps where the myelin coating discontinues and ion channels cluster in a highly complex and specialized region called node of Ranvier. On the contrary, in unmyelinated nerve fibers more axons are included and surrounded by a single Schwann cell giving rise to the Remak bundles and ion channels are widespread along all the fiber.

The axons composing the nerves may come from neurons having different anatomical locations according to their function: anterior horns of spinal cord host motor neurons, dorsal root ganglia (DRG) and trigeminal ganglia contain primary sensory neurons, autonomic neurons are in lateral columns of spinal cord or autonomic ganglia; furthermore, motor, sensory and parasympathetic neurons are also located in brainstem nuclei.

The spinal nerves come from the conjunction of dorsal and ventral roots that are attached to the spinal cord; ventral roots include efferent motor and autonomic fibers coming from cellular bodies located in central nervous system (anterior horns and lateral columns of spinal cord); on the contrary dorsal roots are composed by the afferent projections of the pseudounipolar sensory neurons populating dorsal root ganglia and belonging to the peripheral nervous system. After traversing the subarachnoid space, immediately distally to the spinal ganglion of the dorsal root, the corresponding dorsal and ventral roots join to form the spinal nerve. At this level the dural sheaths containing the spinal cord merge with the epineurium of the spinal nerve.

Cranial nerves differ significantly from spinal nerves due to their different embryologic development. They enter the brainstem in a much more irregular manner without dividing into dorsal and ventral roots; some cranial nerves have ganglion (i.e. trigeminal ganglia), although trigeminal proprioceptive sensory primary neurons are located into brainstem nuclei representing the only exception to the rule for which the cell bodies of the primary

sensory neurons belong to the peripheral nervous system. The optic nerve represents another exception since it is part of the central nervous system and not a peripheral nerve.[1]

Nerve fibers are classified according to their diameter, velocity conduction and type of myelination following the Gasser classification or, limited to the muscle afferent fibers, the Lloyd classification.

Myelinated fibers are further grouped according to their diameter and conduction velocity in Aα (80-120 m/s; 12-21 µm; efferent nerve fibers to extrafusal muscle fibers), Aβ (35-75 m/s; 6-12 µm; afferent fibers from specialized mechanoceptors), Aγ (15-40 m/s; 2-8 µm; efferent fiber to muscle spindles), Aδ (5-30 m/s; 1-5 µm; afferent fibers mediating light stroke, thermal cool and hot pain sensation); whereas the afferent fibers from muscles are named I (Ia from primary muscle-spindles; Ib from Golgi tendon organ), II (from Joint capsule and Pacinian corpuscle) and III (mediating pain secondary to excess stretch), respectively corresponding to Aα, Aβ and Aδ fibers of the Gasser's classification. B fibers are myelinated efferent preganglionic autonomic cholinergic fibers. They have diameter and conduction velocity in the range of Aδ fibers (3-15 m/s; 3 µm) from which they differ for some physiologic characteristics; in particular, B fibers show smooth compound action potentials without discrete peaks, indicating a more uniform distribution of velocity spectrum. Unmyelinated fibers type C in cutaneous nerves and type IV in muscle nerves are the slowest and smallest (1-2 m/s; 0,2-1,5 µm). The type IV fibers mediate muscle and Joint pain, whereas the type C fibers convey cold and polymodal pain sensation, thermal warm sensation and lightest touch. Efferent post-ganglionic autonomic fibers belong to type C.

The unmyelinated fibers outnumber myelinated ones 4 to 1 and at least one third of myelinated fibers are represented by small thinly myelinated Aδ fibers. The distribution of nerve fibers diameter is bimodal, it follows that they are commonly divided into large and small nerve fibers.[2,3]

Sensory fibers

Dorsal root ganglia are populated by sensory neurons of different size from which come axons targeting cutaneous or deep tissues. It has been recently shown that the expression of the transcription factor Runx1 is crucial for driving the projections of the sensory neurons to

superficial tissues by suppressing the molecular program that otherwise leads pain-related sensory neurons to innervate deep tissues.[4]

Large sensory Aβ fibers are low-threshold mechanoreceptors (Aβ-LTMRs) innervating glabrous and hairy skin. According to their firing adaptation rate Aβ-LTMRs of the glabrous skin can be classified as slowly adapting (SA) showing maintained firing during sustained indentation or as rapidly adapting (RA), exhibiting best response to stimuli moving across the skin rather than to static indentation. SA-LTMRs can be further divided into type I (SAI-LTMRs) associated to the Merkel cell complex (present in both glabrous and hairy skin) that respond maximally upon contact with edges and curvature of objects with a very low threshold; whereas type II (SAII-LTMRs), whose responses have been postulated to arise from Ruffini endings, innervate the skin less densely than SAIs, their receptors field are larger and they are more sensitive to skin stretch.

RA-LTMRs in glabrous skin can also be further divided into type I that make contact with Meissner corpuscles and respond to low frequency vibrations (1-10Hz), and type II that are associated to Pacinian corpuscle and respond to high-frequency vibration (80-300 Hz).

Hairy skin covers more than 90 % of the body surface. Although it still has a discriminative touch role with a lower spatial resolution compared with glabrous skin, it is strongly associated with affective touch. It includes the hair follicles that are neurophysiologically complex mechanosensory organs innervated by longitudinal lanceolate ending of several LTMRs belonging to Aβ RA, Aδ and C-type categories, all sensitive to hair deflection and light touch of the skin (Figure 1). In particular, the Aβ RA-LTMRs and Aδ-LTMRs are rapidly adapting sensitive to low-frequency vibration; on the contrary, C-LTMRs that are four times more numerous than A fibers, are intermediately adapting and maximally activated by slow movement across their receptive field, and thus implicated in “emotional touch”[5,6]. Indeed, intriguingly, in human lacking large myelinated fibers, activation of C-LTMRs induce a pleasant sensation associated to activation of the insular but not the somatosensory cortex[7].

Beside LTMRs there is a broad category of mechano-nociceptive sensory neurons that are optimally excited by noxious mechanical stimuli, namely high threshold mechanoreceptors (HTMR). These nociceptors are uniformly distributed in glabrous and hairy skin and are tuned to harmful or potentially damaging stimuli.

HTMRs include Aδ and C fibers free terminal endings that innervate the epidermis. The first are deemed to mediate fast mechanical pain, cool and hot sensations, whereas the latter convey warm and cold stimuli.

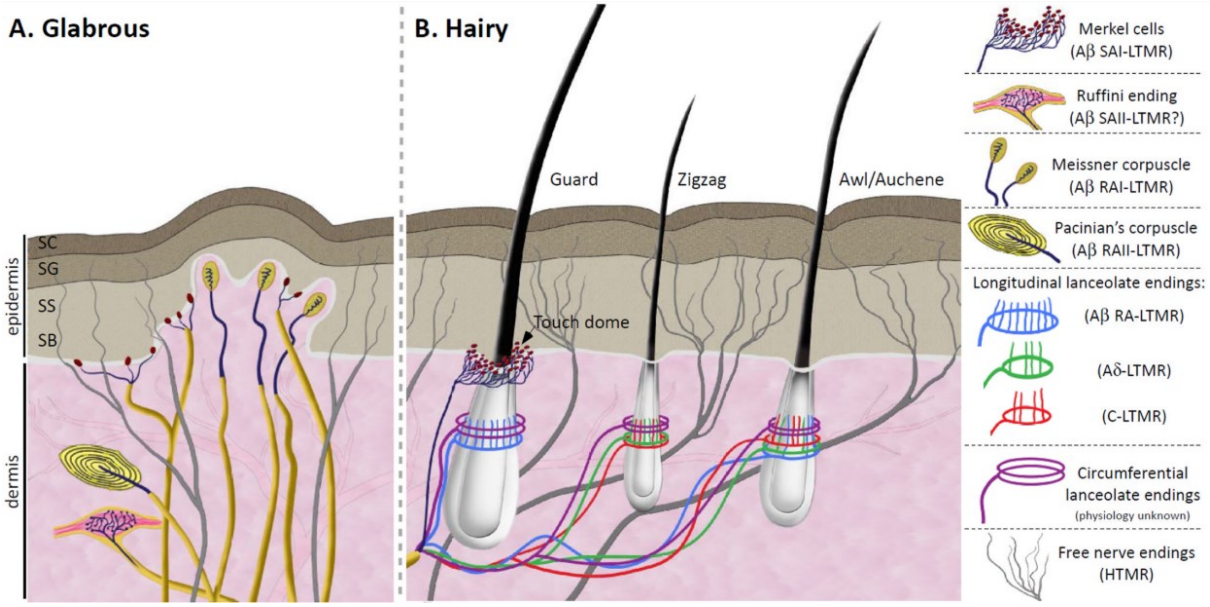

Figure 1. Cutaneous receptors within glabrous and hairy skin[6].

DRG sensory neurons can be divided into several subtypes according to the expression of neurotrophin receptors. They include the tropomyosin-receptor-kinase A (TrkA), TrkB, Trk,C, Met and Ret tyrosine kinase receptors binding nerve growth factor (NGF), brain-derived neurotrophic factor (BDNF), neurotrophin-3 (NT3), hepatocyte growth factor (HGF) and glial-derived neurotrophic factor (GDNF) respectively. These receptors are crucial for cell survival and for driving ion channels expression and appropriate target innervation therefore defining the functional characteristics of each sensory neuron subtype. Large-diameter low-threshold mechanoreceptors innervating the skin are Ret^+ and/or $TrkB^+$; large-diameter low-threshold proprioceptive neurons are $TrkC^+$; $TrkA^+$ small sensory neurons express the calcitonin gene related peptide (CGRP) and substance P thus are defined as peptidergic; conversely, nonpeptidergic nociceptors exhibit Ret. Neurons belonging to these two populations are not uniform and further cytological markers identify subcategories characterized by a specific sensory function. In particular Ret^+ cells include a subtype of neurons expressing cell surface glycol coniugates specifically recognized by isolectin B4 ($IB4^+$) defining a molecular pattern guided by Runx1 that characterizes polymodal pain-sensing

nociceptors. In other Ret^+ neurons the downregulation of Runx1 leads to the expression of Mas-related G protein-coupled receptors (Mrgpr)B3 acting as itch receptors in a subtype of histamine-independent pruriceptors. A subtype of Ret^+ and $IB4^-$ neurons specifically expressing the tyrosine hydroxylase (TH) and the vesicular glutamate transporter VGlut3 identifies the C-LTMRs. A particular group of $TRPM8^+$ very small sensory neurons descending from $TrkA^+$ cells but that are neither IB4 nor peptidergic correspond to neurons activated by cooling or cooling compounds such as menthol[8,9].

Central projections of sensory neurons show different branching according to their diameter. Aβ-LTMRs bifurcated after entering the spinal cord extending rostrally in the dorsal column and then sprouting collaterals that enter the dorsal horn. On the contrary, Aδ and C fibers do not bifurcate after exiting the dorsal root and reach the dorsal horn after travelling one or two segments rostrally.

Dorsal horn neurons are organized in laminae populated by second level sensory neurons receiving different peripheral afferents. Lamina I consists of neurons receiving specific inputs from Aδ and C fibers for noxious or cold stimuli. Lamina II, III and IV include interneurons receiving nociceptive and non-nociceptive afferents. Neurons belonging to lamina V are called wide-dynamic-range neurons since the have dendritic branches extending till lamina II and receive inputs from Aβ, Aδ and C fibers. Large diameter fibers conveying proprioception reach lamina VI, whereas neurons in laminae VII and VIII seem to be responsive to complex noxious stimuli, such as stimuli coming from both side of the body[3,6].

Neuropathic pain

Definition

The International Association for the Study of Pain (IASP) defines pain as "an unpleasant sensory and emotional experience associated with actual or potential tissue damage, or described in terms of such damage"[10]. Pain has a physiological warning function that is crucial for protecting individuals from potentially harmful events and for preserving tissues during healing. On the other hand, pain can represent a severe, chronic and disabling condition assuming features that are far from its original physiological function.

According to the IASP, neuropathic pain is defined as “pain arising as a direct consequence of a lesion or disease affecting the somatosensory system”. This new definition proposed in 2008[11] and introduced in 2011[12] replaces the previous one of 1994[13] (“pain initiated or caused by a primary lesion or dysfunction in the nervous system”). In particular, the new definition replaced the words “dysfunction in the nervous system” with “disease affecting the somatosensory system” therefore better delimiting the frame of neuropathic pain to those condition strictly due to a detriment of the somatosensory system, thus excluding other painful condition also associated to neurological diseases such as spasticity and rigidity in which pain is due to nociceptors activation. Recently, IASP’s Neuropathic Pain Special Interest Group (NeuPSIG) has also proposed a classification of chronic neuropathic pain[14] for the upcoming 11th revision of the International Classification of Diseases (ICD) of the World Health Organization (WHO).

From neural injury to chronic neuropathic pain

Nociception aims to prevent tissue from damaging. When injury already occurred, pain acquires the additional aim of aiding tissue healing. Consequently, the inflammatory response triggered by the injury drives reversible adaptive changes in sensory nervous system leading to an enhanced response to slightly painful stimuli that are perceived as extremely painful (hyperalgesia) and to a widening of the spectrum of stimuli able to elicit a painful sensation including also low-threshold innocuous inputs (allodynia). Typically, this pain amplification is transient and disappear as the tissue injury is resolved. However, in chronic inflammatory conditions such as rheumatoid arthritis pain can persist and become chronic like the underlying condition. Nevertheless, not being related to a lesion or disease of the somatosensory system it cannot be considered neuropathic pain and it is defined inflammatory pain.

On the other side, also a neural lesion does not necessary lead to neuropathic pain. Indeed, neural injury results in a chronic neuropathic pain only a minority of patients and it occurs regardless of the underlying etiology. Studies have reported that risk factors include age, gender and anatomical site of the neural injury. Lesion of ilioinguinal nerve, representing a possible complication of surgery for hernia repair, is associated to neuropathic pain in about 5% of cases, whereas the risk of chronic neuropathic pain rises to 30-60% when larger nerves such as sciatic nerve are involved. Furthermore, brachial root avulsion is not associated with

neuropathic pain in neonates whereas the same lesion causes chronic pain in about 40% of cases when occurs in adults, suggesting a relation with the maturity of the nervous system.[15] These data support an inter- and intra-individual susceptibility to neuropathic pain based on the balance between adaptive peripheral and central response to nervous system damage and a genetic background that might predispose or protect from development of a maladaptive response resulting in chronic neuropathic pain.

Peripheral sensitization

Peripheral nerve injury triggers initial changes at the level of primary sensory neurons of DRG. The damaged axons release CGRP, substance P, bradykinin and nitric oxide inducing vascular changes, immune cells invasion and secretion of sensitizing agents. At the same time, Schwann cells release neurotrophic factors such as NGF and GDNF which are retrogradely transported to cell body of primary sensory neurons after binding the TrkA and Ret receptors expressed by nociceptors, inducing changes in expression of genes coding for ion channels and receptors[16]. The transient receptor potential ion channel TRPV1, well characterized as the capsaicin receptor[17], and TRPA1 are up-regulated in injured sensory fibers in which can be expressed at the level of axon injury besides the terminal ending of nociceptors. This aberrant expression causes a transduction displacement resulting in the clinical "Tinel sign", namely a tingling or electric-shock-like sensation provoked by tapping over the site of nerve injury.

Changes in channels expression involves also VGSC and potassium channels in a manner that contribute to enhance cellular excitability. In particular, injured nerves show an up-regulation of the Nav 1.3 α-subunit of sodium channels normally expressed only during embryonic development. On the contrary, potassium channels TRESK e TREK-2 normally accounting for the 85% of the K^+ background current in primary sensory neurons, are down-regulated by about 40%, significantly contributing together with sodium channels over-expression to membrane depolarization[18]. Furthermore, sensitizing agents act also reducing TRP and VGSC threshold mainly by phosphorylation via protein kinase A (PKA), protein kinase C (PKC) and phospholipase C (PLC)[19]. All together these changes lowering the firing threshold make the nociceptors able to respond to low-threshold stimuli, leading to evoked pain characterized by hyperalgesia and allodynia or to spontaneous pain and paresthesia due to ectopic discharges of action involving Aδ and C or Aβ fibers respectively.

Central sensitization

Persistent exposure to noxious input may induce long-term changes in the central nervous system at cortical, thalamic and spinal cord level, representing an example of stimulus-evoked central plasticity. Most attention has focused on the dorsal horn where mechanisms of sensitization have been mainly studied. Central sensitization consists in an augmented response of central signaling neurons through synaptic potentiation sustaining an enhanced transmission between primary and second-order sensory neurons. At the presynaptic level the downregulation of μ-opioid receptors, GABA-b, and adenosine receptors and the up-regulation of α2δ subunit of voltage-gated calcium channels contribute to increase the release of glutamate and substance P, the main excitatory neurotransmitters. On the postsynaptic side, substance P and glutamate released by C fibers cause a long-lasting depolarization inducing the opening of N-methyl-D-aspartate (NMDA) type receptors. The ion influx from these channels causes the rising of intracellular calcium that mediates over-expression of α-amino-3-hydroxy-5-methylisoxazole-4-propionate (AMPA)-type glutamate receptor owing to modulation of gene expression in the soma. The final result is an increase of the glutamate receptor density improving the synaptic transmission, therefore leading to a postsynaptic potentiation[20].

Central sensitization may occur in a homosynaptic fashion between primary and second-order sensory neurons mediating the same sensory modality, such as Aδ and C fibers of nociceptive neurons projecting to the superficial laminae in dorsal horn. It is responsible of the clinical sings of windup and aftersensation.

The “windup” phenomenon is an increase of the reported intensity of the same nociceptive stimulus as it is repeated. The “aftersensation” is the persistence of a painful or unpleasant sensation lasting longer than the applied stimulus.

Synaptic potentiation involving different sets of afferents is defined heterosynaptic sensitization and it accounts for brush-evoked mechanical allodynia. Mechanisms of tactile allodynia include a phenotypic switch of low-threshold Aβ fibers that express substance P and produce collateral sprouting on nociceptive second-order sensory neurons into lamina II of the dorsal horn in response to peripheral injury[21]. However, recent results suggest that a distinct class C-type sensory neuron expressing VGLUT3 and acting as LTMRs are involved in mechanical hypersensitivity[22].

Synaptic changes similar to those described for central sensitization also occur in structures such as anterior cingulate gyrus, prefrontal cortex and amygdala involved in emotional experience of pain. These changes may play a role in long-term pain-related cognitive and mood changes such as conditioned fear. Furthermore, central sensitization causes a spreading of pain sensitivity beyond the territory of the involved peripheral nerve, resulting in amplification of chronic pain not necessarily sustained by ongoing noxious stimuli that might contribute to patients' pain phenotype in clinical syndromes such as rheumatoid arthritis, osteoarthritis, temporomandibular disorders, fibromyalgia, post-surgical pain and neuropathic pain[23].

Diagnosis and grading system

The new definition of neuropathic pain sets the demonstration of somatosensory system lesion or disease as the key element for neuropathic pain diagnosis. According to this new definition, NeuPSIG recently revised a grading system[24] aiming to ascertain the level of certainty with which the painful symptoms experienced by patients can be defined as neuropathic.

The presence of a history of neurological lesion or disease, the neuroanatomically plausible distribution of pain and even better of clinical signs and the objective demonstration of somatosensory lesion or disease contribute to establish the certainty of the diagnosis of neuropathic pain.

Another important point is to exclude nociceptive or inflammatory pain coming from other causes such as inflammation of non-neural tissue damage. In this respect, several screening tools have been developed and proposed, combining several pain descriptors such as burning, electric shocks, pins and needles, pain evoked by light touch, warm or cold and nonpainful sensation such as numbness and tingling. The main aim of these questionnaires is to help clinicians in identifying, among patients complaining symptoms suggestive of neuropathic pain, those who should undertake further assessment. Some of these screening tools are the Neuropathic pain questionnaire (NPQ)[25], the LANSS[26], the Douleur Neuropathic en 4 questions (DN4)[27], the painDETECT[28] and ID-PAIN[29]. The Neuropathic Pain Questionnaire (NPQ) was among the first tools introduced, exploring 12 items and showing a sensitivity and specificity around 70%. Among the tools proposed for neuropathic pain screening, the DN4 showed a sensitivity of 82% and a specificity of 89%[27]. It includes four

questions investigating seven symptoms, two “negative” signs (pinprick and tactile hypoesthesia) and one “positive” clinical sign (tactile allodynia). More recently, it has been validated in diabetic painful neuropathy being able to discriminate neuropathic pain patients with a sensitivity of 80% and specificity 92%[30]. The ID-PAIN investigate six pain descriptors including pain features and distribution and introduces four level of probability to minimize false negatives (very likely, likely, possible and unlikely).

Two scales are mainly used for investigating pain intensity (PI): the visual analogue scale (VAS) and the numeric rating scale (NRS). The VAS is a 10-cm line anchored at the ends by words that define the bounds of pain intensity (no pain – worst possible pain). The patient is asked to place a mark on the scale to indicate the level of pain intensity. The NRS is a stepwise 11-point Likert scale for which patient is asked to score pain intensity using a number ranging from “0” (no pain) to “10” (worst possible pain).

According to the diagnostic criteria and grading score, a patient complaining of pain can be defined as having a possible, probable or definite neuropathic pain in the light of its medical history, clinical examination and confirmatory tests:

- Possible neuropathic pain

  A patient with pain fulfills the first level of certainty “possible” if there is a history of neurological lesion or disease and pain distribution is neuroanatomically consistent with the suspected location of the disease of lesion in the peripheral or central somatosensory nervous system. Although, in some circumstances (e.g. a history of traumatic lesion of a nerve and pain within that nerve distribution area) these two requirements can be easily addressed, in other conditions the pain distribution may be unusual, such as in painful channelopathies as the familial episodic pain syndrome in which pain involves the chest and proximal regions of upper limbs or the inherited erythromelalgia characterized by a pain distribution at the extremities.

- Probable neuropathic pain

  Clinical examination is the lead character in definition of the next (“probable”) level of certainty. The most reliable sign is the complete or partial loss of one of the sensory modalities in a territory consistent with the suspected lesion or disease of the somatosensory system. Positive sensory signs alone, including allodynia and hyperalgesia

are less specific for a neuropathic etiology of pain since they can be found also in other conditions including inflammatory pain, anxiety, sleep deprivation, etc.

On the other hand, in certain neuropathic pain conditions such as painful channelopathy, thermal allodynia and mechanical allodynia may be present during pain attacks without a detectable sensory loss.

- Definite neuropathic pain

To reach the high level of certainty, the disease or lesion of somatosensory nervous system must be confirmed by an objective diagnostic test. Examples of confirming test include central and peripheral nervous system imaging, neurophysiological studies, skin biopsy showing reduced intraepidermal nerve fiber density, genetic tests for channelopathy-related painful disorders, etc.

However, the "definite" diagnostic level does not exclude that a nociceptive or inflammatory pain may also be present within the area affected by a lesion or disease of nervous system, thus it is always advised to consider other possible causes for pain.

Small fiber neuropathy

Small fiber neuropathy (SFN) is a condition characterized by a selective or predominant impairment of peripheral thinly myelinated Aδ fiber and unmyelinated C fibers in which neuropathic pain is a dominant and often severe feature. The introduction of skin biopsy allowing an objective and reliable quantification of intraepidemal nerve fibers represented the most important milestone in the diagnosis of SFN that entered the differential diagnosis of painful peripheral nervous system disorders.

The frequency of SFN is uncertain. The only epidemiological study available conducted in the Netherlands reported an incidence of 12 cases per 100'000/year and a prevalence of 53 cases per 100'000. However, a recent systematic review and meta-analysis revealed a 49% prevalence of SFN in fibromyalgia[31] that is reported affecting up to 5% of people in Europe[32]. Therefore, it is estimated that only 10% of patients are diagnosed and the global prevalence could far exceed 10 million[33].

Nevertheless, one of the main limitations to exhaustive epidemiological study is the lack of widely shared diagnostic criteria remaining a matter of debate in the scientific community. In particular, one important question still unaddressed is whether the nosographic classification of SFN should consider only patients with pure small nerve fiber involvement or it should also include patients having a mixed small and large fiber neuropathy with predominant symptoms and signs of small nerve fibers disfunction[34].

Clinical features and SFN phenotypes

Clinical presentation of SFN patients include two main different patterns: a length-dependent distal symmetric polyneuropathy and a non-length-dependent ganglionopathy or mono/multineuropathy[35].

Patients with length-dependent SFN usually complain spontaneous pain with burning, electric-like, pins and needles sensation starting at lower limb extremities and progressively ascending to more proximal site than involving also upper limbs again in a distal-to-proximal fashion following a dying-back pathological pattern of peripheral neuropathies. SFN Patients can also present painless forms in which non-painful symptoms include numbness, itching and tingling sensations. This pattern is predominantly seen in patients with metabolic causes such as diabetes or impaired glucose tolerance (IGT) or in neurotoxic exposures.

On the contrary, in non-length-dependent SFN, complaints often present with a proximal, diffuse or patchy distribution involving different parts of the body including face, mouth, scalp, trunk and upper limbs before of simultaneously the lower limbs. This SFN pattern is predominantly seen in immune-mediated disorders (i.e. Sjogren's syndrome), paraneoplastic conditions, idiopathic patients and also in condition characterized by diffuse pain and associated to small fiber pathology such as fibromyalgia[36] and Ehler-Danlos syndrome[37]. Peculiar distribution of symptoms includes tongue and mouth in the burning mouth syndrome or notalgia and meralgia paraesthetica in mononeuropathies.

Patient with SFN may also complain of restless leg, intolerance to bed sheets, shoes and clothes causing dysesthesia or allodynia. Some symptoms seems to be much specific for some form of SFN; for example, patients with oxaliplatin-induced neuropathy symptom are

typically exacerbated by cooling[38], whereas in patients with erythromelalgia, symptoms are exacerbated by warming and relieved by cooling of the skin[39].

Clinical manifestation of SFN encompass "positive" and "negative" symptoms and signs related to the Aδ and C fiber degeneration resulting from conduction impairment or from an augmented function due to the peripheral and central sensitization triggered by neural damage. SFN patient might report a reduced or absent thermal and pain sensation. However, the simultaneous presence of allodynia and hyperalgesia can mask the sensory loss. Furthermore, small fiber neuropathy can also involve autonomic nervous system adding complexity and heterogenicity to the SFN clinical pictures.

Etiology

SFN is associated with several causes that can be classified in four main categories: acquired, hereditary, syndromic and idiopathic[34]. Among the acquired causes diabetes is among the most common accounting for about 20% of cases, with even higher prevalence if prediabetes conditions such as impaired fasting glucose (IFG) and impaired oral glucose tolerance test (OGTT) are included. This high prevalence of neuropathy in patient with prediabetes and the poor preventing effect of metabolic control in type 2 diabetes (T2DM) compared to type 1 diabetes (T1DM) suggested a role for other metabolic causes including hyperlipidemia and metabolic syndrome. Other significant association have been identified with HIV infection, immune-mediated disorders such as Sjogren's syndrome, Celiac disease and Sarcoidosis, and after exposure to neurotoxic drugs.

In the last years, gain-of-function mutations in *SCN9A*, *SCN10A and SCN11A* genes, coding for Nav1.7, Nav1.8 and Nav 1.9 sodium channels α-subunits have been described in SFN patients[40–42], defining the subgroup of sodium-channelopathy-related SFN.

However, as discussed afterwards, the frequency of rare genetic variant is low in SFN patients and some concerns have been raised about their pathogenic role since they might act as modifier rather than directly cause the disease in a fully penetrant manner. Besides sodium channels, mutation in *COL6A5* gene coding for a collagen protein have been described in a peculiar phenotype of familial and sporadic SFN characterized by neuropathic itch[43]. Other genetic conditions associated with SFN include presymptomatic early stages of familial amyloidosis due to *TTR* gene mutations, whereas a mixed neuropathy more often

characterizes the symptomatic stages. SFN is a common adjunctive feature composing the clinical picture of Fabry disease[44], but since it is a rare associated condition, only the presence of other clinical features of the disease should prompt the genetic analysis[45].

SFN has also been identified in syndromic conditions characterized by a diffuse distribution of painful symptoms such as fibromyalgia. A recent meta-analysis reported a SFN frequency of 49% in fibromyalgia patients[31]. I have recently characterized the pain phenotype in a cohort of 25 patients with Ehlers-Danlos syndrome[37] dominated by migratory arthralgias in childhood with a progression to a widespread pain including features of neuropathic pain. I have reported a high frequency of small nerve fiber impairment in Ehlers-Danlos patients, suggesting the SFN might be responsible for chronic pain in these patients. Small fiber degeneration was also described in neurodegenerative disease such as Parkinson's disease[46,47] and ALS[48,49] revealing a concomitant SFN or possibly being part of a neurodegenerative process involving also small sensory neurons[50]. These finding strengthen the importance of consistent clinical sensory symptoms and sings for defining the diagnosis of SFN.

Despite the several conditions identified in association with SFN patients, up to 50% of cases are idiopathic since the underlying cause remains unknown.

Diagnostic criteria

The diagnostic criteria for SFN are not definitely established. In the last decade, two different set of diagnostic criteria have been proposed. The first, published in 2008[51] required the combination of abnormal findings in at least two out of the following three assessments:

1. Clinical signs of small fiber neuropathy, including pinprick and thermal sensory loss or reduction and/or the presence of positive signs (allodynia and hyperalgesia);
2. Abnormal thermal threshold assessed at the foot by QST;
3. Reduced IENFD at the distal leg skin biopsy.

In addition, clinical signs including reduced vibratory sensation and absent deep tendon reflexes and/or electrophysiological evidence of large fibers impairment were considered exclusion criteria, therefore these criteria delimit the frame of SFN to pure SFN, excluding patients with mixed small and large fiber neuropathy.

The second set of diagnostic criteria has been released within the update of the guideline for the diagnosis of diabetic neuropathy by the Diabetic Neuropathy Study Group of the European Association for the study of Diabetes (NEURODIAB). They propose a diagnosis of SFN in diabetic patients based on the presence of symptoms and signs of SFN, normal sural nerve conduction study (NCS), demonstration of small nerve fiber impairment by confirmatory test including skin biopsy and QST, following a grading system in an additive fashion:

1. Possible: presence of length-dependent symptoms and/or clinical signs of small-fiber damage;
2. Probable: presence of length-dependent symptoms, clinical signs of small-fiber damage, and normal sural NCS;
3. Definite: Presence of length-dependent symptoms, clinical signs of small-fiber damage, normal sural NCS, and reduced IENFD at the ankle and/or abnormal QST thermal thresholds at the foot.

The NEURODIAB criteria always require clinical signs to be present for probable and definite diagnosis of SFN, though they include a generic definition of "clinical signs of small-fiber damage" without specifying which signs should be considered.

I have contributed to a recent revision of the SFN diagnostic criteria accepted for publication in *Brain*[52]. The study compared the two sets of criteria into a reappraisal and a validation study showing a strict agreement between the two diagnostic approaches. Furthermore, this study strengthened the role of clinical signs for raising the suspicion of SFN, since sensory symptoms alone are not reliable and confirmed the role of IENFD for the definite diagnosis.

Clinical assessment

Clinical examination of patients aims to disclose clinical signs of polyneuropathy. Motor and large sensory fiber function is usually unaffected in SFN patients. Small nerve fiber function is examined by testing heat, cold and pain sensation. Neurological examination can reveal negative sensory signs such as a reduced pinprick sensation and reduced or absent cold or heat sensation tested with a cooled or warmth water tube. Bedside testing might also reveal positive sensory signs including mechanical or thermal allodynia or hyperalgesia. Patients might also refer paradoxical sensation, for example perceiving cold stimuli as heat.

Inspection of the body might reveal sweating abnormalities such as dry or wet skin, dystrophic changes and skin redness or flushing.

In order to screen patients with SFN, specific questionnaires have been proposed and validated. The Small Fiber Neuropathy – Symptoms Inventory Questionnaire has been validated in patients with SFN associated to sarcoidosis[53] and used to screen patients with SFN associated to SCN9A mutations[40]. It includes 13 items exploring presence of palpitations, flushes, constipation or diarrhea, urination problems (incontinence or hesitation), changes in sweating pattern, restless legs, orthostatic dizziness, dry eyes or mouth, oversensitivity and sheet intolerance of the legs. Another questionnaire specifically investigating autonomic symptoms is the Composite Autonomic Symptom Score-31 (COMPASS-31)[54], a validated self-administrable instrument with a good test-retest reliability able to discriminate patients with and without SFN.

Confirmatory diagnostic tools

Skin biopsy

Thirty years ago, in 1989, two different groups at the Karolinska Institute in Stockholm (from Departments of Anatomy and Plastic Surgery and from Departments of Histology and Dermatology), first provided the demonstration of intraepidermal nerve fibers staining using as marker the protein gene product 9.5, a cytoplasmic ubiquitin carboxyl-terminal hydrolase[55,56]. These evidences further supported by electron microscope studies[57,58], definitely confirmed the presence of nerve fibers in the human epidermis. In fact, although Langerhans back in 1868 first described the presence of nerve fibers within the epidermis layer[59], the actual existence of epidermal innervation remained for long time a debated issue mainly because of technical difficulties in staining and poor reproducibility of results (Figure 2).

In 1995 skin biopsy started to be used for characterization of cutaneous innervation in sensory neuropathies[60] and today the quantification of IENFD is considered the “gold standard” for the diagnosis of SFN, although a true gold standard is lacking[61,62].

Since the classical clinical picture of SFN is characterized by sensory complaints mainly involving distal lower limbs, IENFD quantification has been standardized for diagnosis of SFN collecting skin sample from the lower leg, 10 cm proximal from the lateral malleolus, within

the territory of the sural nerve; although skin biopsy could theoretically be performed at every body site. The number of small nerve fibers crossing the dermal-epidermal junction is quantified in 3 non-consecutive 50 µm slices, then divided by the length of epidermis, resulting in a linear epidermal innervation density value expressed in number of fibers per millimeter (IENF/mm)[61]. Normative reference value for IENFD at distal leg, adjusted for sex and age, are available for bright field[62] and immunofluorescence[63] microscopy techniques, with a consensus study reporting a similar diagnostic accuracy[64], showing a decreasing of IENFD with aging and slightly lower values in men compared to women. The reliability of IENFD parameter has been further strengthened by the demonstration of a stability of IENFD value in healthy subject and patients with length-dependent SFN regardless the side and the time (within 3 weeks) in which skin biopsy is collected[65].

In patients with normal IENFD, the presence of axonal swellings might hint predegenerative changes predicting the loss of fibers[66] and more recent studies have confirmed an increase of IENF swellings ratio from healthy subjects to diabetic patients without neuropathy and diabetic patients with a defined neuropathy[67], although it seems not a discriminating feature between painful and painless phenotype of diabetic neuropathy[68].

Besides intraepidermal nerve fibers, also the assessment of dermal nerves by a method that I contributed to develop consisting in measuring the overall length of dermal nerve fibers of the subepidermal plexus, has been shown to reliably discriminate healthy individuals from SFN patients[69].

The skin is also reached by autonomic nerve fibers for sweat glands, pilomotor muscles and vessels which innervation was investigated and quantification methods have been proposed[70,71], therefore increasing the diagnostic yield of skin biopsy.

Finally, skin biopsy is a minimally invasive procedure, allowing to be repeated for longitudinal disease monitoring or confirming especially when IENFD values are very close to the cut-off. However, it is considered a surgical procedure and can burdened by rare complication such as minor bleeding, surgical site infection and keloid scar formation.

Skin biopsy historical notes and milestones

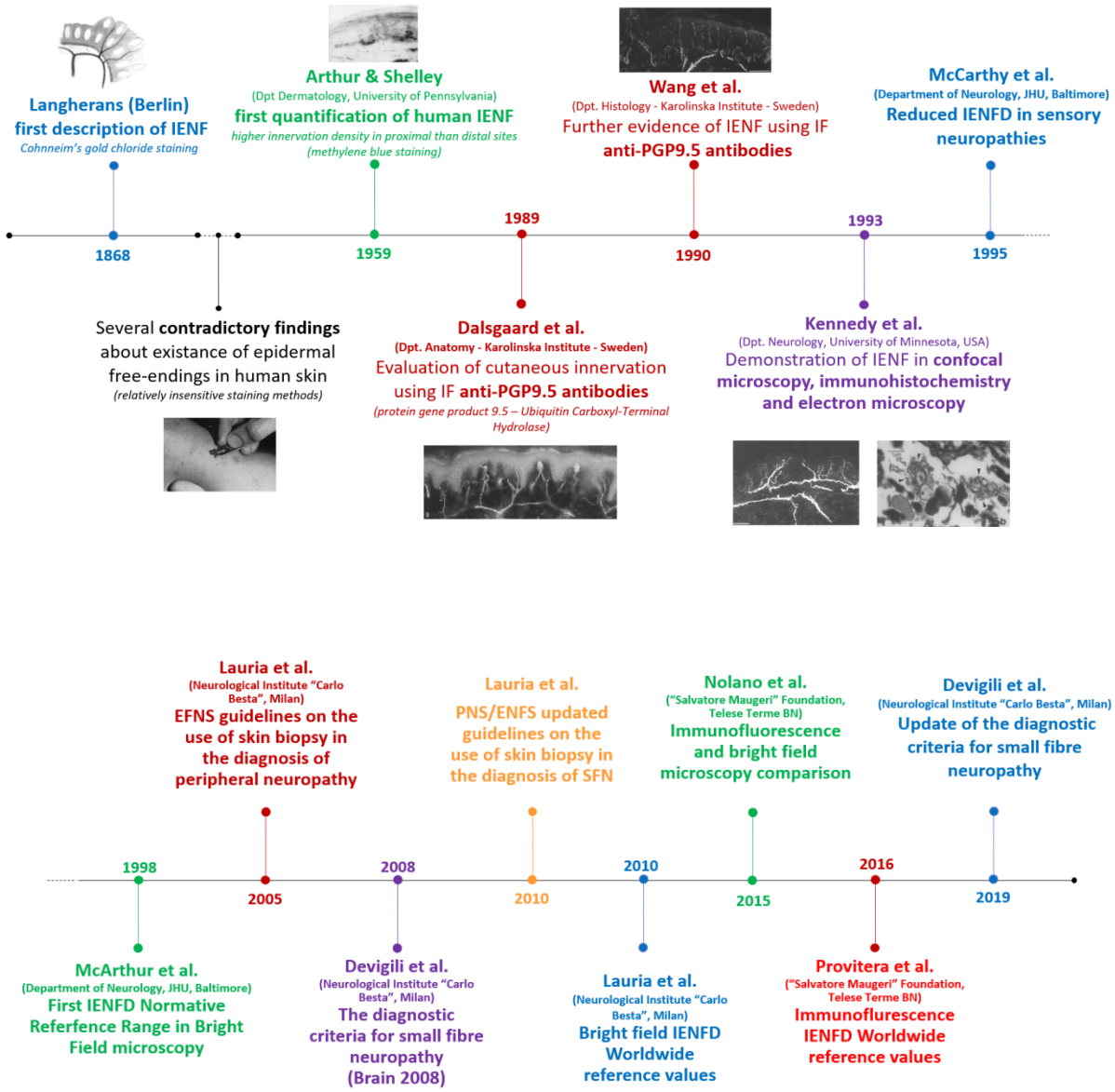

Figure 2. Skin biopsy as a diagnostic tool for SFN - historical notes and milestones. This timeline reports the evolution of skin biopsy for studying the epidermal innervation in humans from the first drawings by Langherans, through the introduction of PGP9.5 axonal marker, until the development of worldwide normative values and diagnostic criteria for SFN.

Quantitative sensory testing

QST is a non-invasive psychophysical examination for quantification of large and small fiber sensory perception. It allows to test several sensory modalities including touch, vibration, warming and cooling, heat and cold pain that the subject has to recognize. It can be used to test the functional impairment of small nerve fiber assessing warming and cooling as well as heat-pain sensation detection thresholds allowing also the evaluation of hypersensitivity and thermal allodynia in case of lower threshold for pain sensation. QST is considered a diagnostic confirmatory tool in SFN and a consensus paper provided recommendations for use in clinical practice summarizing applications and interpretation of results[72]. Normative value are available for sexes, age and body site including face, hand and foot[73] since QST parameters are age, sex and site dependent. However, QST presents some limitations: it is a psychophysical test requiring the patient collaboration and being thus open to bias or malingering; it is not able to discriminate between a central and peripheral somatosensory pathway involvement; it is time-consuming and requires specific equipment available only at specialized centers. The use of the method of levels rely on patient sensing a defined change in temperature. Therefore, being not reaction time dependent, it has the advantage of reducing bias related to cognitive impairment or to the use in children, resulting even more reliable than the method of limits that, on the contrary, require the patient to push a button as soon as a change in temperature is perceived. However, for all the limitations described, QST is not recommended as a stand-alone test for the diagnosis of neuropathic pain and should be used in conjunction with other examinations and in relation to the clinical context.

Other useful diagnostic tools

Corneal confocal microscopy

Corneal confocal microscopy (CCM) is a non-invasive method able to examine the microstructures of the cornea. By means of a light beam focus on the examined cornea layer, CCM allows to in vivo visualize the unmyelinated C fibers originating from the ophthalmic division of the trigeminal nerve[74]. Corneal innervation is evaluated by quantifying four different corneal nerve parameter for which normative value have been provided[75]: 1) corneal nerve fiber density - CNFD (the total number of major nerves per mm^2); 2) corneal nerve branch density - CNBD (the number of branches emanating from all major nerve fiber per mm^2), 3) corneal nerve fiber length - CNFL (the total length of all nerve

fibers and branches within the area of corneal tissue), and 4) corneal nerve fiber tortuosity - CNFT (tortuosity coefficient [TC]), representing the degree of tortuosity from a straight line joining the ends of each main nerve fiber.

Most of the studies have been conducting in diabetic polyneuropathy reporting a diagnostic sensitivity and specificity of 91% and 93% respectively[76]. Moreover, CCM findings are associated with the severity of diabetic polyneuropathy[77] and improvement of CCM parameters following better diabetes control has been reported in patients with type 1 diabetes moving from multiple insulin injections to infusion pump obtaining a more stable glycemic control[78].

Studies conducted on small cohorts of patients with length-dependent[79,80] (25 and 14 patients) and non-length-dependent SFN[81] (6 patients) reported a reduction of CNFD suggesting a diagnostic utility of this tool. Therefore, despite these promising findings of CCM, additional studies are need for determining its diagnostic sensitivity and specificity in patients with suspected SFN.

Nociceptive evoked potentials

Nociceptive-evoked potentials using a scalp derived response evoked by painful selective stimuli applied to the skin can be used to investigate the conduction of nociceptive pathway. A selective and short-lasting nociceptive stimulus is needed to record a synchronized response. It is obtained by a fast heating of the skin generated by either radiant heat using a laser stimulator (laser evoked potentials, LEPs) or contact heat using a plate having an extremely rapid heating rate up to 70°C/sec (contact heat-evoked potentials, CHEPs). Electrical stimulation delivered using customized electrodes has also been used aiming to obtain a selective Aδ and C fiber activation (pain-related-evoked potentials, PREPs), but there are concerns about the nociceptive specificity of this method[82].

The skin denervation induced by topical capsaicin causes a decrease of LEP vertex potential amplitude.[83] More recently, diagnostic accuracy of LEP has been investigated in diabetic neuropathy reporting a sensitivity of 78% and a specificity of 81% in relation to the skin biopsy for the diagnosis of diabetic small fiber neuropathy[84]. Also CHEPs, for which an age- and gender-adjusted normative values have been reported for the clinical use in SFN[85], have

been recently investigated in a large cohort of SFN patients reporting a strong correlation between CHEP amplitude and the degree of skin innervation[86].

However, the vertex potential recorded after laser stimulation does not reflect a nociceptive-specific neural activity since it can be elicited also by non-nociceptive somatosensory stimuli[87] and its amplitude is mainly due to the stimulus saliency rather than the pain intensity[88]. Furthermore, LEP amplitude shows a wide interindividual variability[89] and CHEPs can be absent also in healthy individuals[85], thus caution is needed in interpreting nociceptive-evoked potentials in the context of painful neuropathy.

Similarly to QST, nociceptive-evoked potentials are not able to discriminate between a central and peripheral involvement of the somatosensory system.

Autonomic sweat testing

Autonomic changes can be an early manifestation of SFN and functional tests evaluating the autonomic innervation of the skin has been proposed.

The quantitative sudomotor axon reflex test (QSART) is used to evaluate the function of the postganglionic cholinergic sympathetic C fibers innervating sweat glands. This technique uses the iontophoresis of acetylcholine to stimulate sweat glands, then the sweat production is measured by a sudorometer as an increased or reduced humidity continuously recorded from baseline to 15 minutes post stimulation[90]. QSART can increase the diagnostic yield for SFN especially when QSART findings are associated with autonomic changes[91]. However, normative data are needed for its use in clinical practice.

The postganglionic sympathetic cholinergic sudomotor function can also be investigated by a novel technique, the quantitative direct and indirect axon reflex testing (QDIRT), using a humidity activated dye to display sweating over time. The process is then dynamically observed and acquired through consecutive digital photographs[90]. This tool has been used in selected SFN patients and required further studies to address its diagnostic value in the disorders of autonomic nervous system.

Neuropathic pain treatments in SFN

The primary goal of the management of neuropathic pain in SFN patients is to detect and treat underlying causes of neuropathy. However, many SFN patients have idiopathic form

and typically suffer from sever neuropathic pain that is difficult to treat, thus the approach is mainly symptomatic.

Recommendations for the pharmacotherapy of neuropathic pain have been revised using the Grading of Recommendations Assessment, Development, and Evaluation (GRADE) based on the results of a systematic review and meta-analysis[92]. The three main categories of analgesic drug used for treating neuropathic pain include antidepressants, antiepileptics, and opioids.

In general, there are no evidence of efficacy for particular drug in specific disorders. An exception to this rule is represented by carbamazepine which is specifically effective for trigeminal neuralgia, whether it is not commonly recommended for other neuropathic pain disorders, although it can have a role in patient with painful peripheral neuropathy associated to specific mutation in Nav 1.7 sodium channel[93]. However, the majority of trials includes only patients with neuropathic pain of diabetic, post-herpetic and compressive origin[94].

Drugs with strong recommendation for use and proposed as first-line treatment include: *gabapentin* and *pregabalin* belonging to the family of anticonvulsant and having inhibitory activity on presynaptic calcium channel α2-δ subunit reducing the release of excitatory neurotransmitters as glutamate, substance P; serotonin-noradrenaline reuptake inhibitors (SNRI) *duloxetine* and *venlafaxine*; tricyclic antidepressants such as *amitriptyline* acting as blocker of sodium channels and N-methyl-D-aspartate (NMDA) receptor in the CNS.

Local treatments such as *capsaicin* or *lidocaine patches* as well as weak opioid as *tramadol* have weak recommendation and are proposed as second-line drugs, whereas botulinum toxin A and strong opioids (oxycodone and morphine) are considered third-line medications. In addition to weak recommendation, long-term opioid use might be associated with abuse, thus this class of drug should be managed and used carefully in particular in chronic pain disorders.

However, treatment of neuropathic pain is still disappointing as the overall pain relief is of about 50% in half of patients. Furthermore, available medications have several contraindications which limits their use in older patients who are more prone to have comorbidities and often have to be discontinued because unpredictable side effects.

Intriguingly, advances in understanding the role of genetic variants in VGSCs genes may lead the way for the development of new analgesics or targeting of existing drugs. Interestingly, a recent study investigated the role of the sodium channel blocker lacosamide in patients with Nav 1.7 murations-related SFN reporting a response rate of about 50% with a significant effect on the intensity of surface pain suggesting a possible effect in reducing allodynia[95].

Diabetic neuropathy

Diabetes is defined by the American Diabetes Association as a group of metabolic diseases characterized by hyperglycemia resulting from defects in insulin secretion, insulin action, or both. The chronic hyperglycemia of diabetes is associated with long-term damage, dysfunction, and failure of different organs, especially the eyes, kidneys, nerves, heart, and blood vessels[96].

Diabetes can be classified in two main categories covering the overall majority of cases: type 1 diabetes mellitus (T1DM) and type 2 diabetes mellitus (T2DM) accounting for about 5-10% and 90-95% respectively.

The absolute insulin deficiency, mainly due to cellular-mediated autoimmune destruction of the pancreatic β-cells, is the hallmark of the type 1 diabetes, whereas mechanisms leading to type 2 diabetes include a combination of relative insulin deficiency and peripheral insulin resistance.

Diagnostic test for diabetes based on glycaemic control assessment by either measuring fasting plasma glucose (FPG) after at least 8 without caloric intake, plasma glucose at 2 hours during an oral glucose tolerance test (OGTT) with a 75g anhydrous glucose dissolved in water, or level of glycated hemoglobin (HbA1C) levels.

Diagnosis of diabetes can be confirmed using all of these three diagnostic tests interchangeably, according to at least one of the following diagnostic criteria[97]:

- Fasting plasma glucose ≥126mg/dl (7,0 mmol/L)
- A 2-hour plasma glucose ≥ 200mg/dl (11,1 mmol/L) during OGTT performed with a standard 75g glucose load dose
- Hemoglobin A1C level of ≥ 6,5% (48 mmol/mol) with a laboratory assay NGPS certified standardized to DCCT

- A random plasma glucose ≥ 200mg/dl (11,1 mmol/L) in patients with hyperglycemic crisis or classic symptoms of hyperglycemia

Individuals whose glucose levels do not meet the criteria for diabetes but are too high to be considered normal, are defined as “prediabetes”. This represents a condition conferring an increased risk of developing diabetes and cardiovascular disease and it includes patients with impaired fasting glucose (IFG) defined by the presence of elevated fasting plasma glucose levels and patients with impaired glucose tolerance (IGT) resulting from high 2-hour plasma glucose levels during OGTT.

Diabetic neuropathy is among the most prevalent complications affecting patients with diabetes mellitus (DM)[98]. It represents a burden in terms of patients’ quality of life and healthcare costs, especially when it is combined with the presence of neuropathic pain that worsen the clinical picture of up to 25% of patients with DM[99,100]. The International Diabetes Federation reported a constantly growing trend of incidence of DM in the last two decades and estimates that today DM affects 425 million people worldwide, two-thirds of which are of working age[101]. Therefore, more than 100 million people are expected to suffer from painful diabetic polyneuropathy.

DM can cause several different types of peripheral neuropathy. The distal symmetric polyneuropathy (DSP) is the most common presentation of diabetic neuropathy occurring approximately in half of patients with DM. It is a slowly progressive sensory-motor neuropathy. In the early stages clinical picture is dominated by “positive” sensory symptoms such as tingling and pricking sensations combined with “negative” symptoms such as numbness or decreased sensation in the extremities with a typical “stocking-glove” distribution, classically detectable also at the clinical examination as reduced pinprick, superficial and vibratory sensation. Less frequently neurological examination reveals positive sign such as allodynia and hyperalgesia both configuring different features of evoked pain[102]. Symptoms of neuropathy proceed resembling the dying-back pathological pattern of the neuropathy, they slowly and progressively extend involving more proximal regions with distal-to-proximal gradient. A mild and very distal motor involvement can occur presenting as toe extensor weakness, although, most of the time it remains at a subclinical level. However, the most disabling aspect reported by approximately 25-30% of patients with diabetic polyneuropathy (DPN) is neuropathic pain, most commonly presenting as

spontaneous sharp, aching and burning pain of the feet often present secondary to small nerve fibers involvement. Patients with neuropathic pain also report anxiety, depression, insomnia and poor quality of life directly proportional to the severity of pain, albeit it is not known whether they are consequences of pain or may act as risk factors for pain developing[99].

Mechanisms of nerve damage in diabetic neuropathy

Nerve degeneration in diabetic neuropathy preferentially targets sensory and autonomic axons, whereas motor nerve fibers are usually involved later a to a lesser extent, resembling the clinical pattern observed in patients. This different susceptibility may in part be due to the anatomical localization of the primary sensory neurons within the dorsal root ganglia, thus missing the protection of the blood brain barrier as opposed to motor neurons located in anterior horn of the spinal cord within the central nervous system.

Several mechanisms related to hyperglycemia, dyslipidemia and insulin resistance contribute to neural damage in diabetic neuropathy. These causes changes in axons, especially in distal terminals, or in cell body indirectly conditioning the support of distal axon branches. In addition, although diabetic neuropathy is not considered a demyelinating neuropathy, also Schwann cells are involved in pathogenic steps leading to neuropathy.

Hyperglycemia

Hyperglycemia triggers the dysregulation of different metabolic pathways in diabetes eventually causing intracellular oxidative stress by increasing the production of reactive oxygen species (ROS) and impairing the antioxidant protective mechanisms. Glucose overload causes a partial shift towards polyol pathway with glucose conversion to sorbitol by aldolase reductase. Increased sorbitol levels result in osmotic imbalance within the cell and sodium/potassium ATPase disfunction via the compensatory efflux of myoinositol, thus impairing normal nerve physiology. In addition, sorbitol production by aldolase reductase consumes the cellular storage of nicotinamide adenine dinucleotide phosphate (NADPH) that is needed for regeneration of antioxidant glutathione, therefore resulting in generation of ROSs and cellular dysfunction.

Excess glucose leads also to the increase of glycolysis and levels of glycolysis intermediate fructose-6-phosphate that enters the hexosamine pathway producing pro-inflammatory

metabolite such as the 5-diphosphate-N-acetylglucosamine (GlcNac) contributing to neural damage.

Another disrupting mechanism driven by hyperglycemia is the irreversible glycation of functional and structural proteins producing advanced glycation end-products (AGEs). These AGEs cause cellular damage by altering protein structure and function. In addition, they bind cell surface receptors (RAGE) and modify gene expression and intracellular signaling via nuclear factor κB promoting the release of free radicals and pro-inflammatory molecules[103].

Dyslipidemia

Dyslipidemia is common in type 2 diabetes and prediabetes and contributes to the development of neuropathy. There are clinical evidences suggesting the pathogenic role for diabetic neuropathy is not limited to hyperglycemia. For example, patients with metabolic syndrome have a higher incidence of neuropathy compared with T2DM patients[104], furthermore glycemic control reduces the incidence of neuropathy in T1DM but not in T2DM patients[105] suggesting that further factors other than glucose levels concur to neuropathy.

Different types of lipids take part in the pathogenic process. Excess free fatty acids metabolized by β-oxidation in response to hyperlipidemia cause Schwann cells damage through ROS generation and macrophage activation leading to local inflammation[106]. In diabetes, plasma low density lipoproteins (LDL) are oxidized by ROS to oxLDL and bind oxLDL receptor 1 (LOX1), Toll-like receptor 4 (TLR4) and RAGE expressed by peripheral sensory neurons. These receptors internalize oxLDL and glycated LDL activating an inflammatory signaling pathway mediating additional inflammation and ROS accumulation producing a positive-feedback mechanism of nerve damage[107].

Impaired insulin signaling

Insulin resistance is a major feature of type 2 diabetes. Although neurons are not insulin dependent for glucose uptake, they express insulin receptor[108] on cellular body and axons at node of Ranvier mediating neurotrophic effects promoting neuronal growth and survival. Indeed, near nerve administered insulin was able to repair diabetes induced damage in experimental animal models[109]. However, despite glucose levels correction using insulin is associated with a substantial improvement of diabetic neuropathy in T1DM, it has little effect in T2DM. These findings might be at least in part due to the development of insulin resistance in sensory neurons resulting in reduced insulin neurotrophic signaling[110].

Peripheral receptors and ion channels

The thermal sensitivity and pain in humans is mediated by C and Aδ fibers that express a complex array of specialized receptors and ion channels on their endings which are crucial for stimulus transduction and conveying.

Transient Receptor Potential

Transient Receptor Potential (TRP) is a group of receptor-channels expressed on nociceptive neurons that determine transient variations of potential in response to thermal or chemical stimuli. These non-selective receptor-channels for specific cations, have a structure similar to the sodium dependent voltage channels and consist of four protein subunits each of which contains six transmembrane domains with a pore between the fifth and sixth domain. In humans, 28 different TRP channels have been identified belonging to 6 families of which 3 are of particular interest as thermo-receptors: vanilloid receptors (TRPV), receptors associated with melastatin (TRPM), receptors associated with ankirin (TRPA)[111].

Two classes of TRP receptors are activated by cold and inactivated by heat. The menthol-sensitive TRPM8 receptor is expressed in low and high threshold cold nerve endings and responds to temperatures below 25°C. The TRPA1 receptor, on the other hand, responds to temperatures below 17°C (intense cold) and is expressed only in the high threshold endings of C-fibers in subpopulations of small peptidergic nociceptors at DRG level, nodose ganglion and trigeminal ganglion. TRPA1 is insensitive to menthol while it is activated by allicin, an irritant molecule contained in garlic, and by isothiocyanates contained in wasabi and mustard[112].

Four classes of TRP receptors are activated by heat and inactivated by cold. TRPV4 and the camphor-sensitive TRPV3 respond to a painless warm stimulus at temperatures between 24°C and 34°C and above 35°C respectively. Warm sensation is mediated exclusively by type C fibers. TRPV3 and TRPV4 are also expressed at the level of keratinocytes, providing evidence of their involvement in the mechanisms responsible for heat sensitivity[113]. Unlike the previous two receptors, the TRPV1 and TRPV2 receptors are activated by high temperatures and are responsible for the sensation of heat pain. The TRPV1 receptor was the first vanilloid receptor described as a capsaicin receptor[17]. It is a polymodal receptor activated by temperatures above 43°C, pH reductions, osmolarity changes and inflammation

mediators. In the peripheral nervous system, it is localized in small and medium diameter peptidergic sensory neurons though it is also expressed in the central nervous system, vagal afferents, gastrointestinal tract, bladder epithelium and the skin. The TRPV2 receptor is capsaicin-resistant and is activated by higher temperatures (>53°C). It is expressed in Aδ fibers where it mediates the transduction of the initial sharp sensation to heat pain[111,114].

In addition to the TRP channels, a series of receptors and ion channels specific for sodium, calcium and potassium, expressed by nociceptive neurons, have been identified.

Potassium channels

The potassium channels are crucial for maintaining the resting membrane potential and for the repolarization phase of the action potential modulating its duration and firing frequency. By inhibiting peripheral excitability and limiting neurotransmitter release at central terminals, they provide a brake to spontaneous neuronal activity. Intriguingly, several neurological disorders characterized by neuromuscular hyperexcitability and neuropathic pain such as neuromyotonia or Morvan's syndrome may be caused by the presence of autoantibodies against voltage-gated potassium channels or against protein of the functional K^+ channel complex such as LGI1 or Caspr2 causing channel dysfunction[115].

Four families of potassium channels have been described on the basis of their structural and physiological features: the *voltage-dependent potassium channels (K_v)* which are the most represented K^+ channels, activated by depolarization they drive the repolarization phase of the action potential; the *inward-rectifying potassium channels (K_{IR})* mainly expressed in glial cells, they have the function of reducing the extracellular accumulation of K^+ during neuronal discharges preventing the hyperexcitability of the neuronal membrane; the *two-pore potassium channels (K_{2P})* expressed on C-fibers that limit the axon activation mediated by mechanical and thermal stimuli; the *Ca^{2+}-activated potassium channels (K_{Ca})* are activated by Ca^{2+} input, limiting its further intake with a "feedback" mechanism and thus acting as regulators of synaptic transmission at the nerve endings[116]. The impairment of K_v activation causes threshold lowering and firing rate increasing of action potentials, causing a membrane hyperexcitability. The two-pore potassium channels belonging to the TRAAK/TREK family are reported as playing a role for the cold-induced nociceptors activation, particularly for those nociceptors that are insensitive to menthol[117].

Interestingly, a recent study reported the effect of a novel genetic variant in *KCNQ2* gene coding for Kv7.2 channel responsible for painful phenotype attenuation in a patient harboring also an inherited erythromelalgia-associated mutation in *SNC9A* gene, coding for sodium channel Nav 1.7. Cell electrophysiology revealed a gain-of-function of potassium current induced by the K_V7.2-T730A variant, causing a hyperpolarizing shift due to the enhancing of K current thus resulting in a reduced excitability of iPSC-sensory neurons[118].

Voltage-gated calcium channels

The voltage-gated calcium channels act by increasing the Ca^{2+} conductance thus favoring its entry within the cell in response to depolarization. They influence numerous cellular functions such as membrane excitability, neurotransmitter release and gene expression. Based on the voltage required for their activation, two groups are distinguished: low voltage activated calcium channels (T-type LVA) and high voltage activated calcium channels (HVA). The latter are divided into L, N, P/Q and R types in relation to their pharmacological characteristics. The T-type LVA calcium channels consist of the α1 subunit of which three isoforms are recognized (Cav3.1, Cav3.2 and Cav3.3). In contrast, the HVA channels are heteromultimeric protein complexes made up of several subunits: Cavα1, Cavβ, Cavα2δ and Cavγ[8]. The different isoforms of calcium channels have a distinct cellular and subcellular localization and fulfil specific functions. For example, the release of substance P and CGRP occurs in nociceptive neurons as a result of activation of L, N and P/Q types calcium channels at the presynaptic site[119].

Calcium channels are involved in the transmission of nociceptive afferents and play an important role in neuropathic pain. Indeed, Cavα2δ subunit is up-regulated in neuropathic pain. Furthermore, it represents a key pharmacological target for gabapentinoids[120] such as gabapentin and pregabalin which are a class of drugs used as first-line treatment for neuropathic pain[121].

Acid-sensing ion channels

The acid-sensing ion channels (ASICs) respond to pH changes and play a major role in visceral and muscular afferents rather than in nociceptors innervating the skin. The ASIC channels have been identified at the intestinal level where they also respond to mechanical stimulation such as wall stretching. Currently, five ASIC channels have been identified; ASIC1-5. The ASIC3 subtype is preferentially expressed in sensory neurons receiving input from the

muscle and it has been reported to contribute to muscular mechanical hypersensitivity after exercise[122] and to play a role in pain associated with myocardial ischemia where ASIC3 channels activation is mediated by the rapid drop in pH that occurs after the first minutes of ischemia[123].

Purinergic receptors

Purinoceptors P2 respond to the ATP released by the cells following inflammation, distention and damaging stimuli, making nociceptive neurons sensitive to chemical stimuli as well. P2 receptors are divided in two families: P2X (ligand-gated ion channel receptors) and P2Y (G protein-coupled receptors). Currently, seven P2X subunits (P2X1-7) and eight P2Y receptor subtypes ($P2Y_1$, $P2Y_2$, $P2Y_4$, $P2Y_6$, $P2Y_{11}$, $P2Y_{12}$, $P2Y_{13}$, and $P2Y_{14}$) are recognized. Studies in animal models of neuropathic pain have shown that P2X3 receptors are upregulated in primary sensory neuron, whereas P2X4 receptors expression is increased in microglia[124]. Another purinergic receptor, the P2X7 receptor, has also been reported to play a role in chronic inflammatory and neuropathic pain via regulation of IL-1β.

Among metabotropic P2Y receptors, $P2Y_1$, $P2Y_2$, $P2Y_4$ and $P2Y_6$ receptor mRNA is expressed in DRG neurons. In particular, $P2Y_1$, $P2Y_4$ receptors were identified in a subset of small sensory neurons also expressing P2X3 and TPRV1 receptors. The activation of these receptors in DRG modulates currents generated by N-type calcium channels and P2X3 receptors. $P2Y_1$ receptors are upregulated in lumbar DRG after axotomy in animal model and their inhibition has been reported to prevent induction of thermal hyperalgesia via modulation of TRPV1 expression[125].

Hyperpolarization-activated cyclic nucleotide-gated channels

The hyperpolarization-activated cyclic nucleotide-gated (HCN) channels are activated by membrane hyperpolarization and are permeable to Na+ and K+. Their activation is facilitated by interaction with cyclic nucleotides, in particular adenosine monophosphate (cAMP). The HCN channels produce the I_h current that depolarizes the membrane up to the threshold for the action potential. HCN channels play an important role in membrane potential regulation thus controlling neuronal excitability. Four types (HCN1-4) are described, which are located at the cardiac and nervous tissues. They are primarily responsible for the pace-maker potential of sinoatrial node cells. HCN1 and HCN2 have been identified in the DRG. HCN1 is expressed in Aβ and small cold-sensitive fibers and it is relatively insensitive to cAMP. Its

over-expression has been associated with cold hyperalgesia and allodynia observed in oxaliplatin-induced neuropathy[126]. HCN2 is expressed in Aδ and C fibers and it is sensitive to cAMP. This channel is involved in inflammatory and neuropathic pain. Indeed, HCN2 knockout mice have normal nociceptive threshold but do not develop neuropathic pain or hyperalgesia in response to inflammation[127].

Voltage-gated sodium channels

Sensory neurons express a specific pattern of sodium channels that are key determinants of cellular excitability and action potential generation and propagation. These channels play a crucial role in the pathogenesis of chronic pain since they are involved in the mechanisms of maladaptive plasticity involving the somatosensory system in response to neural injury. The recent description of mutations in VGSCs genes in human Mendelian pain disorders further highlights their pivotal role.

The VGSCs are heterodimeric and heterotrimeric complexes composed of a pore-forming α-subunit and one or two β-subunits (Figure 3) that regulate channel density at the plasma membrane and modulate the activation and inactivation kinetics.

The voltage-gated family of α-subunits includes 9 related isoforms (Na_v 1.1-1.9) that are variably expressed in different tissues (Table 1).

Protein	Gene	Cromosomic locus	Ion selectivity	Sensitivity to TTX	Localization
Na_V 1.1	SCN1A	2q24.3	$Na^+ > K^+ > Ca^{2+}$	TTX-S	CNS, Heart, PNS (Aδ)
Na_V 1.2	SCN2A	2q24.3	$Na^+ > K^+ > Ca^{2+}$	TTX-S	CNS
Na_V 1.3	SCN3A	2q24.3	$Na^+ > K^+ > Ca^{2+}$	TTX-S	(Embryonal isoform) CNS, PNS
Na_V 1.4	SCN4A	17q23.3	$Na^+ > K^+$	TTX-S	Skeletal muscle
Na_V 1.5	SCN5A	3p22.2	$Na^+ > K^+ > Ca^{2+}$	TTX-R	Heart, Skeletal muscle
Na_V 1.6	SCN8A	12q13.13	Na^+	TTX-S	CNS, PNS
Na_V 1.7	SCN9A	2q24.3	Na^+	TTX-S	PNS, Schwann Cells
Na_V 1.8	SCN10A	3p22.2	Na^+	TTX-R	PNS
Na_V 1.9	SCN11A	3p22.2	Na^+	TTX-R	PNS

Table 1. Voltage gated sodium channels α-subunits[128].

Na_v 1.1, 1.2, 1.3 and 1.6 are preferentially expressed in the central nervous system; Na_v 1.7, 1.8 and 1.9 are the primary isoforms of sodium channels in the peripheral nervous system; Na_v 1.4 and 1.5 are the main sodium channels in skeletal muscle and heart respectively.

The α-subunits are composed by 4 domains (I-IV) each consisting of six transmembrane segments (S1-S6). The S1-S4 transmembrane segments constitute the voltage-sensor, whereas the S5 and S6 segments shape the pore. In particular, the S4 segments rich in positively charged arginine and lysine residues is important for voltage sensing. The loops between S5 and S6 segments from each domain form the narrowest external vestibule of the pore determining the ion selectivity. On depolarization, the voltage sensing S4 segment moves outwards drugging the S5 and S6 segments and opening the channel for less than 1 millisecond. The highly conserved cytoplasmic linker connecting the homologous domains DIII and DIV is responsible for the fast inactivation of the channels.

Although the main mechanism of channel regulation is the voltage-dependent gating, channel activity is also modulated by phosphorylation of a series of site in the intracellular loop between domains DI and DII by means of protein kinase A and C. The effect of phosphorylation is specific for each isoform. Indeed, it acts reducing the activity of brain sodium channels $Na_v1.1$ and $Na_v1.2$ by enhancing the slow inactivation and also by subtly slowing fast inactivation, the latter resulting from phosphorylation of a site in the inactivation gate (cytosolic linker domain between DIII and DIV). As opposite, the phosphorylation of analogous sites that regulate brain sodium channels results in enhanced activation of Na_v 1.8 channels that are specifically expressed in sensory neurons[128].

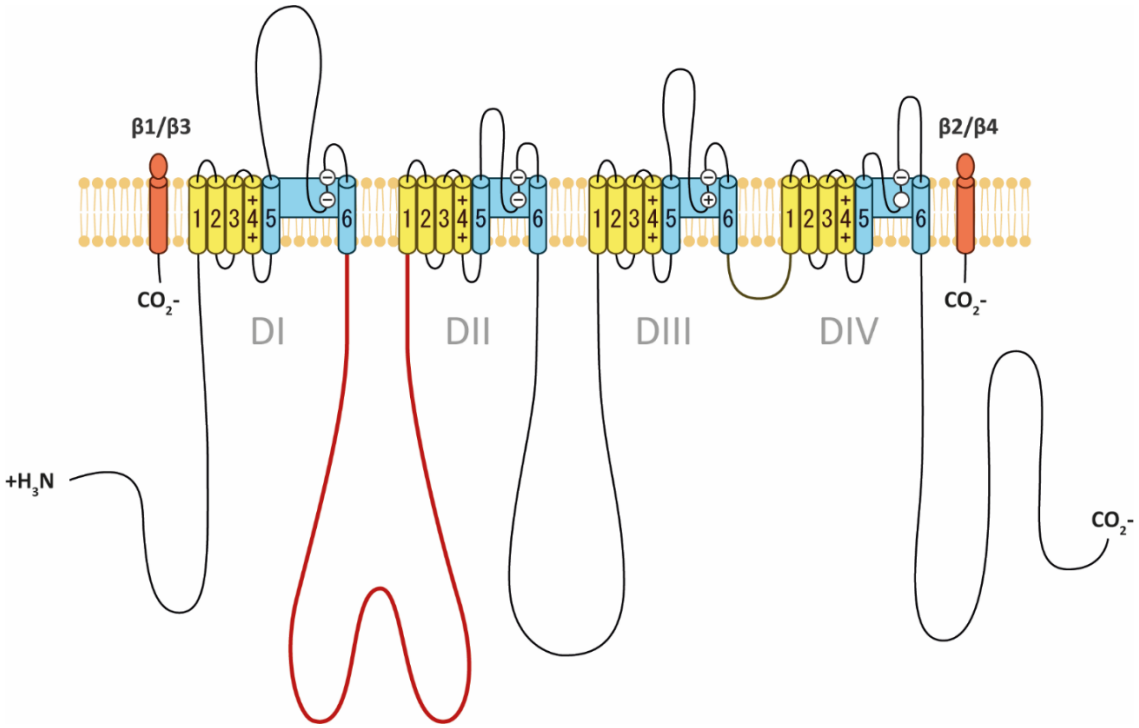

Figure 3. Structure of voltage gated sodium channel. VGSCs are heterodimeric and heterotrimeric complexes composed of a pore-forming α-subunit and one or two β-subunits. α-subunits are composed by 4 domains (DI-DIV) each consisting of six transmembrane segments (S1-S6). The S1-S4 transmembrane segments constitute the voltage-sensor, whereas the S5 and S6 segments shape the pore. The intracellular loop between domains DI and DII act as channel modulator contains a series of phosphorylation sites. The linker between DIII and DIV is responsible for the fast inactivation of the channels. β-subunits are composed by NH2-terminal immunoglobulin-like domain, a single transmembrane segment and a short intracellular segment.

The family of β-subunits includes four different isoforms. An NH_2-terminal immunoglobulin-like domain, a single transmembrane segment and a short intracellular segment compose these subunits. Based on the resemblance of their amino acid sequence and the chemical bond with α-subunits two groups can be identified: β1/β3 which are associated non-covalently with α-subunits and β2/β4 forming disulfide bonds with α-subunits. β-subunits colocalize with several neuronal cell adhesion molecule (NrCAM) including neurofascin-186 and contactin with which they interact through their extracellular Ig-like domain proving their role in subcellular localization of Na_v channels in specific sites such as the node of Ranvier[129], although no evidence has emerged of tissues or cell type specific association of different β-subunits with α-subunits.

Nav have been classified on the bases of their kinetics and sensitivity to the sodium channel blocker tetrodotoxin (TTX) (Figure 4). Focusing on the peripheral nervous system, Nav1.1, Nav1.6, Nav1.7, Nav1.8, and Nav1.9 are all expressed by adult sensory neurons and together

with the embryonal form Nav1.3 have a role in sensitization of sensory neurons in chronic pain states.

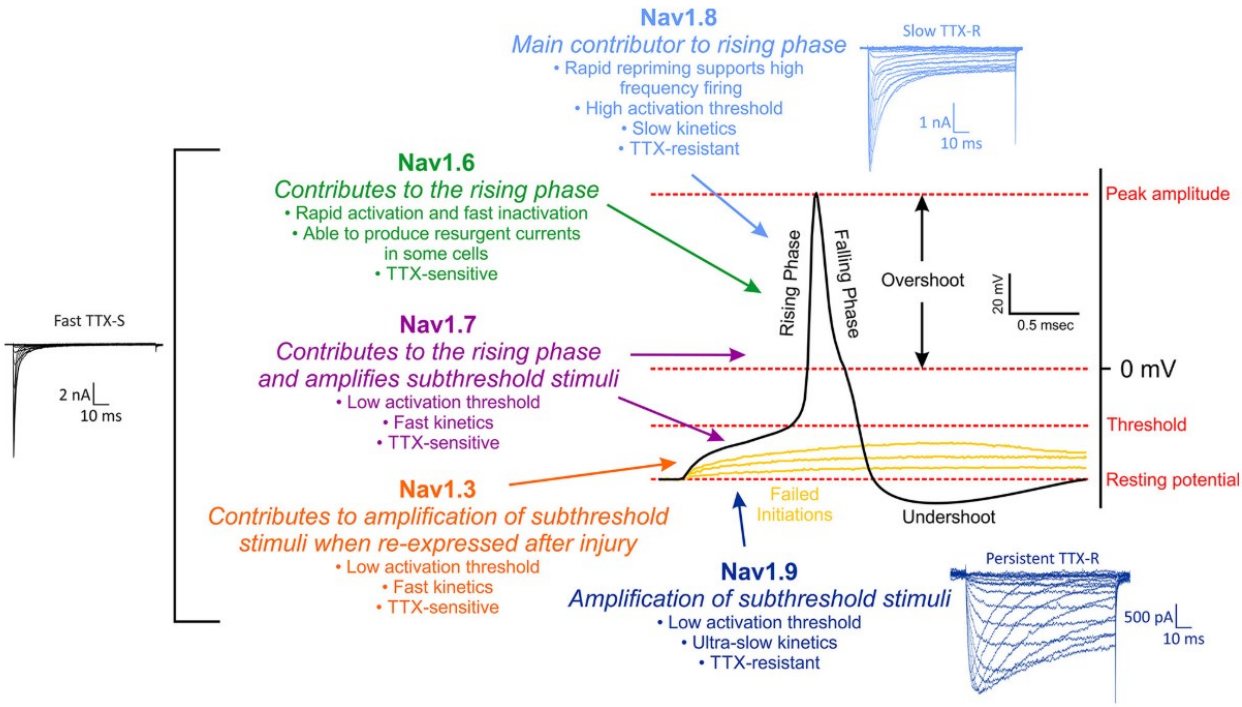

Figure 4. Contribution of different voltage gated sodium channels to action potential generation[130].

Nav 1.3

Nav 1.3 channel is encoded by *SCN3A* gene on chromosome 2q24. It is expressed in central and peripheral nervous system during embryonal development then its expression declines till becoming undetectable in adulthood. However, neural injury triggers a reexpression of this channel which contribute to mechanisms of sensitization, although these data come from studies on mouse animal models and no data are available in humans about expression in embryos and post-injury reexpression in DRG. Nav 1.3 has fast activating, fast inactivating and rapid-repriming (recovery from inactivation) kinetics and produces tetrodoxin-sensitive (TTX-S) currents that amplify small subthreshold depolarizing inputs.

There are no evidences of *SCN3A* mutations in patients with painful disorders, whereas Nav 1.3 channel have been identified in human neuromas[131] thus suggesting that the upregulation of Nav 1.3 following nerve injury represent the primary mechanism by which

this channel contributes to the development of ectopic discharge and mechanical allodynia[130].

Nav 1.6

Nav 1.6 is a TTX-S VGSC coded by *SCN8A* gene on chromosome 12q13.13. It is widely expressed in peripheral and central nervous system and its mutations have been linked to epilepsy. Nav 1.6 channels are densely expressed at the node of Ranvier of myelinated fibers whereas they are scattered in a continuous fashion in unmyelinated C fibers. These channels show a rapid repriming kinetics and are able to produce resurgent currents promoting the repetitive firing features of DRG neurons[132]. This specific kinetic feature of Nav 1.6 is supposed to be responsible for Oxaliplatin induced cold allodynia[133]. The role of Nav 1.6 in human painful disorders has recently emerged. A novel Met136Val missense mutation in Nav 1.6 has been described in a patient with trigeminal neuralgia. The electrophysiological characterization of the mutated channel revealed that the p.Met136Val substitution potentiates transient and resurgent sodium currents resulting in increased excitability of trigeminal ganglion neurons expressing the mutant channel, therefore suggesting a pathophysiological role of Nav 1.6[134].

Nav 1.7

Nav 1.7 is the major sodium channel expressed in peripheral neurons. It has been identified in sensory neurons from distal ending, along the axon to the presynaptic terminal in the dorsal horn of the spinal cord as well as in sympathetic and parasympathetic ganglion neurons. It is a TTX-S sodium channel encoded by *SCN9A* gene in the chromosome 2q24. For its fast-kinetic and low activation threshold it is designed as a threshold channel since it contributes to the amplification of subthreshold stimuli and to the rising phase of action potential.

Studies in animal models reported an upregulation of Nav 1.7 in DRG neurons in inflammation along with a switch from slow-repriming kinetic to rapid-repriming in injured DRG neurons. In addition, accumulation of Nav 1.7 in painful neuromas has also been reported following nerve injury in humans[131]. However, the stronger association between Nav 1.7 channel and human pain come from the recent identification of fully penetrant gain-of-function mutation of *SCN9A* gene in individuals with familial painful disorders with a dominant Mendelian inheritance pattern such as inherited erythromelalgia and paroxysmal

extreme pain disorder. On the contrary, recessively inherited loss-of-function mutations of *SCN9A* gene causing a completely absence of functional Nav 1.7 channels, are associated with a clinical phenotype of congenital insensitivity to pain[135].

Gain-of-function variants in Nav 1.7 have also been identified in patients with painful idiopathic small fiber neuropathy[136] and painful diabetic neuropathy[137] defining the new entity of channelopathy-related painful neuropathy.

Nav 1.8

Nav 1.8 is a TTX-resistant VGSC encoded by S*CN10A* gene in the chromosome 3p22.2. Nav 1.8 is the major contributor to the rising phase of the action potential. It has a high activation threshold, a slow inactivation from open-state causing the channel to remain open longer and a rapid repriming. These features are even more pronounced in human Nav 1.8 compared to rat Nav 1.8 and make the channel able to drive repetitive firing in DRG neurons[138].

Nav 1.8 was considered a sensory neuron channel owing to its preferential expression in DRG and trigeminal ganglion (TRG) where it was first identified. In addition, it is present in the nodose parasympathetic ganglion but it is absent from sympathetic superior cervical ganglion. Interestingly, this tissue-specific distribution and the relative resistance of Nav 1.8 to depolarization-induced inactivation explain the dual effect of I739V Nav 1.7 mutation resulting in the hyperexcitability of DRG neurons where Nav 1.8 is highly expressed, as well as an hypoexcitability of sympathetic ganglion neurons missing this sodium channel subunit[136].

Nav 1.8 channel has the unique feature to be resistant to cooling-induced enhancing of slow inactivation which cause inactivation of TTX-S channels at low temperatures, therefore this channel is essential for sustaining nociceptors excitability when the skin is cooled[139].

Mutations of *SCN10A* gene are associated with familial episodic pain syndrome (FEPS) type 2, a dominantly inherited Mendelian painful disorder. Gain-of-function mutations of Nav 1.8 producing DRG neurons hyperexcitability have been identified in patients with painful neuropathies[41] and recently the Nav 1.8 S424T mutation has been reported in a patient with painful diabetic neuropathy[140].

Nav 1.9

Nav 1.9 is TTX-R VGSC encoded by *SCN11A* gene mapped in the genome region 3p22.2. It is preferentially expressed in somatosensory nonpeptidergic nociceptors $IB4^+$ and in peptidergic myoenteric neurons. Nav 1.9 channels have a low activation threshold near the resting membrane potential and a very slow inactivation kinetics producing a persistent current at hyperpolarized potentials, amplifying small subthreshold stimuli.

Interestingly, Nav 1.9 gain-of-function mutations have been linked to human pain disorders ranging from FEPS type 3, characterized by severe pain, to the hereditary sensory and autonomic neuropathy (HSAN) type VII in which affected individuals experience a complete loss of pain perception. Genetic variants in *SCN11A* gene have also been reported in patients with sporadic form of painful SFN[42].

Nav β-subunits

The family of β-subunits includes four different isoforms (β1-4). An NH_2-terminal immunoglobulin-like domain, a single transmembrane segment and a short intracellular segment compose these subunits. Based on the resemblance of their amino acid sequence and the chemical bond with α-subunits two groups can be identified: β1/β3 which are associated non-covalently with α-subunits and β2/β4 forming disulfide bonds with α-subunits. β-subunits colocalize with several neuronal cell adhesion molecule (NrCAM) including neurofascin-186 and contactin with which they interact through their extracellular Ig-like domain proving their role in subcellular localization of Na_v channels in specific sites such as the node of Ranvier[129], although no evidence has emerged of tissues or cell type specific association of different β-subunits with α-subunits.

β-subunits act also modulating the channel kinetics and in particular influencing channel activation and inactivation. Recently, a mutation in the β2-subunit has been described in a patient with painful diabetic peripheral neuropathy having a negative screening for mutation in genes encoding for α-subunits. Cell electrophysiology confirmed a gain-of-function profile of the β2-D109N mutation which rendered DRG neurons hyperexcitable. These evidences confirm the role of β-subunits in contributing to channel kinetics and expand the frame of pain-related genes including also the genes coding for β-subunits[141].

Diabetes and sodium channels

Human pancreatic β-cells express a subset of potassium (voltage-gated and Ca^{2+}-activated), calcium (L-, P/Q- and T-type) and sodium (Nav 1.3, 1.6 and 1.7) channels. All these channels contribute to modification of β-cells membrane potential initiated by the glucose-induced closure of ATP-sensitive K^+ channels eventually resulting in Ca^{2+} influx and insulin granules exocytosis[142].

Pancreatic α-cells secreting glucagon are also equipped with voltage-gated sodium channels. Nav 1.3 is the most abundant isoform in the α-cells, whereas β-cells mainly express the Nav 1.7 channel. However, Nav 1.3 seems to be the functionally important sodium channel both in α- and β- cells because Nav 1.7 is largely inactivated at physiological membrane potential and its ablation in mice has been shown to have little effect on glucose-induced insulin secretion. Interestingly, Nav 1.7 channel inactivates at a voltage about 30 mV more negative in β-cells compared to neurons providing only a minor contribution to Na^+ current, thus the physiological role of Nav 1.7 in β-cells remain largely unkown[143].

A role for insulin and glucagon secretion has also been provided for VGSC β-subunits. A study revealed that loss of VGSC β1-subunity reduces glucose-stimulated insulin and glucagon secretion without affecting Nav 1.7 membrane localization. The extent of hormone secretion impairment was greater for glucagon compared to insulin resulting in a severe hypoglycemia in the in vivo model[144]. Furthermore, increased Na^+ current may trigger apoptotic cascade through an augmented Ca^{++} influx which can be prevented by VGSC blocking that eventually promotes cells survival[145].

On the other hand, diabetes is involved in the pathogenesis of peripheral neuropathy which represents one of its more common complication. In addition, it contributes to promote neuropathic pain not only enhancing sodium channels expression but also producing post-translational changes of VGCSs mainly through channel phosphorylation[146,147]. A crucial example is provided by the glycolytic metabolite methylglyoxal which plasma levels increase in diabetic patients and are associated with higher incidence of painful features. Intriguingly, post-translational modification induced by methylglyoxal show opposing effects on TTX-S Nav 1.7 and TTX-R Nav 1.8 channels. The phosphorylation of arginine residues within the inactivation gate (cytosolic loop between DIII and DIV) of Nav 1.8 is associated with increased excitability of nociceptors. As opposite, the major slow inactivation of Nav 1.7

could mainly affect postganglionic autonomic neurons not expressing the Nav 1.8, thus contributing to autonomic impairment associated with diabetes[148].

A fine regulation of membrane potential is therefore crucial for the neuronal and pancreatic cells function and its modification induced by constitutional of acquired changes in sodium channels can influence pancreatic cells hormone secretion as well as hyperexcitability of DRG neurons. These evidences raised an alternative hypothesis according to which in both diabetes and neuropathy might represent parallel events resulting from common underlying predisposing factors, therefore explaining why some patients developed neuropathy before the onset of diabetes[149].

The genetic hypothesis for neuropathic pain

Neuropathic pain is a complex multifactorial disease in which the environment and the genetic substrate participate in pathological process. Neural injury results in a chronic neuropathic pain only in some of patients irrespective of the underlying etiology. Likewise, pain features and intensity as well as response to analgesic treatments show a wide interindividual variability.

In the last years, the identification of several gene variants affecting the threshold to pain perception and analgesic response (e.g. in KCNS1[150], SCN9A[42], CGH1[151] genes) has raised the hypothesis of a genetic substrate for neuropathic pain[152]. The recognition of loss- or gain-of-function mutations of voltage gated sodium channels causing rare familial painful disorders, ranging from congenital insensitivity to pain to extremely painful syndromes such as primary erythromelalgia or paroxysmal extreme pain disorders has further strengthened this assumption[135]. However, despite accounting for familiar cases these Mendelian disorders do not address the variability of pain features presentation in much more common neuropathic pain conditions. The genotyping of polymorphisms of single nucleotides (SNPs) of the entire genome or exome and their association with particular phenotypes has made it possible to identify genetic determinants, presenting a more complex heritability pattern, capable of conferring protection or susceptibility to pain.

One of the most studied candidate genes codes for the catechol-O-methyl transferase (COMT) which is involved in the inactivation of dopamine, adrenaline and noradrenaline. Haplotypes associated with increased enzyme activity and reduced pain susceptibility have been described[153]. A polymorphism of the KCNS1 gene coding for the α subunit of the

potassium channel, involved in the regulation of neuronal excitability, is associated with an increased intensity of pain in various painful conditions with an additive risk profile: the most if the variant is present in homozygosis, intermediate if in heterozygosis, the least if the variant is not present[150].

Further evidence of genetic predisposition for pain comes from the identification of a haplotype of the gene encoding for the GTP cyclohydrolase 1 (GCH1) which is associated with a protective phenotype. The activity of the GCH1 and the sepiapterin reductase regulate the synthesis of tetrahydrobiopterin (BH4), an important cofactor for the synthesis of catecholamines, serotonin and nitric oxide. The increased activity of GCH1 triggered by a nerve injury causes an increase in BH4. In the animal model, inhibition of BH4 reduces inflammatory and neuropathic pain and the production of nitric oxide in DRGs, whereas intrathecal infusion of BH4 causes increased pain. The identified variant of the GCH1 gene with an allele frequency of about 15% in the general population, is associated with a reduced activation of GCH1 in response to nerve damage and with a significant reduction in chronic lumbar pain in patients undergoing discectomy[151,154].

Polymorphisms have also been associated with response to opioid therapy. A polymorphism of the *OPRM1* gene that encodes for the μ receptor of opioids was associated with a lower analgesic response causing patients requiring higher dosages. On the other hand, polymorphisms in genes coding for COMT, melanocrotine-1 receptor (MC1R) and cytochrome CYP2D6 were associated with an increased opioids effect at lower dosage, whereas the normal therapeutic dosage easily produced intoxications and adverse events[155].

Inherited pain disorders

Congenital insensitivity to pain

Congenital insensitivity to pain (CIP) is a very rare disorder characterized by the complete inability to perceive pain from birth leading to contusions, cuts, fractures, burns and finger mutilation. Over the years, many traumas can accumulate and mortality in juvenile age is significantly increased, especially in males due to risky behaviors resulting from absence of pain perception. On the other hand, temperature perception is preserved, but patients do not experience painful sensation even at temperatures above 50°C. Different biallelic

mutations have been described in *SCN9A* gene, associated with CIP phenotype[156], causing a complete absence of functional copies of Nav 1.7 channel. A new SCN9A splicing mutation causing a premature stop codon and resulting in truncated Nav 1.7 protein compound with a missense mutation has been recently identified in a patient with CIP phenotype with hyposmia and hypogeusia[157]. The effect of suppression of Nav 1.7 expression has also been investigated in animal models resulting in an altered behavior in response to painful mechanical stimuli[158]. A frame-shift mutation in the *SCN9A* gene, responsible for the appearance of a premature stop codon, was described in two Japanese families associated with a new CIP phenotype classified as HSAN type IID[159]. It is characterized by a variable age of onset of symptoms ranging from birth to third decade, distal extremities distribution, reduction of intraepidermal innervation density, involvement of small and large sensory fibers with a mononeuropathy multiplex pattern, hearing loss, hypogeusia, hypo/anosmia and dysautonomia including urinary disorders and reduced sweating and lacrimation. More recently, a phenotype of congenital insensitivity to pain associated with a significant impairment of gastrointestinal motility has been described associated to a de novo mutation in the *SCN11A* gene encoding the sodium channel Nav1.9. Such gain-of-function mutation might block the transmission of pain signals impairing the recovery from inactivation of Nav1.7 and Nav1.8 channels by causing a sustained depolarization of nociceptors[160].

Inherited Erythromelalgia

Inherited erythromelalgia (IE) represents a model of a genetically determined pain-disorder in humans. It has been the first painful syndrome to be related to sodium channel dysfunction. IE has an autosomal dominant pattern of inheritance and it is caused by gain-of-function missense mutations in the *SCN9A* gene encoding for the α-subunit of the sodium channel voltage dependent Nav1.7[161]. Onset may occur in childhood, adolescence or adulthood with attacks of severe burning pain, edema, congestion and intense redness at the extremities, in particular the feet and hands and occasionally nose and ears triggered by heating, prolonged standing and exercise and relieved by cold. Pain free intervals between attacks may reduce as the disease progress leading to constant pain with some fluctuation. Mutations in the *SCN9A* gene responsible for the erythromelalgia fall into a region of the sequence coding for the loop between the 4th and 5th trans-membrane segments of the Nav1.7 channel. This region is the linker between the voltage-sensor (1st-4th segment) and

the pore-forming region (5th and 6th segment), thus mutations in this domain could have an effect on channel activation. Electrophysiological studies revealed that mutations causing erythromelalgia produce a hyperpolarizing shift of activation threshold of the Nav1.7 channels expressed by nociceptors. Other mutations may result in slower inactivation kinetics and increased current in response to slow depolarization. There is a correlation between the biophysical characteristics of the mutated channel and the severity of the disease. It has been reported that the magnitude of the shift of the activation threshold of the channel towards a more "hyperpolarized" membrane potential correlates with the age of onset of the disease, so mutations that cause a greater reduction in the activation threshold of Nav1.7 are associated with an earlier age of onset[162]. Electrophysiological changes are sensitive to high temperatures, explaining the clinical phenomenon of heat-triggered painful episodes. Although treatment of IE is challenging, some evidences support the use of carbamazepine and mexiletine in the context of specific mutations[163].

Paroxysmal extreme pain disorder

Paroxysmal extreme pain disorder (PEPD) is an autosomal dominant inherited condition with incomplete penetrance. A correlation with gain-of-function missense mutations in the *SCN9A* gene was first demonstrated in 2006 [164]. Typical clinical features include paroxysmal urethral, perineal, rectal, ocular and mandibular pain attacks associated with autonomic manifestations such as skin reddening (sometimes with patchy distribution configuring the Harlequin phenomenon), bradycardia and syncope, lacrimation and rhinorrhea. Pain episodes can be spontaneous or evoked by mechanical stimuli. Four types of painful attacks are described: 1-child crisis at birth in which the newborn appears red and stiff; 2-rectal crises that may be spontaneous or triggered by defecation and tend to decrease in frequency with age; 3-eye crises, most often spontaneous; 4-jaw crises in which the triggering phenomenon is often represented by chewing. The last two, ocular and mandibular, unlike the rectal ones, seem to become more frequent in adulthood. More frequently in childhood are reported episodes of non-epileptic tonic seizures characterized by apnea, flushing and bradycardia that sometimes can reach asystole, lasting up to a minute. These features seem to be associated with the most acute episodes of pain. Missense mutations have been reported in the Nav1.7 sodium channel causing alteration of fast inactivation and enhanced channel repriming (earlier recovery from the inactivation

phase). Unlike erythromelalgia, PEPD is associated with neuronal hyperexcitability caused by mutations that alter inactivation rather than promoting activation of sodium channels[165]. Carbamazepine therapy has been shown to be effective in reducing the frequency and intensity of pain attacks.

Family episodic pain syndrome

Familial episodic pain syndrome was first described in 2010 associated to a gain-of-function missense mutation of the *TRPA1* gene encoding the homonymous non-selective ion channel receptor. This autosomal dominant inherited painful condition has an onset in childhood and is characterized by episodes of pain in the chest and upper limbs occasionally radiating to the abdomen and lower limbs. Pain attacks are triggered by fasting, fatigue, cold and physical stress. They last about 60-90 minutes and are preceded by a prodromal phase during which rest can avoid evolution towards an established painful attack. During the phase of intense pain, breathing difficulties, tachycardia, sweating, paleness, cyanosis of the lips and abdominal rigidity may occur. Episode resolution is followed by a phase of exhaustion and deep sleep. In the period between attacks, neurological examination is unremarkable. In particular, there is no evidence of reduced superficial, thermal or pinprick sensations. Nerve conduction study and IENFD at skin biopsy are normal. Cell electrophysiology revealed an increase in the cationic current through the TRPA1 ion channel, leading to enhanced cellular excitability. Individuals harboring pathogenic mutations have a greater area of skin inflammation associated with hyperalgesia and allodynia in response to the application of mustard oil (containing an isothiocyanate that binds the TRPA1 receptor) compared to normal subjects[166].

More recently, two large Chinese families have been described with familial episodic pain syndrome, defined as type III, associated with gain-of-function mutations of the SCN11A gene encoding the sodium channel Nav1.9[167]. Unlike type I (due to *TRPA1* mutations), familial episodic pain syndrome type III is characterized by a distal distribution of complaints and a preferential presentation late in the day. A pharmacological response to anti-inflammatory analgesic drugs is also described. Functional study of DRG sensory neurons in mice induced to express the mutated Nav1.9 channel demonstrated cellular hyperexcitability with increased peak of current density and neuronal firing.

Mutations in *SCN11A* responsible for familial episodic pain syndrome do not determine depolarization of the resting membrane potential, which instead occurs in the congenital insensitivity to pain syndrome associated to "gain-of-function" missense mutations of *SCN11A* (see Congenital insensitivity to pain). This shows how different mutations of the *SCN11A* gene, all responsible for an increased function of the sodium channel Nav1.9 but with different biophysical characteristics, can have opposite effects on sensory neurons excitability and translate into opposite clinical phenotypes.

Channelopathy-related peripheral neuropathy

Up to 50% of cases of SFN do not have a defined cause and are therefore defined as idiopathic. The identification of gain-of-function mutation in sodium channels causing painful disorders prompt the investigation for genetic variants also in this much more common condition whose cause often remains unclear.

A seminal study in 2012 described gain-of-function missense mutations in the SCN9A gene in about 30% of patients with idiopathic SFN[40], though a recent study reported a lower rate of mutated patients[168]. Gain-of-function mutations in patients with painful neuropathy were also identified in *SCN10A*[41] and *SCN11A*[42] genes, defining the subgroup of sodium-channelopathy-related SFN.

The main electrophysiological alterations of the Nav1.7 channels change in SFN include a reduction in slow inactivation and an increased current leading to hyperexcitability of sensory neurons. However, these mutations do not show the electrophysiological characteristics typical of extreme paroxysmal pain syndrome (incomplete rapid inactivation) and erythromalgia (hyperpolarization of the activation threshold). Most SFN variants in VGSCs genes are associated with distal pain, but single mutations can cause different phenotypes and electrophysiological changes[169], though some variants have been associated to specific phenotype such as the G856D variant in *SCN9A* gene identified in a complex phenotype including severe pain, dysautonomia and acromesomelia[170]. The increased levels of intracellular calcium due to an altered functioning of the sodium-calcium exchanger is the proposed mechanism leading to small nerve fiber degeneration in sodium channelopathy[171].

Clinical and genetic risk factors for neuropathy and pain in diabetes: state of the art

Risk factors for diabetic neuropathy

Diabetic neuropathy is a complex process in which hyperglycemia seems not to be the only actor playing a role in the pathophysiology of neuropathy. Although the duration of diabetes and glycated haemoglobin (HbA1c) levels are considered major predictors of diabetic neuropathy[172], a systematic review of clinical trials in patients with DM suggested that glucose lowering therapies do not significantly prevent patients with type 2 DM (T2DM) from developing polyneuropathy. Conversely, enhanced glucose control notably reduces the incidence of clinical neuropathy and ameliorate nerve conduction abnormalities in patient with type 1 DM (T1DM)[105]. Interestingly, a study comparing C-fiber function in patients with T1DM and impaired glucose tolerance (IGT) investigating the axon reflex with laser doppler, revealed a disfunction of C-fibers in IGT patients whereas no small nerve fiber involvement was detected in those with longstanding type 1 diabetes[173]. These results suggest that other factors besides hyperglycemia likely contribute to the development of neuropathy in T2DM patients. Indeed, recent studies identified metabolic syndrome components, including obesity, hypertriglyceridemia and hypertension as independent risk factors for developing polyneuropathy[174,175]. Moreover, the lipid profile abnormalities often identified in prediabetes, which is highly prevalent in obese patients, further strengthen the role of obesity and dyslipidemia in the pathophysiology of polyneuropathy[176].

Nevertheless, several evidences are accumulating for the role of genetic susceptibility to DPN. Although several genes have been investigated as candidate genes for DPN susceptibility, most of the studies were underpowered because of the small sample size and only few genes have been studied in large and independent cohorts. In particular the *ACE* (encoding angiotensin converting enzyme) and MTHFR (encoding methylenetetrahydrofolate reductase) polymorphisms have been associated with an increased risk of development of DPN[177,178].

Risk factors for painful diabetic neuropathy

Neuropathic pain is defined as a pain occurring as a result of a lesion or a disease of the somatosensory nervous system[12]. Although neuropathy occurs in up to 50% of patients with

DM, only a part of them develop pain. The reasons why some patients are more likely than others to develop neuropathic pain remain unclear. This likely reflects a complex interplay of several factors conferring vulnerability to noxious agents such as the metabolic dysfunction of DM.

A recent cross-sectional study investigated the frequency of neuropathy and pain in a cohort of 816 diabetic patients. Diabetic polyneuropathy showed a frequency of 36% and was associated with different variables including severity and duration of diabetes, BMI, glycated hemoglobin and male sex. On the contrary, diabetic pure SFN was unrelated to the investigated clinical variables. Only 13% of patients had a painful polyneuropathy and the further analysis of the differences between painful and painless polyneuropathy patients revealed that the female sex was the only variable significantly associated with pain[179] and also confirmed in other studies[100,180,181] . Interestingly, the study reported no relation between the sural nerve sensory action potential amplitude and the painful phenotype, supporting the role of nociceptive fibers damage rather than the large sensory fiber axonal loss in developing of neuropathic pain.

Patients with more severe neuropathy, poor glycemic control and higher BMI had higher prevalence of pain, as also reported other cross-sectional studies[102,180,181]. However, these variables were also associated with the development of polyneuropathy and might not be specific of painful form. Indeed, from the comparison between painful and painless polyneuropathy, female gender remained the only significant associated factor[179].

Type of diabetes has been also reported to be associated with painful phenotype. In particular, T2DM patients have double risk of painful neuropathic symptoms compared to T1DM patients[100]. This finding further underlines how hyperglycemia represents only one actor of a wider scenario in which several other players contribute to the development of pain.

Mechanisms causing neuropathic pain encompass a variety of changes occurring at the level of injured sensory neurons leading to nociceptors hyperexcitability. Upregulation and phosphorylation of ion channels expressed by sensory neurons are critical determinants of cellular excitability by increasing the number of channels or modifying channels properties in terms of kinetics and conductance. The glycolytic metabolite methylglyoxal can alter the function of ion channels causing post-translational modification of Nav 1.7 and Nav 1.8 (see

Diabetes and sodium channels). In addition, it can enhance the activity of TRPA1 channel leading to neuron hyperexcitability in animal models[182]. Plasma levels of Methylglyoxal above 600 nM have been reported in association with higher risk of painful diabetic neuropathy[148].

In the last decade, the identification of pathogenic gain-of-function mutations in *SCN9A* gene (encoding for Nav 1.7) causing inherited pain disorders, raised the interest for genetic mutation in this channel also in other much more common conditions such as painful diabetic neuropathy. Candidate-gene studies reported a higher frequency of rare variants in *SCN9A* gene in patients with painful diabetic neuropathy compared to painless patients[137,183] and some of these variants resulted in gain-of-function of the Nav 1.7 at cell electrophysiology. In addition, gain-of-function variants in the *SCN10A*[41,140] gene and more recently in the gene coding for the β2-subunit of sodium channel have been identified in patients with painful diabetic neuropathy.

Another candidate-gene investigated a single-nucleotide polymorphism, at nucleotide 118 for opioid receptor mu 1 (OPRM1) showing a prevalence of A118G polymorphism in patients having a painless form (VAS ≤3) of diabetic foot ulcer[184].

Only two genome wide association studies (GWAS) in the same Scottish diabetic cohort have been conducted in order to investigate genetic determinants for painful diabetic neuropathy.

These GWAS studies[185,186] identified an association at chromosome 8p21.3 near the gene GFRA2 with a narrow-sense heritability of 11% as painful diabetic neuropathy patients had been selected considering the use of at least one from five recommended neuropathic pain analgesic drugs and a monofilament test positive for sensory neuropathy; the elimination of monofilament test from the inclusion criteria widened the association results including a sex-specific associations at chromosome 1p35.1 in the ZSCAN20/TLR12P gene regions in females and chromosome 8p23.1 next to HMGB1P46 in males and a narrow-sense heritability of 30% in males and 14.7% in females.

HYPOTESIS AND SIGNIFICANCE

The typical clinical picture of small fiber neuropathy presents with excruciating burning sensation at feet and hand. However, pain features are not homogenous among different

subjects. Some patients have painless form of SFN while among those complaining painful form the intensity of dolorous symptoms may significantly differ irrespectively of the underlying etiology.

The identification of several gene variants affecting the threshold to pain perception and analgesic response (e.g. in KCNS1, SCN9A, CGH1 genes) has raised the hypothesis of a genetic substrate for neuropathic pain susceptibility (see The genetic hypothesis for neuropathic pain). The recognition of very rare gain or loss-of-function mutations of voltage gated sodium channels as responsible for rare mendelian familial painful disorders, ranging from congenital insensitivity to pain to extremely hyperalgesic syndromes such as primary erythromelalgia or paroxysmal extreme pain disorders further strengthened this concept.

Based on these considerations, the studies published in the last years argued the role of a genetic substrate for painful small fiber neuropathy, focusing on the screening for rare variants in candidate pain-related genes, in particular voltage gated sodium channels (VGSC) genes, that might be able to explain the clinical phenotype also in patients affected by much more common conditions such as painful neuropathy. Indeed, many different rare variants in VGSC genes have been described as associated to painful phenotype in idiopathic or diabetic neuropathic patients, some of which conferring a gain-of-function to the channels as demonstrated by cell electrophysiology (see *Diabetes and sodium channels* and *Channelopathy-related peripheral neuropathy*).

The demonstration that these variants have a pathogenic role in neuropathic pain is challenging. In familial cases, it derives from the multigenerational segregation between genotype and phenotype of affected family members. However, this cannot be applied to the majority of sporadic cases for which the pathogenic role is addressed by the demonstration of impaired cellular excitability of nociceptors and biophysical changes of the channels by cell electrophysiology. Nevertheless, concerns have been raised about the pathogenicity of single rare gain-of-function variants, since some of them have been identified also in healthy subjects or did not produce changes in terms of cellular excitability[187]. As a result, most of the identified variants are classified as VUS (variants of unknown significance).

Available evidences suggest that the vast majority of the heritability in adult-onset diseases is mediated by a polygenic architecture composed by numerous common and low-frequency

gene variants having a small effect size and considered as modifiers, whereas rare high-risk variants only account for approximately 1–10% of the disease incidence. A recent theoretical development has proposed an extreme representation of this model according to which all complex traits and diseases share a single "omnigenic architecture"[188]. In the omnigenic model, all genes expressed in a disease-relevant cell are sufficiently interconnected to contribute with a non-zero effect on phenotype.

This thesis proposes to move from the customary approach of seeking for rare variants with large effect to a groundbreaking approach in this clinical context of a complex and the most of times sporadic disease, looking also at the frequency of common variants in candidate pain-related genes in painful and painless cohorts of patients. This approach, by computing a polygenic risk score, aims at identifying the weight of a "cluster" of variants that, together with other environmental factors, might be able to discriminate with sufficient accuracy painful from painless patients (Figure 5).

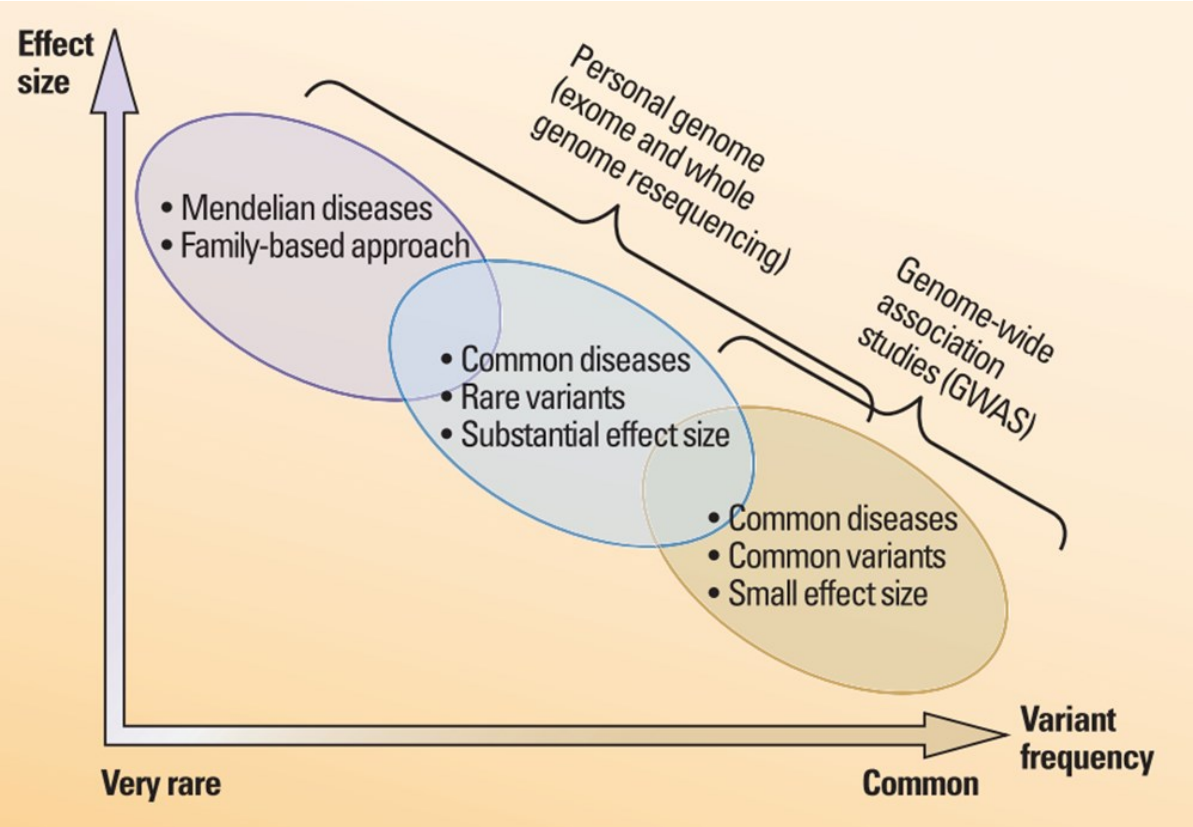

Figure 5. From Kaiser J. *Science* 2012[189]. For common disorders individual variants give only a minor contribution to the overall risk of developing a disease, thus the resulting phenotype comes from a combination of many common variants contributing with a small effect size to compose the clinical phenotype.

Considering the hypothesis of a polygenic architecture of SFN, phenotype represents the clinical marker sustained by the right combination of multiple genetic variants having different weight. In these terms, the assessment of a deep clinical phenotyping is a crucial step that aims of identifying a well-defined and homogeneous cohort of idiopathic painful and painless small fiber neuropathy patients. In addition, it is essential for interpretation of genotyping data and for increasing the statistical power by narrowing the clinical variability of the cohort.

AIMS

- **CLINICAL PHENOTYPING**
  1. To design a standardized protocol for evaluation of patients with suspected SFN and to develop a tool for integrating data coming from clinical, neurophysiology, skin biopsy and genetics for an accurate, systematic and thorough patients' phenotyping.

     Study 1: Deep clinical phenotyping of patients with suspected SFN and relational database design
  2. To evaluate changes in diagnostic accuracy of IENFD for addressing the diagnosis of SFN based on a comprehensive review of skin biopsies performed over a period of twenty years in patients with suspected SFN.

     Study 2: 20 years of skin biopsy at Neurological Institute C. Besta
  3. To investigate the circadian variability of pain intensity in a cohort of patients referred for suspected SFN.

     Study 3: Circadian variability of pain features in suspected SFN patients

- **PAIN GENETICS: From candidate-gene to polygenic risk score**
  4. To identify rare variants in VGSC genes and describe their frequency in phenotypically well-defined cohorts of small fiber neuropathy patients according to the etiology and presence or absence of pain.

     Study 4: *Candidate-gene* analysis of rare variants in VGSCs study
  5. To propose a pilot model for pain risk prediction in patients with diabetic neuropathy combining clinical and genetic variables into an individual-level risk score.

     Study 6: *Pilot polygenic* model for risk stratification on painful diabetic neuropathy

METHODS

CLINICAL PHENOTYPING

Study 1: Deep clinical phenotyping of patients with suspected SFN and relational database design

Study design

A standardized protocol for evaluation of patients with suspected SFN was developed and integrated in clinical practice. In addition, the design of a dedicated database for accurate and systematic data collection represented a crucial step of this study.

The study had a cross-sectional design and consisted of a single clinical assessment appointment for thorough clinical evaluation of patients with suspected SFN to be performed in outpatient clinical setting. Evaluation included also questionnaires that were completed before the appointment and then returned at the time of the visit.

Study population

Patients referred to the Neuroalgology Unit of Neurological Institute "Carlo Besta" in Milano with suspected SFN or neuropathic pain have been consecutively recruited for detailed phenotype assessment and genetic analysis starting from 2017. All study participants signed written consent before participating.

In addition, we retrospectively collected available data from medical records of patients evaluated from 1998 to 2016.

Demographics and medical history

During clinical evaluation patients had a detailed medical history including age, sex, symptoms onset and progression, familiarity, pain features, comorbidities and drug history.

Information about onset included date of onset, time of symptoms onset distinguishing between a rapid or slow progression (depending on whether symptoms developed in less or more than 8 weeks respectively), presence/absence of pain and distribution of symptoms.

Where available, biochemical parameters were also collected including glycaemia, Hb1Ac, thyroid function, serum electrophoresis, autoimmunity, vitamin B12, lipid profile, HIV, HCV and HBV serology. Height and weight parameters were measured for each patient.

Customized neurological examination

All patients underwent a comprehensive neurological examination including a customized assessment of sensory function. In particular, it included the following assessments:

- evaluation of sensory functions: pin-prick using disposable examination pins, light touch using a cotton swab, temperature using tubes filled with cold or warm water, joint position, vibration sense using a 64 Hz Rydel Seiffer tuning fork[190]
- sensory positive signs such as hyperalgesia (defined as augmented pinprick sensation characterized by abnormal painful sensations including electric-like sensation) and mechanical allodynia (tested using a cotton swab)

  Presence and distribution of positive and negative sensory signs were recorded
- muscle strength examined bilaterally in foot dorsal flexors and extensor hallucis longus. Strength was graded in 4 categories: normal strength, slightly reduced (< 50%), severely reduced (> 50%), paralytic[191]
- Deep tendon reflexes examined in lower limbs (knee and ankle jerk). Tendon reflexes were grades as: normal, reduced (when present with reinforcement maneuvers, e.g. Jendrassik), absent.

Neurophysiology

Standardized nerve conduction study was performed in every patient using conventional techniques with surface electrode recordings with skin maintained at 32°C. At least one motor nerve (peroneal or tibial) and one sensory nerve (sural) were included in the neurophysiological study:

- Sural sensory nerve conduction was performed antidromically recording at the ankle posterior to lateral malleolus and stimulating 12 cm proximally at posterior-lateral calf.
- Peroneal motor nerve conduction was performed recording from extensor digitorum brevis (EDB) muscle and stimulating at ankle, below fibular head and at lateral popliteal fossa.
- Tibial motor nerve conduction was performed recording from abductor hallucis brevis (AHB) and stimulating at the ankle and popliteal fossa.

The nerve conduction velocity and the amplitude of sensory action potential (SAP) and compound motor action potential (CMAP) were recorded for sensory and motor nerves, respectively.

Patients having previous electrophysiological study testing at least one sensory nerve conduction of sural nerve and one motor conduction either of peroneal or tibial nerve did not repeated the study. Abnormal nerve conduction study was defined according to the laboratory normal values.

Skin Biopsy

We used the quantification of IENFD for addressing a definite diagnosis of SFN[61]. Skin biopsy was collected from lower distal leg about 10 cm proximal from the lateral malleolus. Skin biopsy were collected from the most affected side or from the right side in those reporting a symmetrical distribution of complaints[65].

Skin biopsy was taken with a disposable 3-mm circular punch. The immunostaining processing was performed following published guidelines using polyclonal anti–protein gene product 9.5 antibodies[61] (Ultraclone, Isle of Wight, UK). Briefly, specimens were fixed (2% paraformaldehyde–lysine–sodium periodate, 4°C overnight) and cryoprotected. Sections with 50-mm thickness were cut on a cryostat from each punch biopsy. Count of dermal-epidermal junction crossing fibers for assessing the density of intraepidermal nerve fiber (IENFD) per millimeter was performed on 3 non-consecutive central sections (e.g., n. 25, 27, 29) by bright-field microscopy using a stereology workstation (Olympus BX50, Tokyo, Japan; PlanApo oil-objective 40 3/NA 5 1.0). IENFD was compared to sex- and age-adjusted normative value[62].

Questionnaires

A standardized set of validated questionnaires were used for assessing presence, intensity and distribution of neuropathic pain, autonomic symptoms, small-fiber-related symptoms, mood and anxiety.

- *The Douleur Neuropathique 4 Questions (DN4)* was used as screening tool for neuropathic pain. It includes two questions focusing on pain features (burning, painful cold, electric shocks) and associated abnormal sensations (tingling, pins and needles, numbness, itching) which were reported by patients by filling a form, and

two questions investigating presence of three signs assessed by neurological examination (touch hypoaesthesia using a soft brush, pinprick hypoaesthesia using disposable examination pins, tactile dynamic allodynia using a soft brush).

- *ID-PAIN* and *painDETECT* questionnaires including questions on pain determinants, spatial and temporal distribution were used as a self-administered screening tool for Neuropathic pain.
- *The Small Fiber Neuropathy and Symptoms Inventory Questionnaire (SFN-SIQ)* including 13-items assessing autonomic symptoms (e.g., changes in sweating pattern, presence of diarrhea, constipation, urinary tract problems like hesitation and incontinence, dry eyes, dry mouth, dizziness when standing up, palpitations, hot flashes) and pain symptoms (e.g., sensitive leg skin, burning feet, sheet intolerance, and restless legs at night) was administered for scoring the number of SFN-related symptoms.
- *The Composite Autonomic Symptom Score-31 (COMPASS-31)*, validated in patients with small fiber neuropathy, was used to measure autonomic symptoms encompassing six domains (orthostatic intolerance, vasomotor, secretomotor, gastrointestinal, bladder and pupillomotor functions)
- *The hospital anxiety and depression scale (HADS)* was administered to assess mood and anxiety components.

Pain assessment

Presence of pain as well as pain determinants and intensity were assessed in all patients.

Each patient was asked to define his painful sensation according to:

- Presence / absence of pain or positive sensory symptoms such as tingling and/or itch;
- Pain determinants: choosing one or more among burning, pins and needles, electric-like, cold pain or cramp-like pain;
- Spatial distribution: highlighting it on a body map, reporting whether pain was perceived predominantly as deep or superficial and if any prevalence over a side was observed;
- Temporal distribution: reporting the number of days a month when they experienced pain and if pain was constant or paroxysmal with or without pain free intervals within a single day;

- Pain intensity: the *11-point Likert Pain Intensity Numeric Rating Scale (NRS)* was used for scoring the severity of pain. Patients were asked to report the mean intensity of pain experienced in the 2 weeks preceding the clinical evaluation in the morning, in the afternoon, in the evening and at night, respectively, as well as an average of whole day using the NRS. Patients that had a normal sleep scored "0" at night.

Clinical phenotype definition

Patients were initially classified in four different main categories according to symptoms and sings presence and distribution:

- *Classic SFN phenotype*: patients having a length-dependent distribution of pain or sensory positive symptoms;
- *Diffuse SFN phenotype:* patients having diffuse distribution of pain or sensory symptoms but still including features of length-dependent distribution;
- *Atypical SFN phenotype:* patients having a non-length-dependent or patchy or focal distribution of pain or sensory symptoms not including extremities;
- *No SFN symptoms:* patients not complaining pain or sensory positive symptoms.

Comorbidities

Associated medical conditions were collected for each patient and classified in four main categories: acquired, hereditary, syndromic and idiopathic. Year of onset was also collected for each comorbidity when available. Medical relevant comorbidities, other than those clearly associated to SFN[34], were also reported including tumors, neurodegenerative diseases, diagnosed psychiatric disorders, migraine and headache or other non-predefined medical conditions.

Patients who had no definite SFN-associated conditions were defined as idiopathic.

Analgesic treatment

Analgesic medication history was collected. Each patient was asked to report which medication he or she had used, at what dosage and for how long. Efficacy of the drug was scored according to the extent of pain reduction: good (at least 50% of pain relief), partial (pain relief between 30% and 50%), absent (no pain relief). Drug discontinuation was also recorded reporting any adverse effect.

Blood sample

Blood sample for DNA and serum bank was taken from all the patients who had given written informed consent.

Relational database

A database was developed using Microsoft Access software. It has been conceived as a relational database connecting different tables containing clinical, neurophysiological, neuropathological and genetics data sets.

A unique identification number (ID patient) was assigned to each patient and represents the database *key* connecting all tables. Objects stored in the database were grouped in logical sessions (tables) encompassing demographics, medical history, comorbidities, clinical evaluation, laboratory tests, analgesic treatments, nerve conduction study, skin biopsy, genetics.

User-friendly input masks were designed to provide users with a guided and standardized data entry system. These masks were also designed as a tool for quick data visualization through the implementation of a patient search form.

Two different exporting modalities were integrated:

a. clinician-oriented report including all data for each patient suitable for storage in patients' clinical records.
b. researcher-oriented data export by means of customized queries for addressing sample description, patients' selection for further studies and statistical analysis.

Database was password-protected and stored in a network path accessible only to authorized users.

Study 2: 20 years of skin biopsy at Neurological Institute C. Besta

Study population

In this retrospective study, all patients who underwent skin biopsy for IENFD quantification at the Neurological Institute "C. Besta" from 1999 to 2019 were included. Clinical and skin biopsy information collected in Study 1 was used to investigate the diagnostic accuracy of IENFD for defining SFN patients.

Cut-off values comparison

Three different cut-off values have been used over time for diagnosis of SFN patients, based on the best reference normal values available for each period (Table 2):

- from 1999 to 2007 the normative reference value published by McArthur[192] was adopted, consisting of a single cut-off value (IENFD 6.8/mm) regardless the age and sex.
- from 2007 to 2009 the cut-off value was slightly modified according to results from a small group of healthy subjects (IENFD 7.6/mm)
- starting from 2010 the age- and sex-adjusted normative values provided by the IENFD worldwide normative reference study[62] for bright field microscopy were used.

Cut-off values expressed in IENFD/mm for each period

	1999 - 2007[192]	**2007-2009***	**2010 – in use**[62]	
Age (years)	Females and males	Females and males	Females	Males
20-29	6.8	7.6	8.4	6.1
30-39			7.1	5.2
40-49			5.7	4.4
50-59			4.3	3.5
60-69			3.2	2.9
70-79			2.2	2.1
>80			1.6	1.7

Table 2. Cut-off values of IENFD/mm adopted for each period. Starting from 2010, sex- and age-adjusted IENFD normative values have been used[62]. *Not published.

Data analysis

We conducted an analysis of the diagnostic accuracy of IENFD quantification at distal leg from 1999 to date, comparing the different normative values used over time. All skin biopsies performed from 1999 and 2009 were re-evaluated considering the last cut-off values, thus we compared the diagnostic accuracy of the different normative values by computing the number of patients who had a change in SFN diagnosis.

We compared the number of patients with normal or reduced IENFD according to gender using chi-squared test.

Study 3: Circadian variability of pain features in suspected SFN patients

Study population

We conducted a retrospective analysis of patients with suspected SFN evaluated at the Neuroalgology Unit of Neurological Institute "Carlo Besta" in Milano. Patients who completed neurological examination, questionnaires for pain features and intensity assessment and skin biopsy for IENFD quantification as described for Study 1 were included (see pag.52).

Patients were asked to report the mean intensity of pain experienced in the 2 weeks preceding the clinical evaluation in the morning, in the afternoon, in the evening and at night, respectively, as well as an average of whole day using the NRS. Patients that had a normal sleep scored "0" at night.

Statistical analysis

We divided patients into two groups according to normal or reduced IENFD at skin biopsy or gender. Between-group comparison of average PI-NRS was performed using Wilcoxon-Mann-Whitney or Wilcoxon rank sum test.

Multiple paired comparison among average PI-NRS at different moments of the day (morning, afternoon, evening and night) was performed using Friedman rank sum test with the alternative hypothesis that the distributions across repeated measures are different.

To find out which pairs (morning/afternoon, morning/evening, morning/night, afternoon/evening, afternoon/night, evening/night) of our groups were significantly different among each other, we performed a post-hoc analysis.

The significant p-value threshold was set to 0.05.

Statistical analysis was conducted using R software (version 3.6).

PAIN GENETICS STUDIES

The following studies have been performed in the context of the multicentre international study "*PROPANE – Probing the role of sodium channels in painful neuropathies*", funded by the European Union 7th Framework Programme (grant no. 602273) which included patients recruited by four sites: IRCCS Foundation Neurological Institute Carlo Besta, Milan, Italy; Maastricht University Medical Centre, Maastricht, the Netherlands; University of Manchester, Manchester, UK; Deutsche Diabetes Forschungsgesellschaft (DDFG), Heinrich Heine University, Düsseldorf, German.

Study population

Patients referred with the suspicion of small fiber neuropathy have been consecutively recruited. Screening process aimed to identify two cohorts based on etiology: patients with diabetic neuropathy and patients with idiopathic neuropathy. Each cohort was then further divided in two groups according to the presence or absence of pain.

The “Candidate-gene analysis of rare variants in VGSCs study” (study 4) was conducted using the entire dataset including all patients recruited by the four sites. Conversely, to conduct PRS analysis (study 5) we considered the cohort of diabetic patients only recruited by German and UK sites.

Definition of aetiology: idiopathic and diabetic neuropathy

Patients with diabetic neuropathy had to meet the diagnostic criteria for type 1 or type 2 diabetes and had to have a diagnosis of possible, probable or definite mixed or pure sensory small fiber neuropathy according to international diagnostic criteria (see Diabetic neuropathy) .

Subjects with idiopathic neuropathy had to meet the international diagnostic criteria for definite small fiber neuropathy (see *SFN Diagnostic criteria*).

All patients had to sign informed consent prior to enter the study.

Patients were excluded from the protocol in case of:

- absence of neuropathy or subclinical neuropathy
- presence of any other cause for neuropathy: hypothyroidism, renal failure, vitamin B12 deficiency, monoclonal gammopathy, autoimmune diseases, alcohol abuse

(more than 5 IU/day), malignancies, drugs causing neuropathy (e.g. chemotherapy, amiodarone, propafenone); diabetes (only for idiopathic cohort)

- presence of concomitant diseases (psychiatric or mental illness of physical condition) that might interfere with the ability of the patients to give free informed consent and to accurately report pain features.

Definition of phenotype: painful and painless neuropathy

Neuropathic pain has been diagnosed based on the accepted definition and grading system (see Neuropathic Pain Diagnosis and grading system). Information on pain duration, pain intensity of the mean value of the previous 24 hours rated on the pain intensity numerical rating scale (PI-NRS) were collected at screening visit.

Patients with neuropathic pain for more than 1 year and PI-NRS ≥ 4 despite analgesic or before starting treatment were defined as having "painful neuropathy (PN)", whereas those with PI-NRS ≤3 were defined as having "painless neuropathy (PLN)".

Patients evaluation

All patient had a neurological examination, electrophysiological study and skin biopsy (see methods section of "Study 1": *Demographics and medical history*, *Customized neurological examination*, *Neurophysiology*, *Skin Biopsy*).

In addition, patients had quantitative sensory testing (QST) where available. In particular, QST was performed to assess warm/cold and heat-pain thresholds using a TSA-2001 (Medoc, Ramat-Yishai, Israel) instrument, on the dorsum of the non-dominant foot, using ascending/descending (warm/cool) thermal ramp stimuli delivered through a thermode. Results were compared with reported normative values and measurements were considered abnormal when Z-values of method-of-level exceeded 2.5.

Next generation sequencing and bioinformatics analysis

For each patient 3 ml blood sample was collected after providing specific informed consent for genetic analyses. Blood samples from patients recruited in UK and Italy were processed and stored (in the Molecular Genetic Laboratory) at "C. Besta" Neurological Institute in Milan, whereas samples from patients recruited in Germany and in The Netherlands where processed in Maastricht. Genomic DNA was extracted from whole blood by a manual commercial kit, following the manufacturer instructions (Puregene Blood Kit, Qiagen®).

A set of 107 pain-related candidate genes (grouped in 5 different categories (Table 3), were sequenced by single molecule Molecular Probes (MIP)-Next Generation Sequencing, entirely designed at Maastricht University Medical Centre. The complete list of 107 genes included in the study is reported in Table 8.

Group	Category	Number of genes
Group 1	Sodium channels genes	10
Group 2	Ion channels	20
Group 3	Nav/Na-channel interacting partners	36
Group 4	Pain phenotype, receptor/channel interacting partners	25
Group 5	Co-expression with Nav channels	16

Table 3. **Sequenced pain-related candidate genes, divided into 5 different groups**

Data were analyzed using an in-house MIP-pipeline. A first quality control step was performed with FastQC (http://www.bioinformatics.babraham.ac.uk/projects/fastqc/) to identify base quality drops across cycles and adapter contamination, and to evaluate overall data quality. To ensure the best mapping performance, both adapter trimming and quality trimming were performed using Trimmomatic[193]. Then, high-quality reads were mapped to the hg19 reference genome using bwa (mem algorithm)[194]. Hence, we performed duplicated read marking, local realignment, and base quality score recalibration as suggested by Genome Analysis Toolkit (GATK) best practices[195]. We performed single-nucleotide variant (SNV) and INDEL calling using the GATK module Unified Genotyper.

Statistical Analyses

Continuous variables are presented as mean and standard deviation, categorical variables as numbers and percentages. Between-group comparison of continuous variables was performed using t-test or Mann-Whitney test. For categorical variables, the χ^2 test was used or the Fisher's exact test when necessary.

We performed different genetic analysis both on single or on aggregated variants. The following paragraphs report the methods explaining each study.

Study 4: Candidate-gene analysis of rare variants in VGSCs study

Variants selection

To identify the possible pathogenic variants in candidate VGSCs, all the data were filtered according to the following criteria:

1. Variants in VGSCs genes (*SCN3A, SCN7A, SCN8A, SCN9A, SCN10A, SCN11A, SCN1B, SCN2B, SCN3B, SCN4B*) among the 107 pain-related sequenced genes
2. Rare (Minor allele frequency (MAF) <0.01) and low frequency (MAF <0.05) variants based on SNP databases (dbSNP, GnomAD, Exome Aggregation Consortium, 1000 Genome Database)
3. Mutation type (non-synonymous: non-sense, missense, frameshift, splicing)
4. Intraexonic (±20bp) location
5. Interallelic variation >30% for heterozygous genotypes
6. High coverage (>20 reads for the genomic locus; >10 reads for the mutated allele)

These stringent criteria were adopted in order to exclude NGS artefacts, general and study population polymorphisms with a minor allele frequency (MAF) higher than 5% and low NGS coverage variants from analysis.

Pathogenicity classification

The resulting annotated variants were classified according to Wallis' criteria[196] for evaluation of pathogenicity based on the presence or absence on genome databases, familial co-segregation analysis, species conservation, eventual in silico prediction of pathogenic effect and functional studies.

Wallis' criteria identify 5 different classes:

1. Clearly not pathogenic
2. Unlikely to be pathogenic
3. Unknown significance or variant of uncertain clinical significance (VUS)
4. Likely to be pathogenic
5. Clearly pathogenic

We considered only variants classified as class 3, 4 and 5.

In addition, we further classified selected variants according to Waxman criteria[187], providing a more specific classification for sodium channel gene variants into 4 classes, based on predictive algorithms suggested pathogenicity, segregation and ion channel functional studies:

1. Pathogenic if one of these conditions is met:
    - Multigenerational segregation with the disease in a family spanning more than three generations, predictive algorithms unequivocally suggesting pathogenicity.
    - Multigenerational segregation with the disease in a family spanning more than three generations and the variant displays gain-of-function changes by voltage-clamp or current-clamp studies, or both.
    - Segregation with the disease in a nuclear, single-generation family, and predictive algorithms unequivocally suggesting pathogenicity, and the variant displays gain-of-function changes by voltage-clamp and current-clamp studies.
    - A patient with insensitivity to pain has a homozygous nonsense variant or substitutions that disrupt the consensus splice sites, or compound heterozygous mutations of nonsense or splicing-disrupting substitutions, with missense mutations shown as non-functional after voltage-clamp studies.
2. Probably pathogenic, if one of these conditions is met:
    - Segregation with the disease in a nuclear, single-generation family, predictive algorithms unequivocally suggesting pathogenicity.
    - Segregation with the disease in a nuclear, single-generation family and the variant displays gain-of-function changes by voltage-clamp or current clamp studies.
3. Possibly pathogenic, if one of these conditions is met:
    - Predictive algorithms unequivocally suggest pathogenicity, but segregation cannot be tested or is unclear (e.g. sporadic cases) and no functional studies are available.
    - Only one family member and the variant displays gain-of-function changes through voltage-clamp or current-clamp studies.
4. Variants with uncertain clinical significance (VUS) if:
    - Variants for which predictive algorithms suggest pathogenicity, that do not belong to any of the previous categories

Study 5: Pilot polygenic model for risk stratification on painful diabetic neuropathy

This study focused on risk assessment for painful form of diabetic neuropathy. In particular, we investigated painful and painless diabetic neuropathy patients from two different cohorts recruited within the "PROPANE" study from Germany and UK sites. We set German (GER) cohort as discovery (base) and UK cohort as validation (target).

To select the variants for the polygenic model analysis, all the data were filtered according to the following criteria:

1. Variants in all 107 candidate pain-related genes (Table 8)
2. Good coverage
3. Genotype call rate >0.8 (called in at least 80% of samples)
4. Hardy-Weinberg equilibrium P-value < 0.000048
5. No filter for location in the gene, considering both exonic and intronic variants
6. No filter for minor allele frequency, considering both rare and common variants

In the discovery cohort (GER sample), each quality controlled variant was tested for association with painful diabetic neuropathy (PDN) or painless diabetic neuropathy (PLDN) trait using a logistic regression adjusting for sex, age, ethnicity and diabetes type, using PLINK software[197]. Odds ratio (OR) and relative 95% confidence intervals were measured.

PRSice-2 software[198] was utilised to generate the polygenic risk score (PRS) for PDN cases and PLDN controls in validation dataset, using summary statistic data from the association analysis in discovery. Effect sizes from discovery cohort were used as the base dataset to generate the best PRS model which was then applied to the validation target dataset.

In particular, a PRS was calculated for each individual based on the weighted sum of the number of carried risk alleles multiplied by the trait-specific weights (log OR).

The best PRS model was derived from testing the inclusion of all SNPs from a range of p value thresholds in the base dataset (0.001, 0.05, 0.1, 0.2, 0.3, 0.4, 0.5, 1), to see which threshold gave the largest Nagelkerke's R2 value to select the best-fit PRS.

The effect of significant non-genetic predictors was included with PRS in logistic regression analysis to enable incorporation into the predictive model.

The significance of differences in mean PRS between the PDN and PLDN was tested in the validation sample using one-way ANOVA.

Predictive ability of the PRS for identifying PDN was calculated using Area Under Curve (AUC) in StataSE software. AUC was calculated to identify predictive ability, values range from 0 to 100%, where 0% is random classification and 100% is perfect classification.

RESULTS

CLINICAL PHENOTYPING

Study 1: Deep clinical phenotyping of patients with suspected SFN and relational database design

Clinical phenotyping of suspected SFN patients

From 2017 we evaluated 346 patients who were referred for suspected SFN or neuropathic pain, of which 258 patients had also blood sample for genetic analysis after giving informed consent. Further 239 patients referred before 2017 also had clinical information about pain features, among these, 107 had also blood sample for genetic analysis.

Among a total number of 585 patients, diagnosis of SFN was confirmed in 362 (61.8%) patients of which 164 (45%) men and 198 (55%) women. Mean age of patients was 53.1 ± 16.2.

No significant correlation was identified between IENFD reduction and NRS score (spearman's rho 0.07, p=0.1747) (Figure 6).

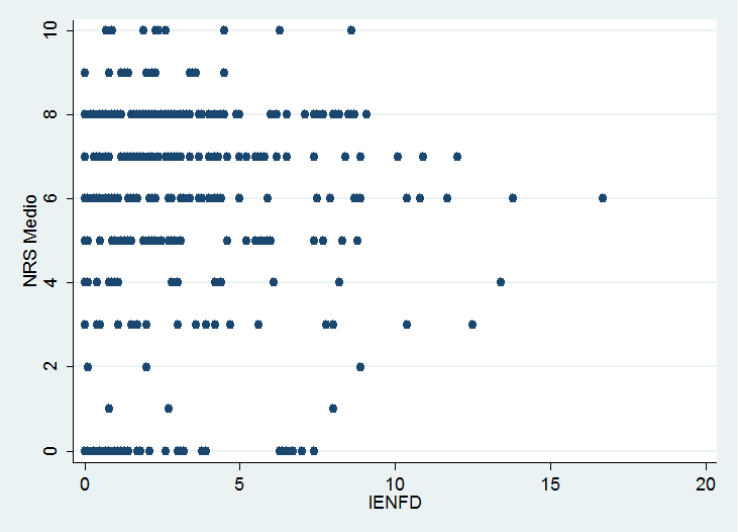

Figure 6. Correlation analysis between IENFD and NRS in patients with confirmed diagnosis of SFN showing no significant correlation (spearman's rho 0.07, p=0.1747).

The DN4 screening tool score was available for 270 patients. It demonstrated a sensitivity of 84% and specificity of 19% in identifying patients with a definite neuropathic pain confirmed by reduced IENFD at skin biopsy.

Information about onset were collected for 134 patients. Symptoms at the onset included pain for 89 (66%) patients, whereas 45 (34%) patients had only sensitive non-painful complaints as initial symptoms with no differences between those having a normal or reduced IENFD at skin biopsy. Among patients who were painless at the onset, 28 (62%) developed pain.

According to the phenotype classification based on symptoms and sings presence and distribution, we identified 66 (48%) with classic SFN (*patients having a length-dependent distribution of pain or sensory positive symptoms*), 17 (12%) with diffuse SFN (*patients having diffuse distribution of pain or sensory symptoms but still including features of length-dependent distribution*), 38 (28%) with atypical SFN (*patients having a non-length-dependent or patchy or focal distribution of pain or sensory symptoms not including extremities*), 16 (12%) not having SFN symptoms (Figure 7). No significant association was found between IENFD reduction and each clinical phenotype, therefore epidermal denervation seems to be an independent factor and symptoms distribution does not provide clues for predicting the presence of neuropathy. This is consistent with the results of a recent systematic review reporting IENFD reduction in 45% of patients with fibromyalgia[31] who would belong to the "atypical" phenotype.

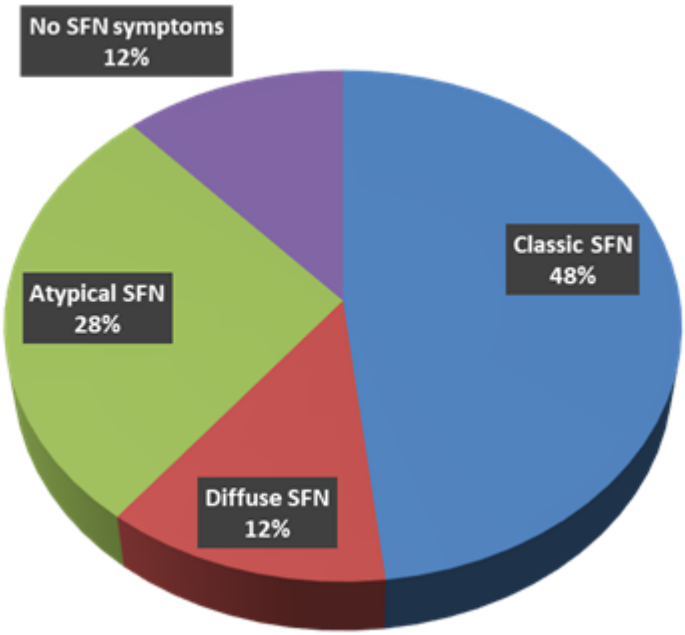

Figure 7. Clinical phenotypes according to presence and distribution of symptoms. Definitions are reported in the text.

Among evaluated patients, 270 had data about comorbidities. Figure 8 shows the frequency of different etiologies in our cohort of SFN patients. Immunological conditions represented the most frequent associated condition being present in 44 (16%) patients. Other associated conditions include diabetes in 25 (9%) patients, hypothyroidism in 18 (7%), pre-diabetes in 11 (4%), Celiac disease in 8 (3%), familial amyloidosis in 8 (3%), vitamin B12 deficiency in 5 (2%) and hepatitis C in 4 (1%). In 147 (54%) no underlying conditions were identified therefore these patients were considered idiopathic. With particular reference to the most frequent conditions, these results are in line with those reported in a recent study investigating a large cohort of 921 SFN patients[199] in which immunological conditions were the most frequent acquired comorbidity (19%), followed by diabetes and pre-diabetes (7.7% and 9.7% respectively), whereas in more than half of patients (53%) underlying cause ramained unseen.

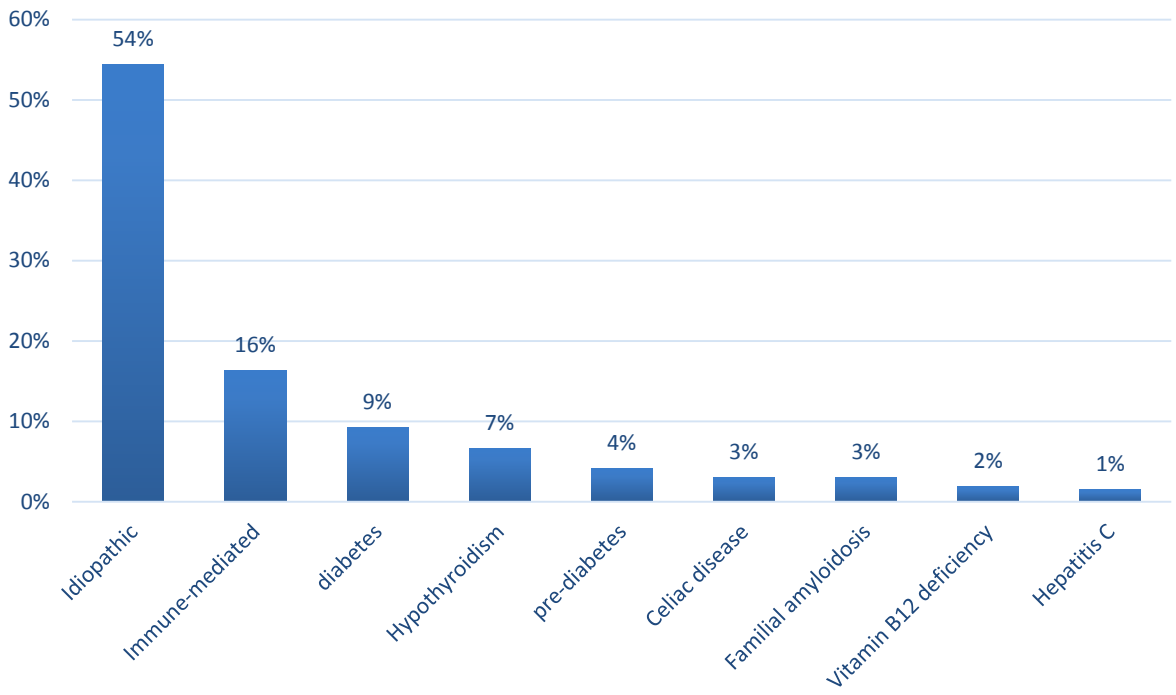

Figure 8. Frequency of different aetiology in our cohort of patients di SFN.

Relational database

A customized relational database was designed and developed to systematically and accurately collect, store and integrate clinical information including symptoms onset and progression, neuropathic pain features and distribution, sensory symptoms and sign, familiarity, comorbidities and response to analgesics, nerve conduction study and neuropathological skin biopsy data.

This database represents a crucial preliminary result necessary for further analysis. It was designed and developed at the beginning of the study for being implemented in clinical practice and allowing a systematic data collection from patient consecutively evaluated. In addition, available clinical and skin biopsy information from clinical records of patients evaluated before the introduction of database have been also collected and stored.

The database included logical sessions encompassing demographics, medical history, comorbidities, clinical evaluation, laboratory tests, analgesic treatments, nerve conduction study, skin biopsy, genetics organized in twelve tables connected by a unique identification number for each patient (ID patients). Figure 9 shows relations among different tables.

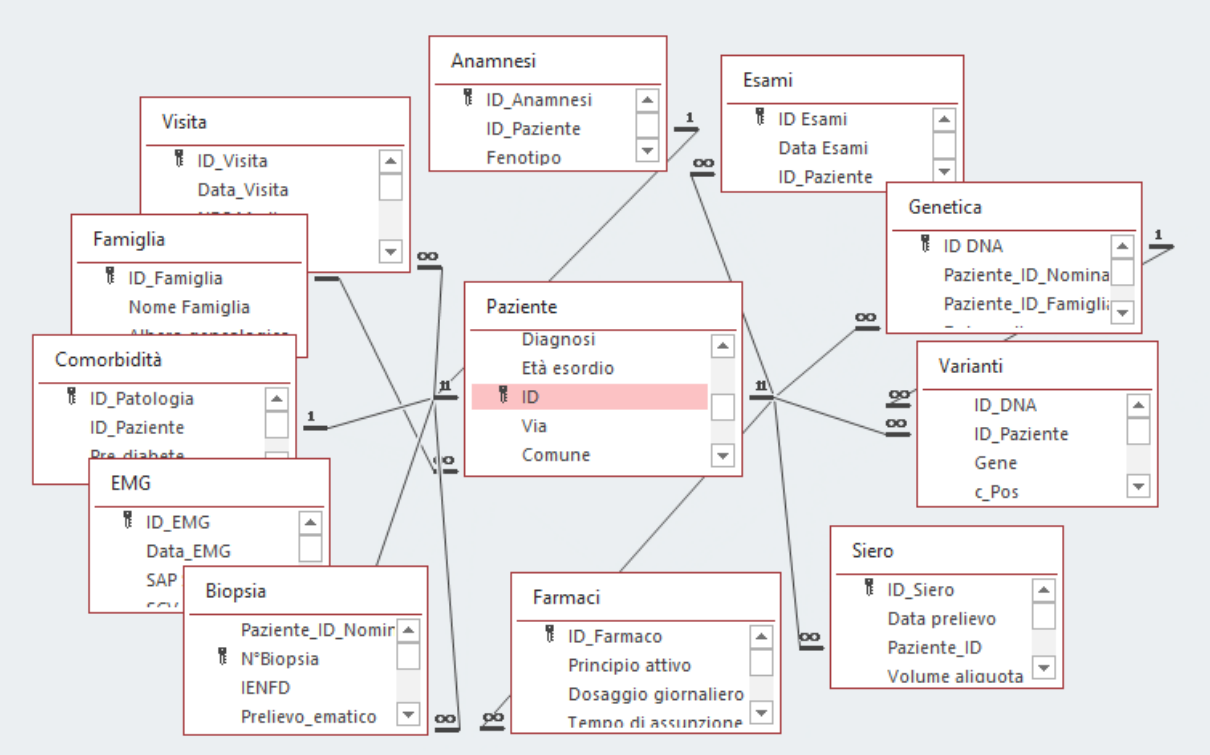

Figure 9. Database relations among different logical sections

Eleven user-friendly input masks were designed, for standardized data entry and quick data visualization and sharing among clinicians and researchers. The masks encompass all the assessments included in patients' evaluation. The upper part contains a toolbar with a search box. Toolbar includes also labels for selecting and open each mask. The images below report a sample with details included in each mask.

Sample images of the different masks composing the database

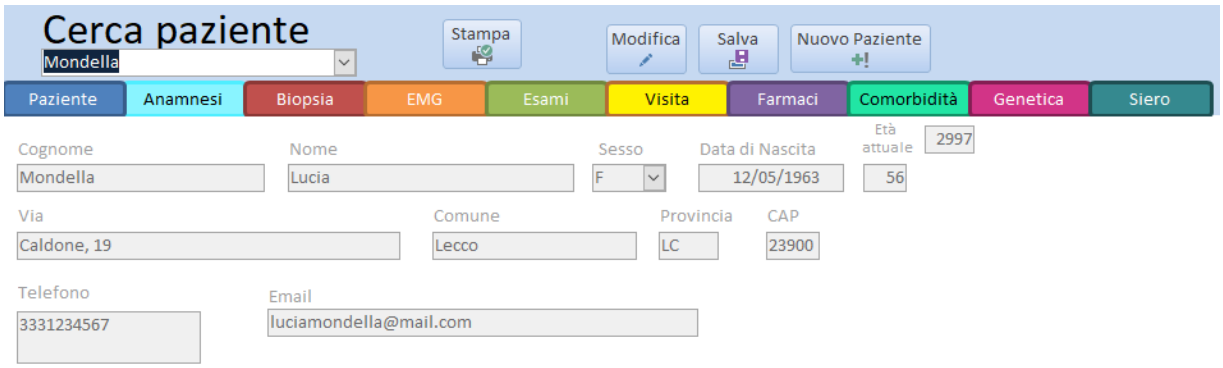

Figure 10. The mask "paziente" includes personal data. Information included in the forms does not belong to a real patient and all data are fictional for illustrative purposes only.

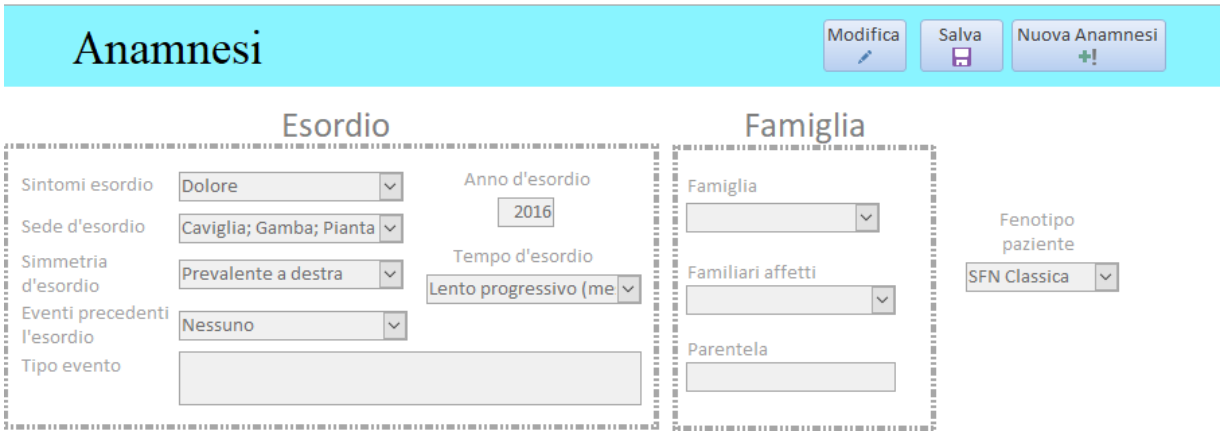

Figure 11. The mask "Anamnesi" collects information about symptoms onset, clinical phenotype and familiarity

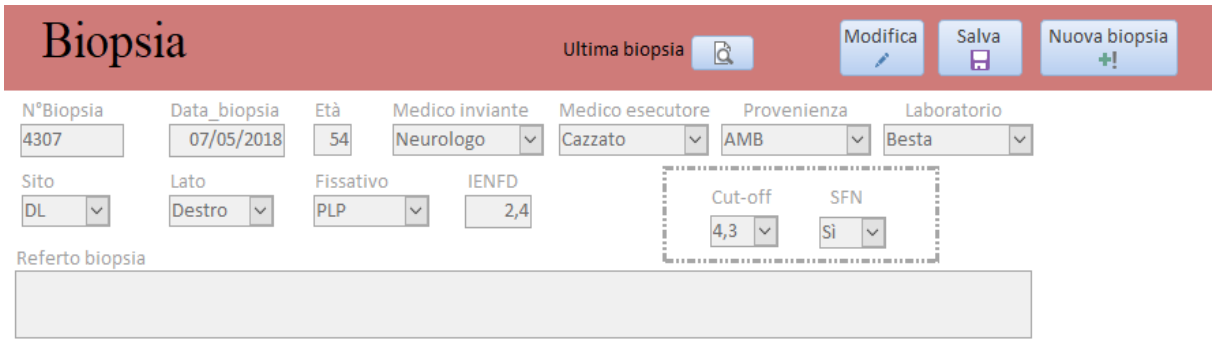

Figure 12. The mask "Biopsia" includes information about skin biopsy collection and results, reporting the IENFD cut-off value specific for the specific patient according to gender and age at the biopsy.

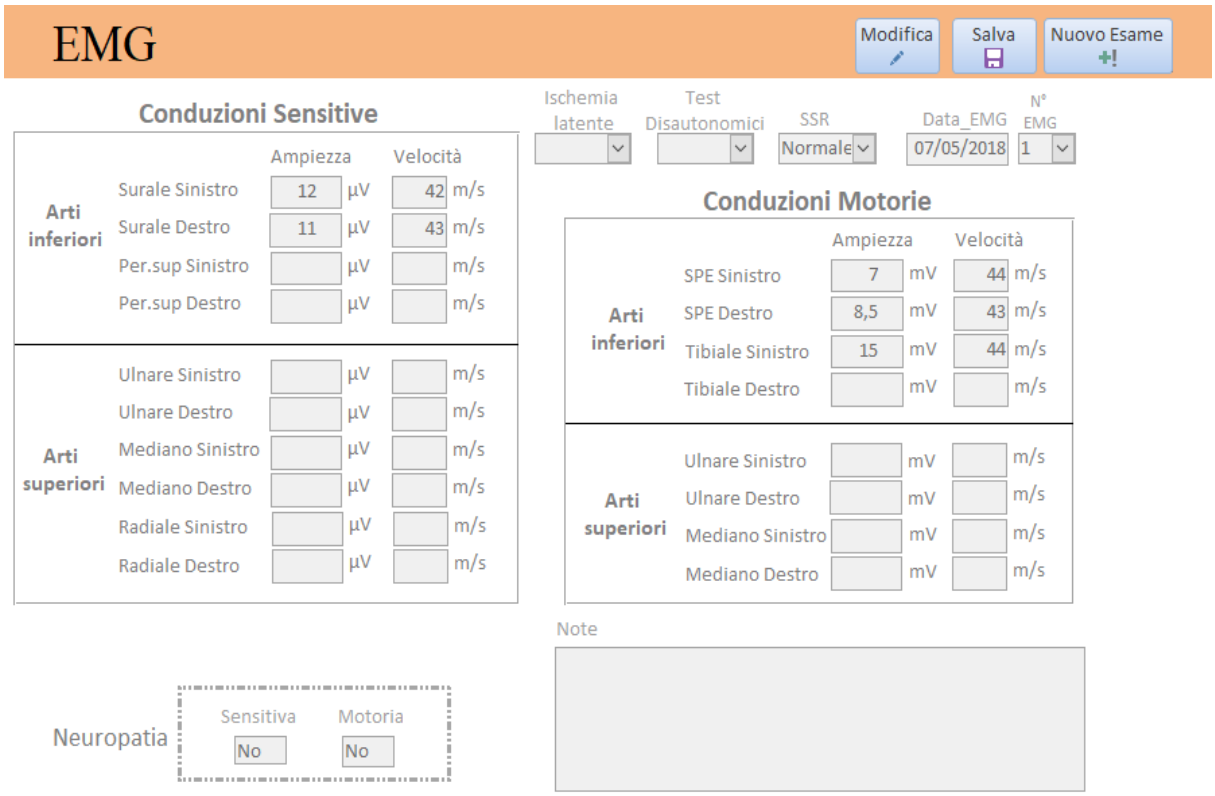

Figure 13. The mask "EMG" reports data about sensory and motor nerve conductions. Where available results of autonomic nervous system testing such as sympathetic skin response can be reported.

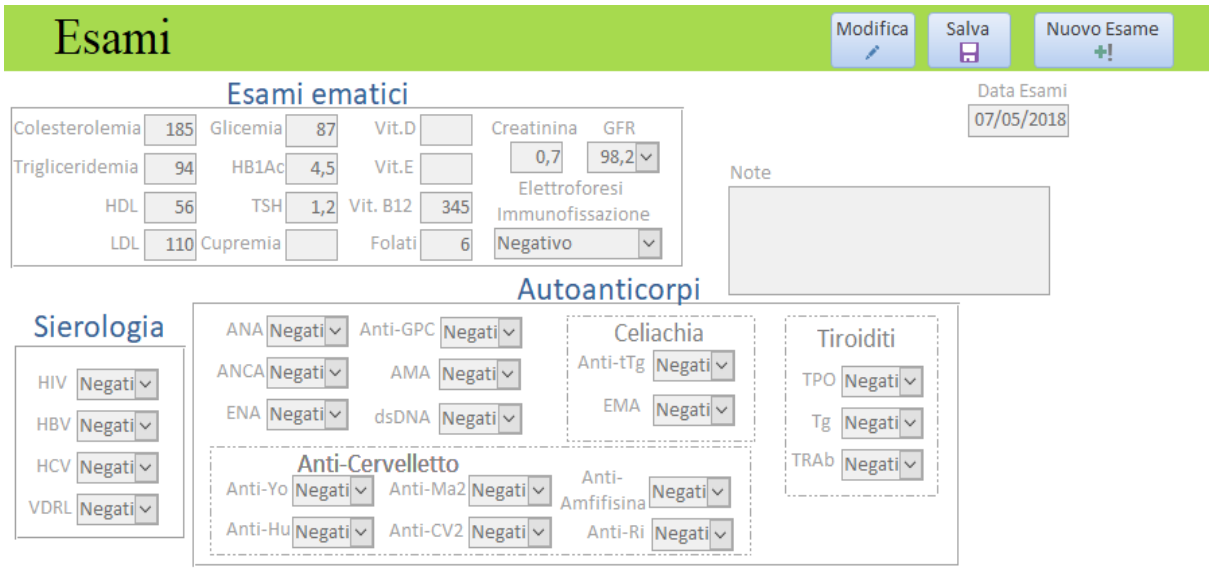

Figure 14. This mask named "Esami" allows to collect results of biochemical tests, serology and immunology.

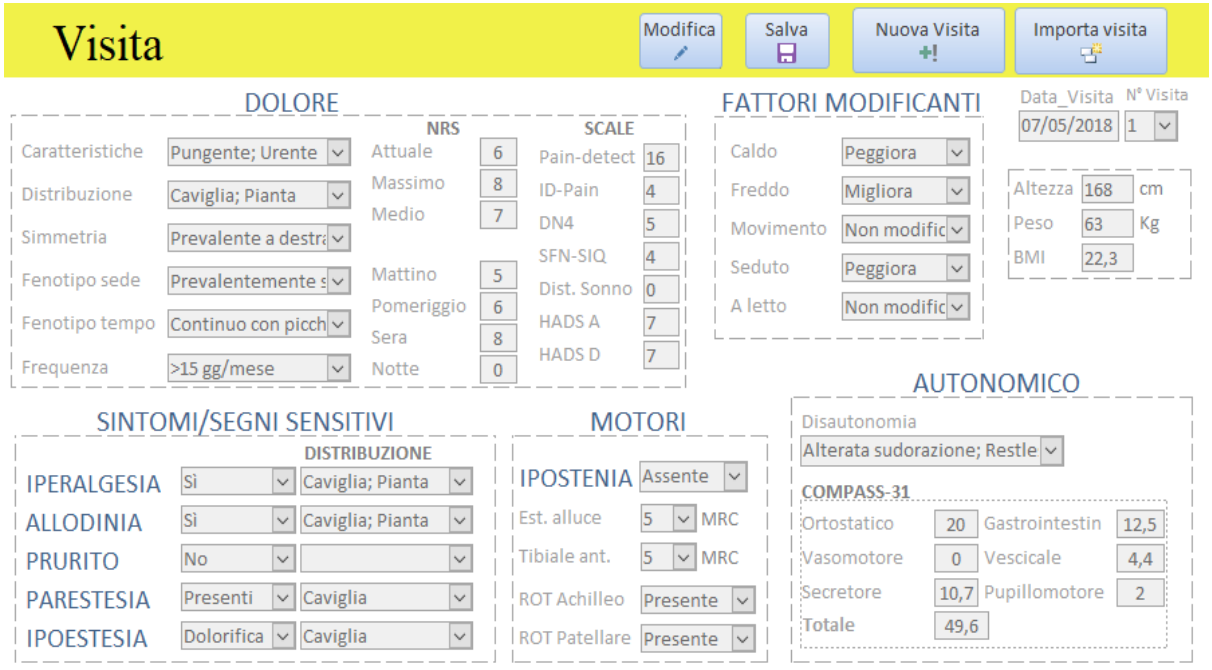

Figure 15. The tab "Visita" encompasses all the clinical information about pain features, modifying factors, symptoms and signs and the scores of selected scales and questionnaires.

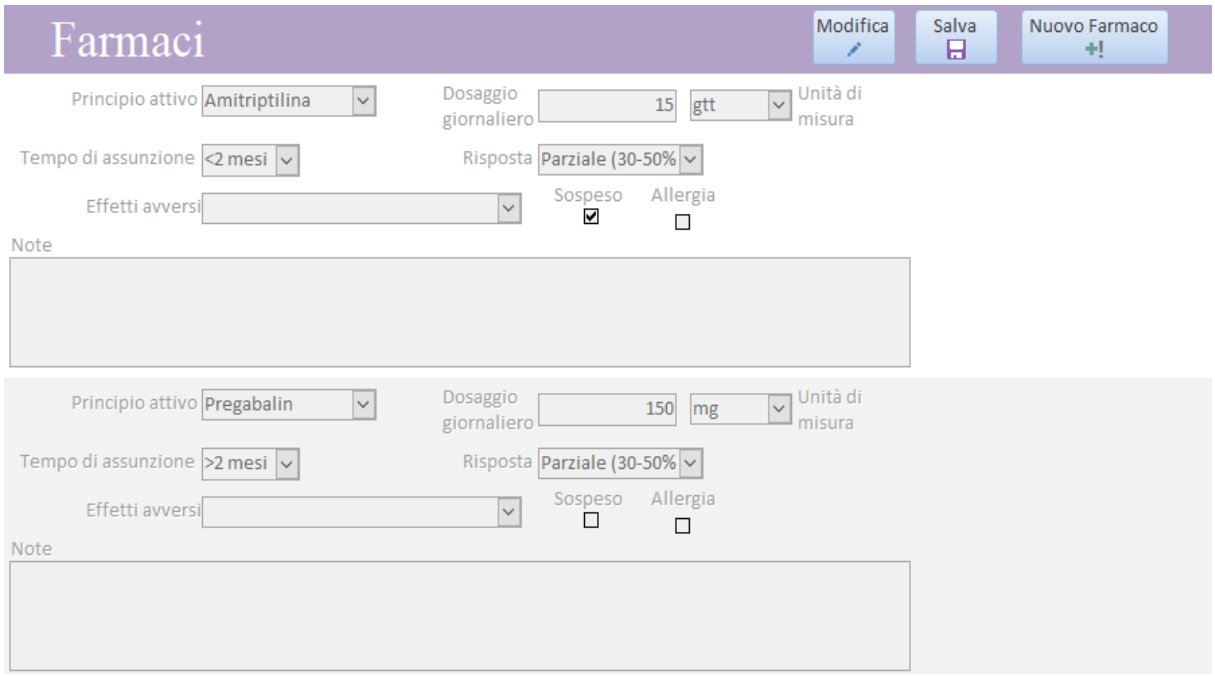

Figure 16. This form named "Farmaci" collects information about analgesics, reporting time taking, dosage, efficacy and eventual discontinuation or side effects for each analgesic drug used by the patient.

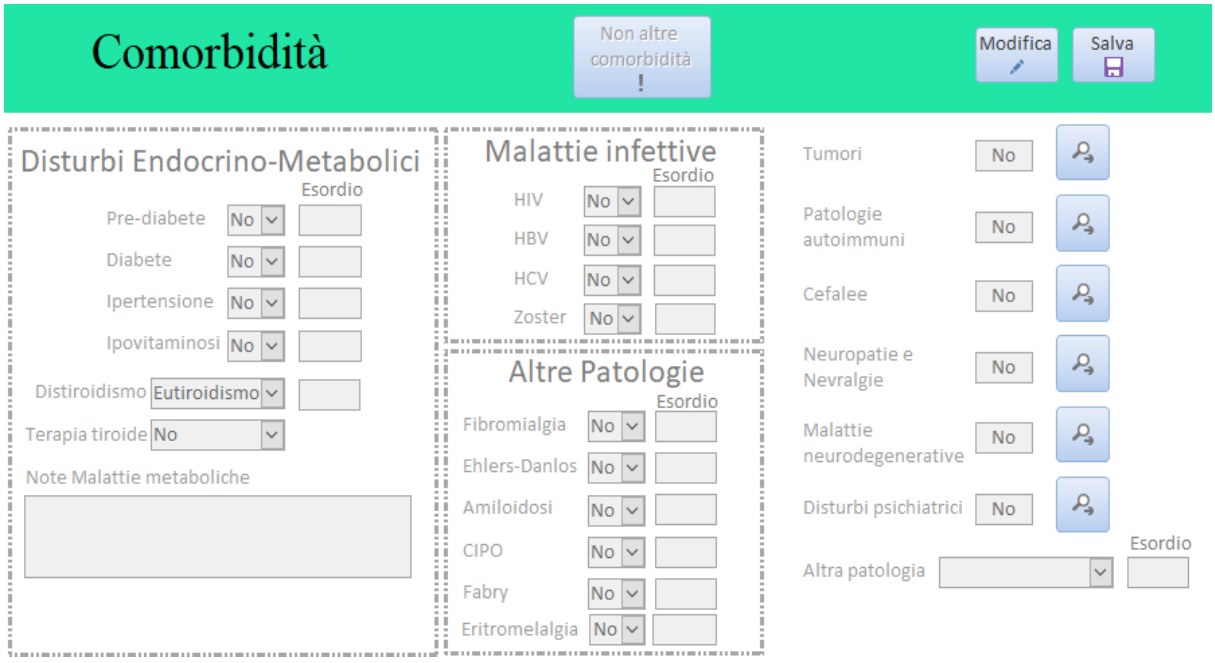

Figure 17. The tab "Comorbidità" shows comorbidities reported in patient's medical history. It includes a predefined set of associated conditions, however other not listed potentially interesting comorbidities can be added.

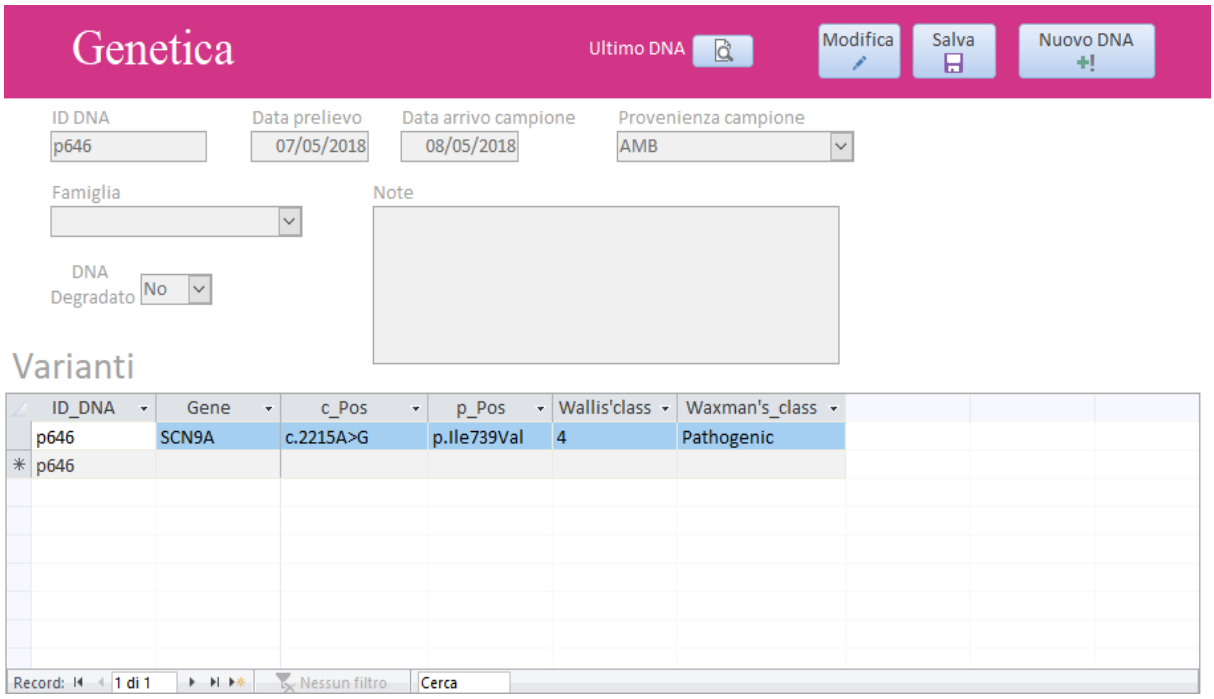

Figure 18. The mask "Genetica" includes genotyping data and the list of identified variants.

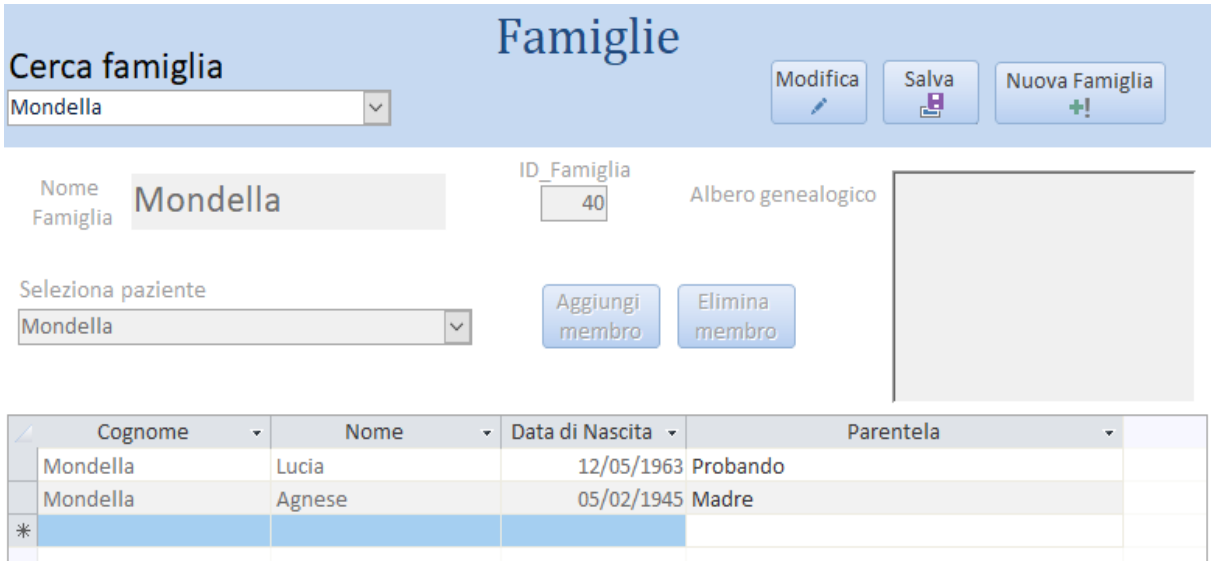

Figure 19. This mask "Famiglie" contains information about pedigree of familial cases reporting a list of relatives to quickly access information about each family member.

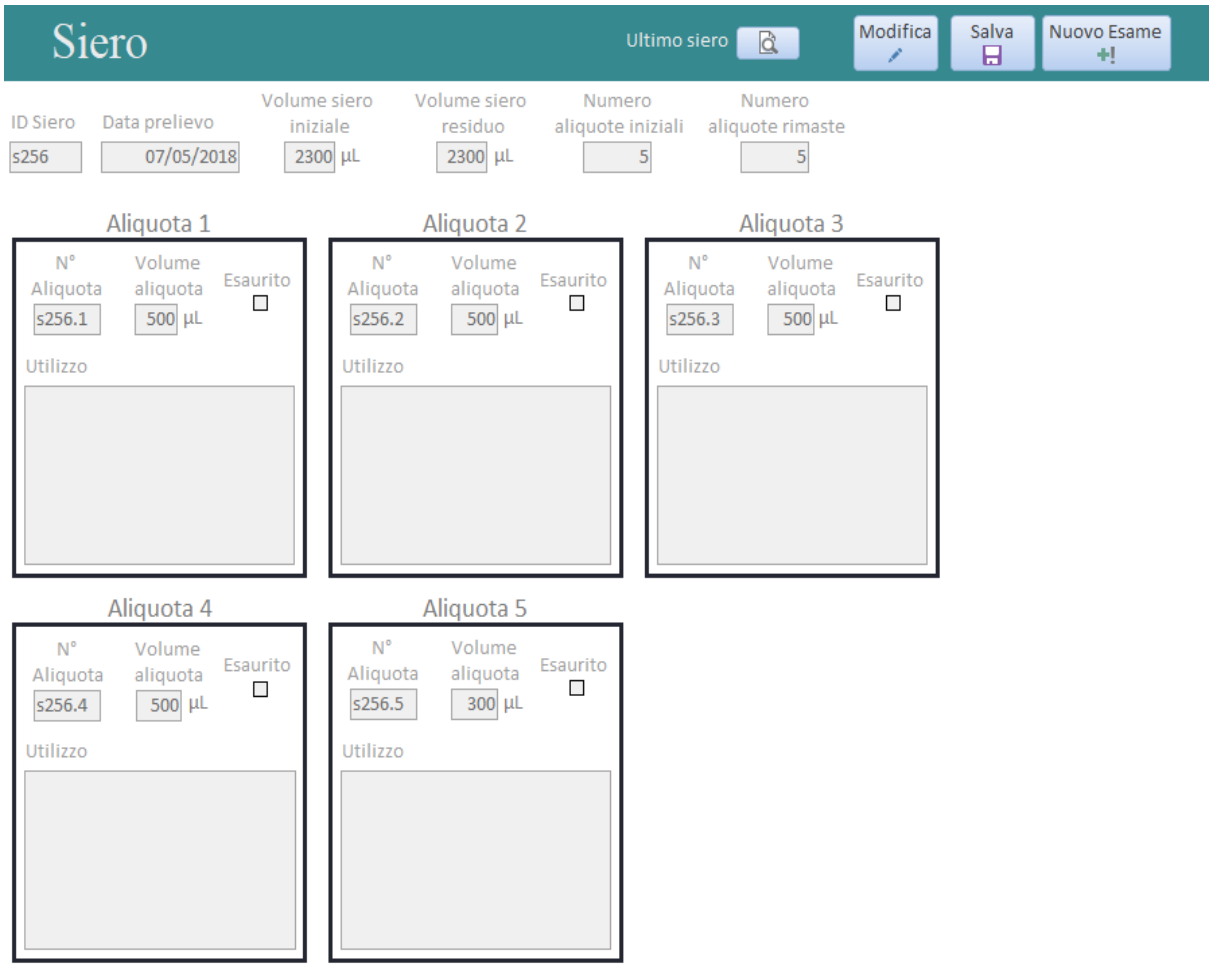

Figure 20. This form named "Siero" report data about serum sample collection and storage for patients who had blood samples for DNA and/or serum bank after giving informed consent.

Example of clinician-oriented database report

FONDAZIONE I.R.C.C.S. ISTITUTO NEUROLOGICO CARLO BESTA

13/11/2019

Cognome	Mondella				
Nome	Lucia				
Data di Nascita	12/05/1963	Età	56	Sesso	F
Via	Caldone, 19				
Comune	Lecco				
CAP	23900	Provincia	LC		
Telefono	3331234567				
Email	luciamondella@mail.com				

Biopsia

N°Biopsia	Fissativo	Data biopsia
4307	PLP	07/05/2018

Sito	Lato	Medico inviante
DL	Destro	Neurologo

Anamnesi		DNA		Siero	
Fenotipo paziente	SFN Classica	p646	07/05/2018	s256	07/05/2018
Famiglia	2997				

Visita — Data Visita 07/05/2018

DOLORE

Altezza 168 cm BMI 22,3

Peso 63 Kg

Caratteristiche Dolore	Pungente; Urente
Distribuzione Dolore	Caviglia; Pianta
Simmetria	Prevalente a destra
Frequenza	>15 gg/mese
Fenotipo sede	Prevalentemente superficiale
Fenotipo tempo	Continuo con picchi di dolore

Fattori modificanti	
Caldo	Peggiora
Freddo	Migliora
Movimento	Non modifica
Seduto	Peggiora
A letto	Non modifica

Scale	
Pain-detect	16
ID-Pain	4
DN4	5
SFN-SIQ	4
Dist. Sonno	0
HADS A	7
HADS D	7

NRS	
Attuale	6
Massimo	8
Medio	7
Mattino	5
Pomeriggio	6
Sera	8
Notte	0

ALLODINIA	Sì	Caviglia; Pianta
IPERALGESIA	Sì	Caviglia; Pianta
PRURITO	No	
PARESTESIA	Presenti	Caviglia
IPOESTESIA	Dolorifica	Caviglia

IPOSTENIA: Assente — Est. alluce 5 — Tibiale ant. 5

RIFLESSI: Achilleo Presente — Patellare Presente

DISAUTONOMIA: Alterata sudorazione; Restless leg; Xeroftalmia; Xerostomia

COMPASS-31 49,6

Note

Pagina 1

Figure 21. Example of report including all data collected and suitable for storage in patients' clinical records. Information included in this report do not belong to a real patient and all data are fictional for illustrative purposes only.

FONDAZIONE I.R.C.C.S. ISTITUTO NEUROLOGICO CARLO BESTA

13/11/2019

Elettroneurografia

Data EMG 07/05/2018

Conduzioni Sensitive

		Ampiezza		Velocità	
Arti inferiori	Surale Sinistro	12	µV	42	m/s
	Surale Destro	11	µV	43	m/s
	Per.sup Sinistro		µV		m/s
	Per.sup Destro		µV		m/s
Arti superiori	Ulnare Sinistro		µV		m/s
	Ulnare Destro		µV		m/s
	Mediano Sinistro		µV		m/s
	Mediano Destro		µV		m/s
	Radiale Sinistro		µV		m/s
	Radiale Destro		µV		m/s

Ischemia latente

Test Disautonomici

SSR: Normale

Conduzioni Motorie

		Ampiezza		Velocità	
Arti inferiori	SPE Sinistro	7	mV	44	m/s
	SPE Destro	8,5	mV	43	m/s
	Tibiale Sinistro	15	mV	44	m/s
	Tibiale Destro		mV		m/s
Arti superiori	Ulnare Sinistro		mV		m/s
	Ulnare Destro		mV		m/s
	Mediano Sinistro		mV		m/s
	Mediano Destro		mV		m/s

Note

Comorbidità

Disturbi psichiatrici	No
Tumori	No
Patologie autoimmuni	No
Cefalee	No
Neuropatie e Nevralgie	No
Malattie neurodegenerative	No

Esordio

Disturbi Endocrino-Metabolici	Pre-diabete	No
	Diabete	No
	Ipertensione	No
	Ipovitaminosi	No
	Distiroidismo	Eutiroidismo

Malattie infettive	HIV	No
	HBV	No
	HCV	No
	Zoster	No

13/11/2019

Altra patologia

Note

Altre Patologie		
	Fibromialgia	No
	Ehlers-Danlos	No
	Amiloidosi	No
	CIPO	No
	Fabry	No
	Eritromelalgia	No

Farmaci

Farmaco	Dosaggio	Assunzione	Risposta	Effetti avversi	Sosp.	Aller.	Note
Amitriptilina	15 gtt	<2 mesi	Parziale (3		☑	☐	
Pregabalin	150 mg	>2 mesi	Parziale (3		☐	☐	

Study 2: 20 years of skin biopsy at Neurological Institute C. Besta

From 1999 to 2019, 2132 skin biopsies were collected at distal site from 1849 patients referred with suspected SFN at Neurological Institute "C. Besta" in Milan.

We evaluated 398 skin biopsies between 1998 and 2007 using the 1st cut-off, 133 skin biopsies between 2007 and 2009 using the 2nd cut-off value and 1600 specimens from 2010 up to 2019 using the latest age-and-sex-adjusted reference values. Globally, 439 patients had skin biopsy before 2010 and 1356 from 2010 to 2019, of which 1010 were women (55%) and 839 men (45%) with a mean age of 54 (±15).

The overall number of patients with abnormal IENFD after recalculating according to the current cut-off was 890 (48%), whereas 959 (52%) patients had normal IENFD. A similar rate of normal/abnormal IENFD was observed also when considering men (49% normal and 51% abnormal IENFD) and women (53% normal and 47% abnormal) with no significant difference between groups (Figure 22).

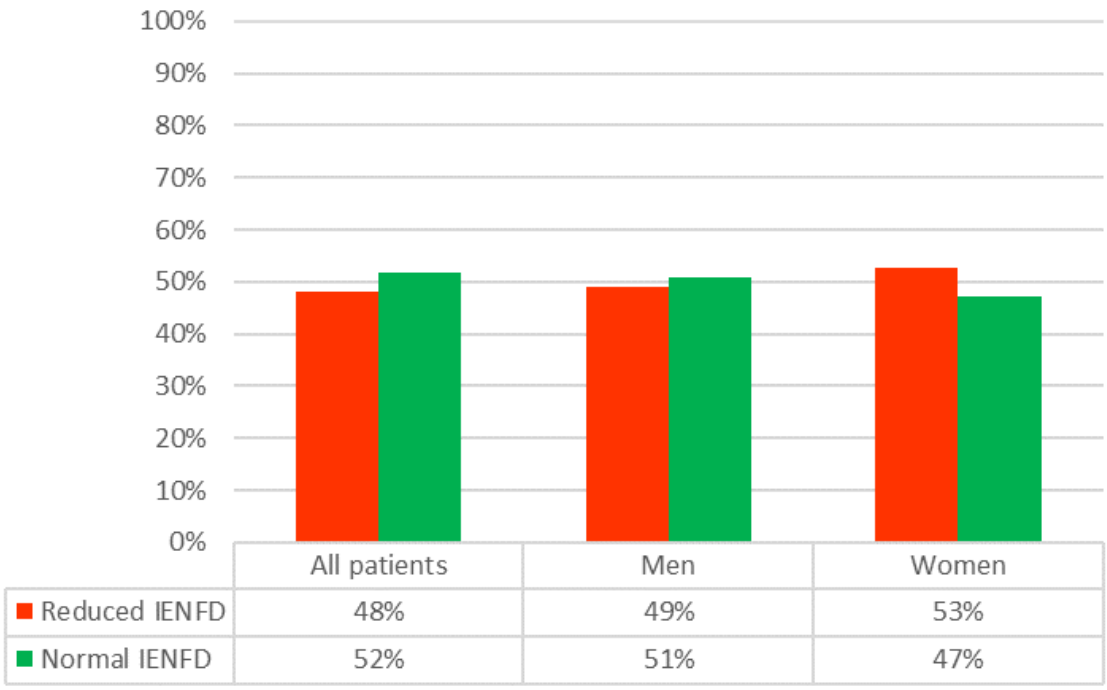

	All patients	Men	Women
Reduced IENFD	48%	49%	53%
Normal IENFD	52%	51%	47%

Figure 22. **Rate of patients having a normal or reduced IENFD** considering the entire cohort of skin biopsy analysed from 1999 to 2019 and having all results recalculated according to the current cut-off[62].

After re-evaluating IENFD of biopsies from 1999 to 2009 in light of the available reference values, 128 out of 219 patients (58%) changed from reduced to normal IENFD, indicating they had been wrongly diagnosed as having a pathological loss of IENF using the previous cut-off values (false positive). Only 1 patient among the 274 patients with normal IENFD according to the previous cut-off values changed to a reduced IENFD (false negative) (Figure 23 and Figure 24).

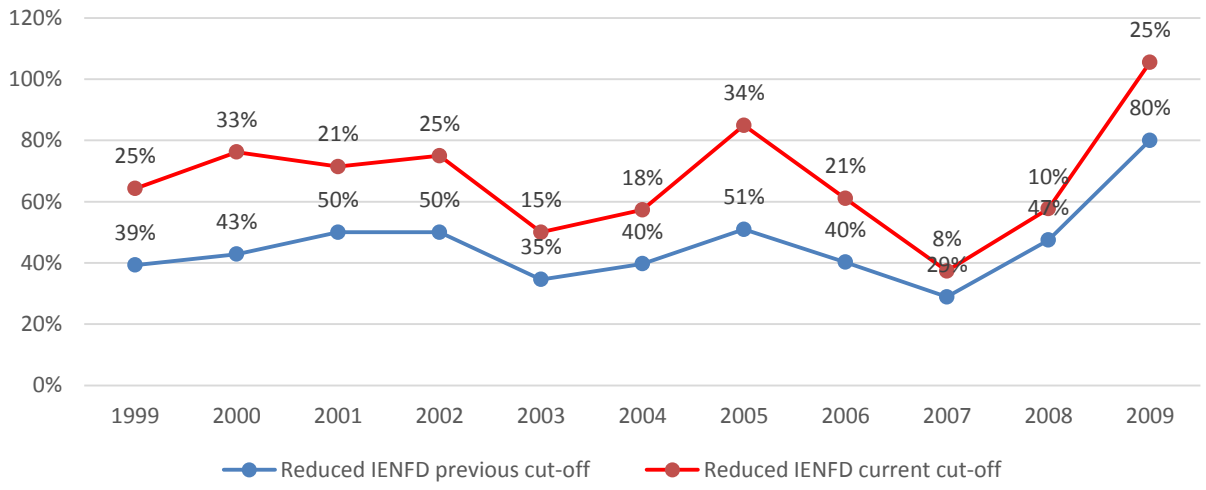

Figure 23. **Comparison of different IENFD reference values used over time**. Blue line shows the rate of patients from 1999 to 2009 having a reduced IENFD at skin biopsy according to the original cut-off value in use at the time; red line shows the rate of reduced IENFD after recalculating using the 2010 sex- and age- adjusted normative values currently adopted.

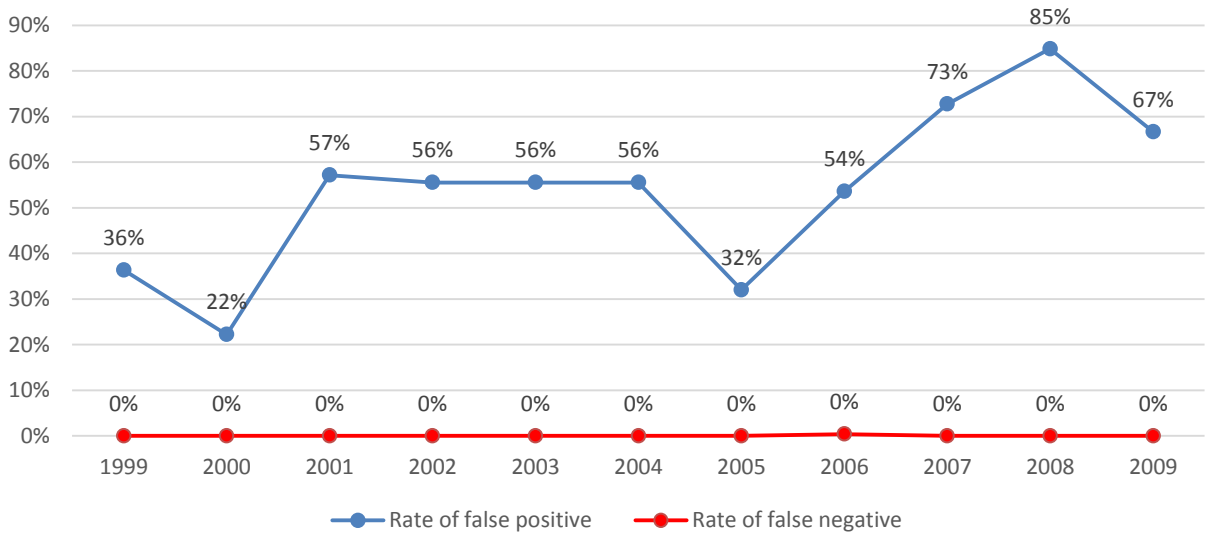

Figure 24. **Rate of false positive and false negative skin biopsy results.** Blue line shows the rate of patients who were wrongly addressed as having a reduced IENFD using the previous cut-off values (false positive). Only one patient (a woman in 2006) having normal IENFD with previous cut-off values changed to reduced IENFD (false negative).

Study 3: Circadian variability of pain features in suspected SFN patients

We included 253 patients with suspected SFN. We confirmed the diagnosis of SFN in 171 patients having an IENFD below 5th centile of sex- and age-matched normative value at distal leg skin biopsy.

Comparing average PI-NRS reported for whole day in subgroups of patients we found that women experienced significantly more pain than men (average NRS: 4.98 men; 5.94 women; p<0,01). On the contrary, PI-NRS comparison between subjects with reduced or normal IENFD revealed no significant difference (average NRS 5.5 for subjects with reduced IENFD; NRS 5.9 for those having a normal IENFD; p<0,13), confirming that reduction of IENF does not correlate with pain intensity (Figure 25).

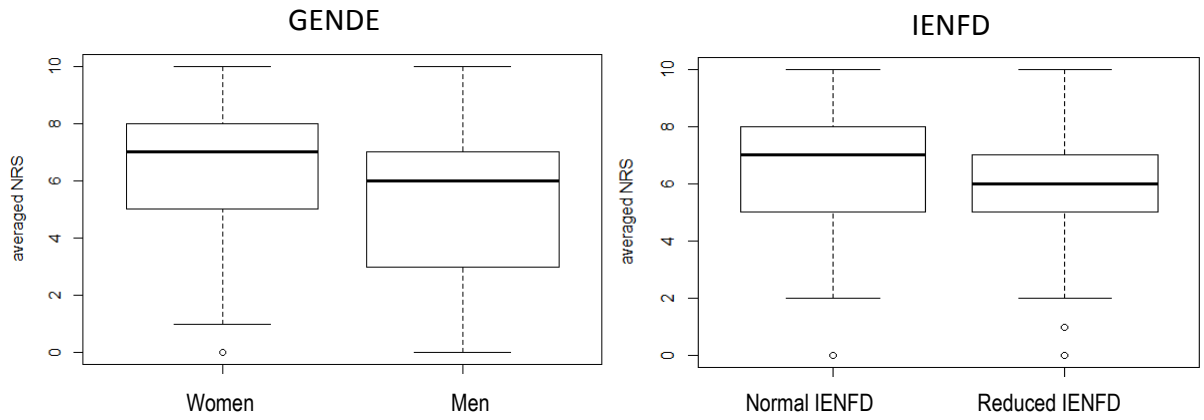

Figure 25. Comparison of the average whole day NRS according to gender and IENFD. Wilcoxon-Mann-Whitney test showed a significant difference between women and men (p<0,01) (left box), whereas comparison between subjects with normal or reduced IENFD showed no significant difference (p=0.13) (right box).

The analysis of circadian PI-NRS pattern in the 171 SFN patients revealed mean PI-NRS values of 5.12 in the morning, 5.36 in the afternoon, 5.99 in the evening and 3.84 at night. Post-hoc analysis showed that PI-NRS has a slight but significant rising trend from the morning or afternoon to the evening, whereas at night PI-NRS significantly declines since in 54 (31%) of 171 patients the intensity of pain was not such as to prevent sleep, therefore scored “0” (Figure 26).

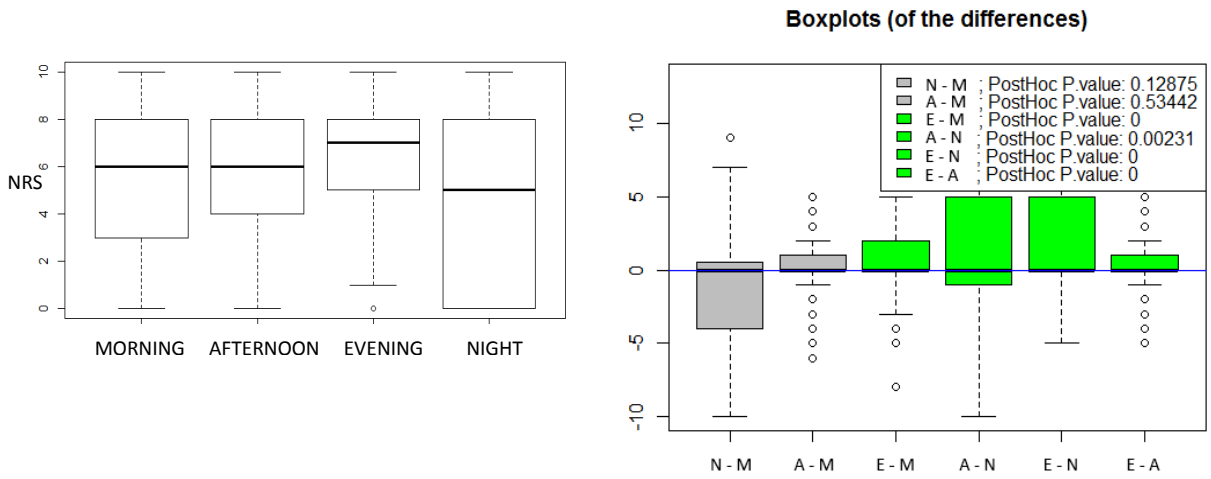

Figure 26. **Comparison of NRS among periods of the day for paired samples.** Friedman test and post hoc analysis showed a significant difference of NRS scores between morning/evening, afternoon/evening, afternoon/night and evening/night.

Figure 27 shows the rate of patients reporting an increase or reduction of PI-NRS during the day. Considering PI-NRS change from the morning to the afternoon (blue bars), 33% of patients had an increased PI-NRS, whereas 15% showed a PI-NRS reduction. When moving from morning to the evening (red bars), NRS increased in 42% and reduced in 14% of patients. A high discrepancy in NRS change was also observed from afternoon the evening (green bars) with 39% of patients reporting an increase and 8% a reduction of PI-NRS.

A similar trend was observed when considering a PI-NRS change of more than 2 points. In particular, patients having a PI-NRS increase outnumber those having an PI-NRS reduction four to one when moving from the morning to the evening (red bars) and five to one when moving from afternoon to evening (green bars).

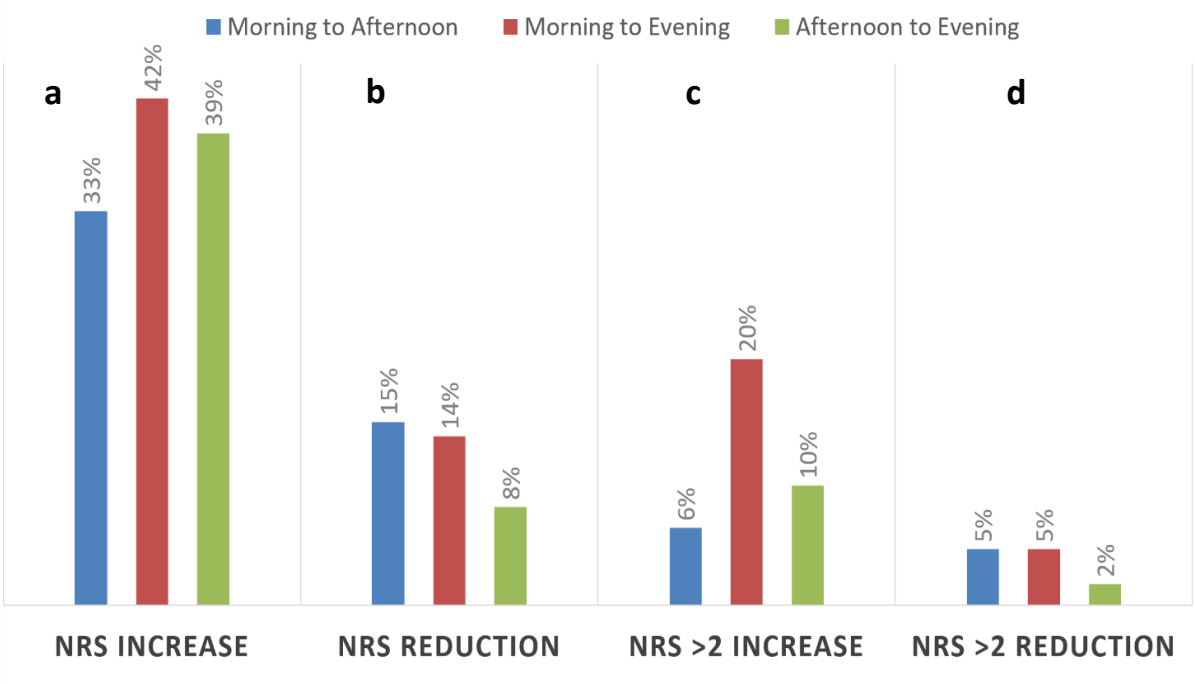

Figure 27. Rate of patients showing a PI-NRS increase (a) or reduction (b) between different moments of the day. Fig c and d show rate of patients having a PI-NRS variation higher than 2 points.

PAIN GENETICS STUDIES

Patients recruitment

The study included 1,015 patients: 513 fulfilling the criteria for diabetic neuropathy and 502 meeting the criteria for idiopathic small fiber neuropathy or predominantly sensory neuropathy. Over the 513 diabetic patients, 332 were recruited from the Heinrich Heine University in Düsseldorf, Germany, and 181 from the University of Manchester in Manchester, UK. Of the 502 patients with idiopathic neuropathy, 402 were recruited from Maastricht University Medical Centre in Maastricht, Netherlands, and 100 from Neurological Institute Carlo Besta in Milan.

According to the presence or absence of pain, within the idiopathic cohort 482 patients were defined as having a painful neuropathy and 20 as having a painless neuropathy; within the diabetic cohort 213 were defined as having painful diabetic neuropathy and 300 as having painless diabetic neuropathy (Figure 28).

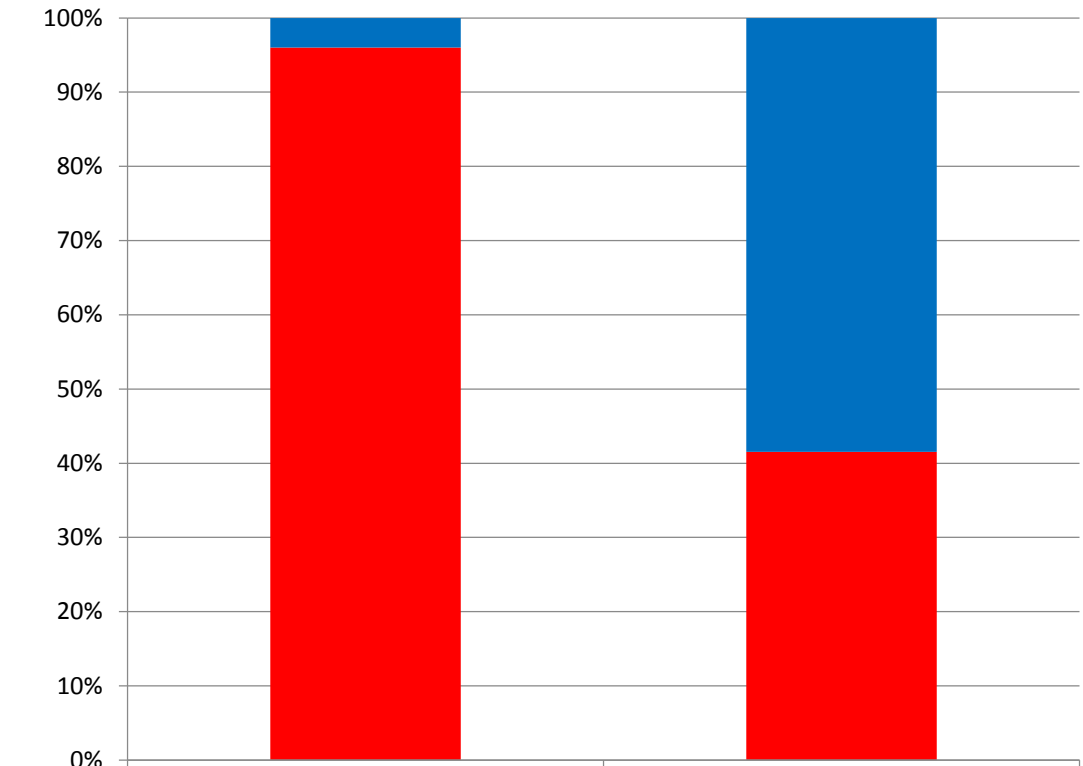

	Idiopathics	Diabetics
Painless	20	300
Painful	482	213

Figure 28 Distribution of the 1015 included patients according to aetiology and pain phenotype.

Study 4: Candidate-gene analysis of rare variants in VGSCs study

In this study, we investigated the incidence of potential rare pathogenic variants in VGSCs genes considering the entire dataset including all idiopathic and diabetic patients recruited by the four sites. We described and compared the frequency of non-synonymous variants and their topological distribution in VGSC domains, according to the aetiology and presence or absence of pain. Eventually, pathogenicity classification for each variant is reported.

Idiopathic Small Fiber Neuropathy

The genetic analysis of 502 patients with idiopathic SFN, identified 74 genetic variants distributed among 68 patients (13.5%), of which 4 patients carrying more than one variant (2 patients had 2 variants and 2 patients had 3 variants). Of these, 53 variants were found in only one patient, 3 in 2 patients, 4 in 3 or more patients, for a total number of 60 different unique variants.

In particular, painful SFN patients carried 72 exclusive variants and painless SFN carried 2 VUS variants (in SCN3A and SCN4B).

Among the total number of variants exclusively found in patients with painful idiopathic SFN, 63 variants were in VGSC α-subunits (4 in *SCN3A*; 3 in *SCN8A*, 23 in *SCN9A*, 16 in *SCN10A*, 17 in *SCN11A*), 3 in VGSC β-subunits (2 in *SCN2B*, 2 in *SCN3B*) and 6 in *SCN7A* (Figure 29).

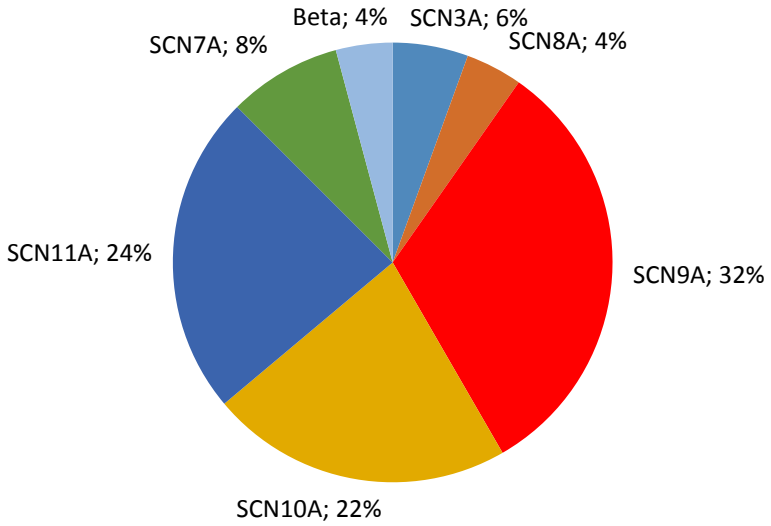

Figure 29. Genetic variants' frequencies in painful idiopathic neuropathy according to their distribution in VGSCs genes.

In α-subunits, we described the topological distribution of variants in different VGSC domains. In particular 22 (30.6%) were located in the linker domains, 13 (18.1%) in the small loops between transmembrane segment, 12 (16.7%) in the transmembrane segments themselves, 6 (8.3%) in the voltage-sensor segment (S4), 1 (1.4%) in the pore-forming regions, 1 (1.4%) in the N-terminus and 5 (6.9%) in the C-terminus (Figure 30). Additionally, 7 (9.7%) variants involved β-subunits genes whereas 5 (6%) were splicing variants.

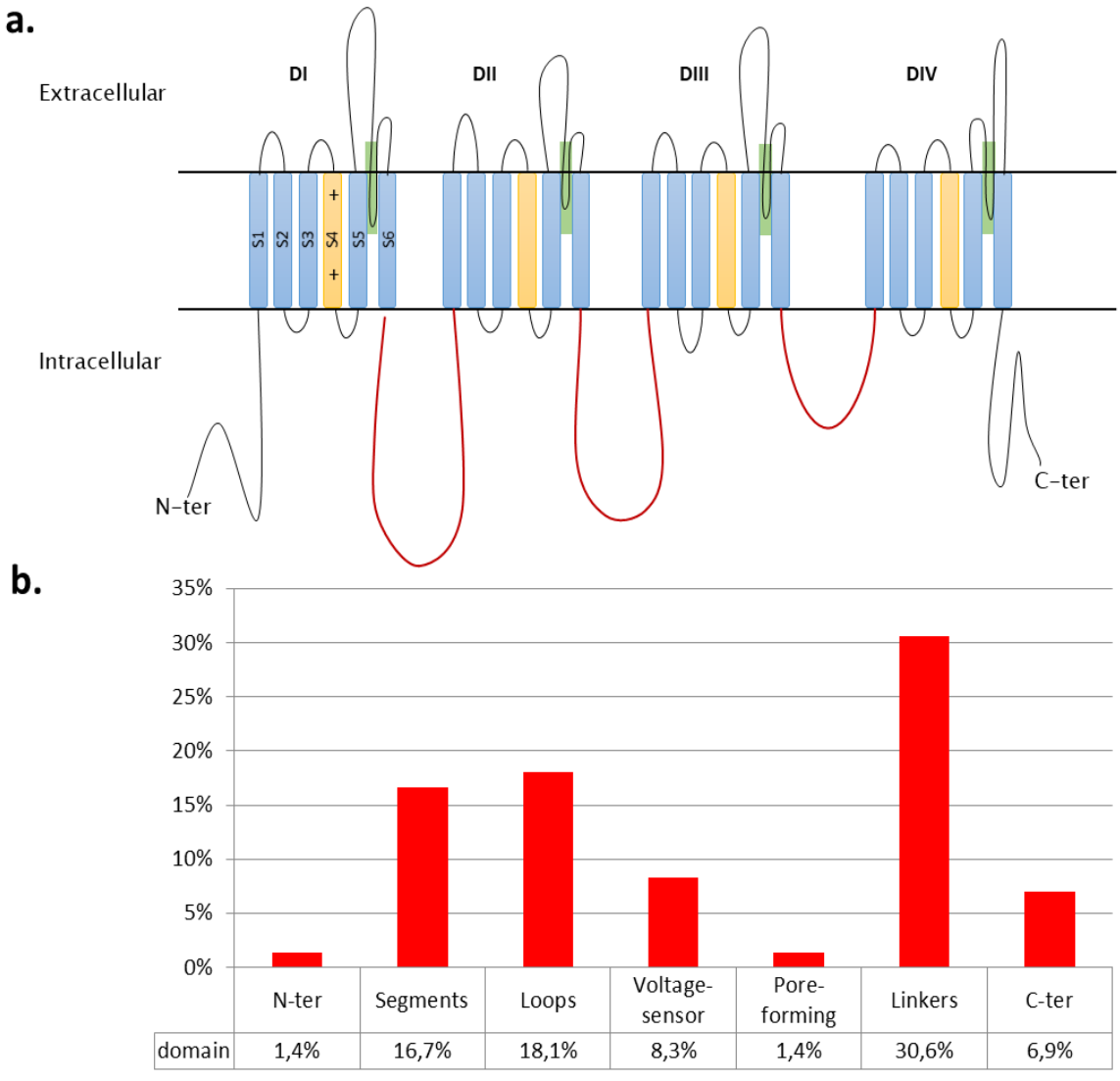

Figure 30. **Topological distribution of VGSCs variants in painful idiopathic SFN cohort**. a) Schematic representation of VGSCs showing the 24 trans-membrane segments contained within four regions (DI-IV). Within each region, there are six segments (S1-S6). The fourth segments, S4, within each region acts as the voltage sensor (yellow), whereas S5 and S6 come together to form the channel pore (green). N-ter, Amino-terminal region; Loop, extra-cellular and intra-cellular regions connecting adjacent segments; C-ter, Carboxyl-terminal region. b) Bar plot of mutation rate among topological regions of VGSCs.

According to Wallis' criteria, 54 (75%) variants (43 unique) were class 3 and 18 (25%) variants (15 unique) were class 4, whereas no variants were classified as class 5. Differently, according to Waxman's criteria, 55 (50%) variants (45 unique) were VUS, 15 (22.2%) variants (9 unique) were pathogenic and 4 unique (5.6%) possibly pathogenic. **Errore. L'origine riferimento non è stata trovata.** reports the list of pathogenic variants according to Waxman's classification, associated to painful idiopathic SFN.

Diabetic Neuropathy

Among the 513 patients with diabetic neuropathy, 75 genetic variants were selected in 68 patients (13.3%), of which 7 patients carrying 2 rare variants. Of these, 57 distinct variants were found in only one patient, 6 in 2 patients, 2 in 3 patients, for a total number of 65 unique variants identified. Three variants, Pro991Leu (*SCN10A*), Val940Ala (*SCN9A*) and Arg1460Gln (*SCN10A*), have been shared by painful and painless samples.

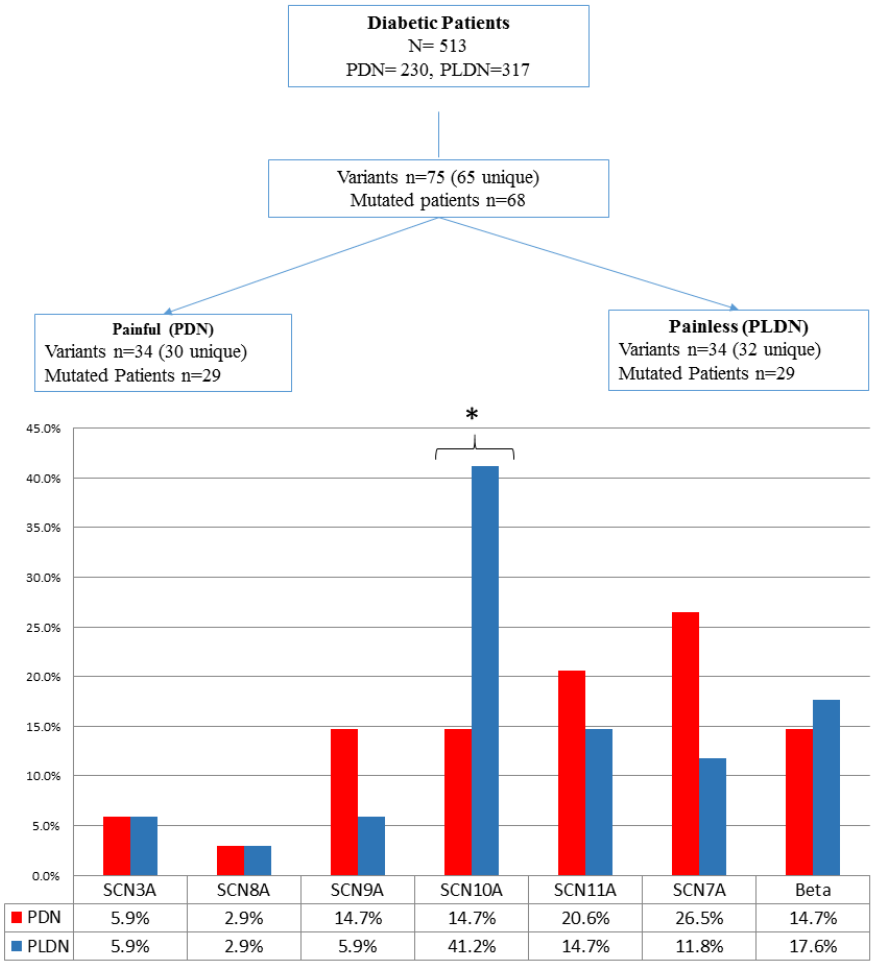

Figure 31. **Flowchart for genetic analysis of Diabetic neuropathic patients.** The Flowchart shows the distribution of potential pathogenic VGSCs variants according to phenotypes (painful/painless). **Bar plot of mutation rate among VGSCs genes according to pain phenotype**. PDN, Painful Diabetic Neuropathy; PLDN, Painless Diabetic Neuropathy. *<0.05, p-value from Fisher exact test

Among the 34 variants exclusively found in patients with **painful diabetic neuropathy** and not in painless group**,** 20 variants were located in VGSC α-subunits (2 in *SCN3A*; 1 in *SCN8A*, 5 in *SCN9A*, 5 in *SCN10A*, 7 in *SCN11A*), 5 for VGSC β-subunits (1 in *SCN1B*, 2 in *SCN2B*, 1 in *SCN3B*, 1 in *SCN4B*) and 9 in *SCN7A*. Conversely, among the 34 variants exclusively found in patients with **painless diabetic neuropathy** and not in the painful group**,** 24 variants were located in VGSC α-subunits (2 in *SCN3A*; 1 in *SCN8A*, 2 in *SCN9A*, 14 in *SCN10A*, 5 in *SCN11A*), 6 for VGSC β-subunits (1 in *SCN1B*, 3 in *SCN2B*, 2 in *SCN3B*) and 4 in *SCN7A*. Comparing PDN versus PLDN in relation to the distribution of the mutations in VGSCs genes, we observed a slight prevalence of SCN9A and SCN7A mutations in PDN mutated patients whereas we observed a significant predominance of *SCN10A* mutations in PLDN mutated patients (p=0.029) (Figure 31).

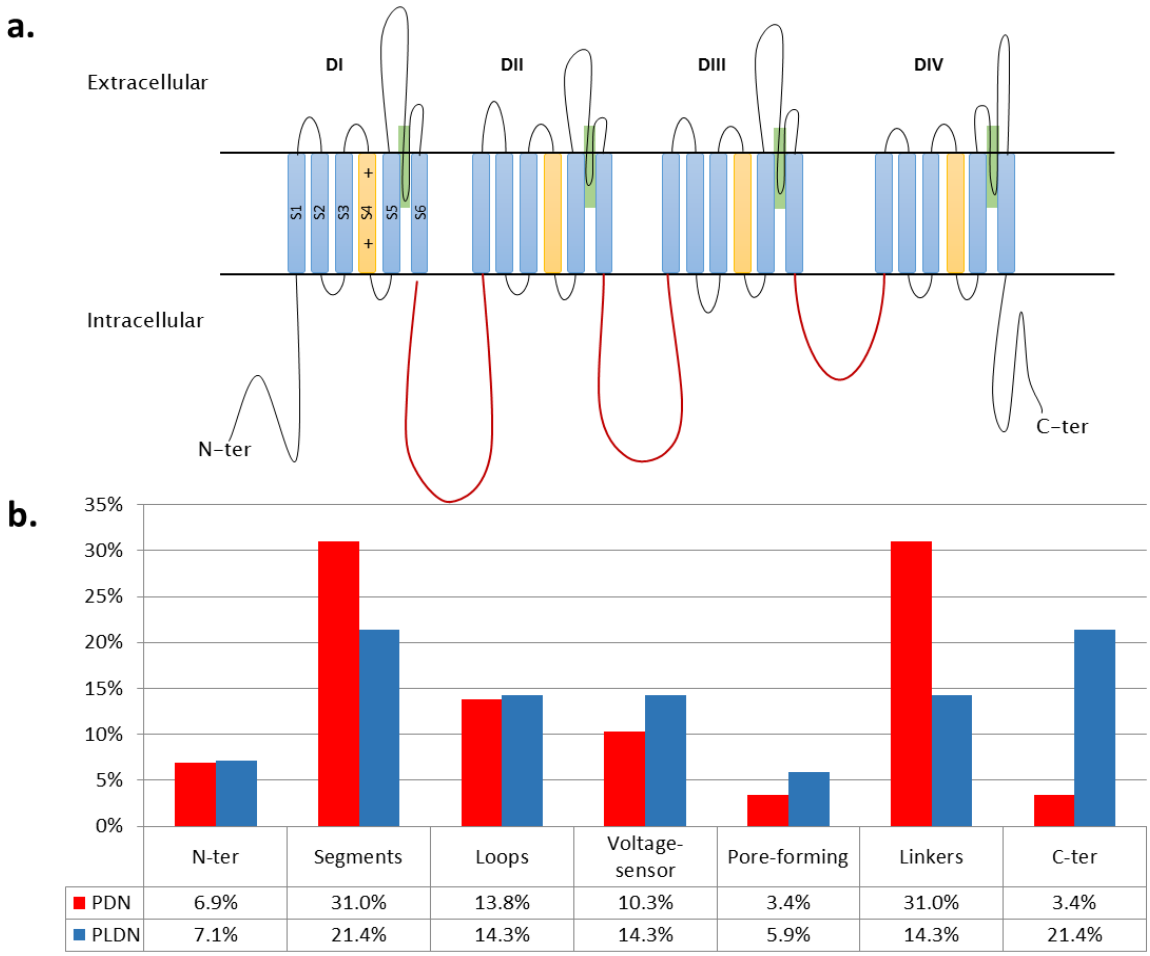

	N-ter	Segments	Loops	Voltage-sensor	Pore-forming	Linkers	C-ter
PDN	6.9%	31.0%	13.8%	10.3%	3.4%	31.0%	3.4%
PLDN	7.1%	21.4%	14.3%	14.3%	5.9%	14.3%	21.4%

Figure 32. **Topological distribution of VGSCs variants according to pain phenotype in diabetic cohort.** a) Schematic representation of VGSCs showing the 24 trans-membrane segments contained within four domains (DI-IV). Each trans membrane domain contains six segments (S1-S6). The fourth segments, S4, within each region acts as the voltage sensor (yellow), whereas S5 and S6 come together to form the channel pore (green). N-ter, Amino-terminal region; Loop, extra-cellular and intra-cellular regions connecting adjacent segments; C-ter, Carboxyl-terminal region. b) Bar plot of mutation rate among topological regions of VGSCs according to pain phenotype. PDN, Painful Diabetic Neuropathy; PLDN, Painless Diabetic Neuropathy.

In α-subunits, we described the topological distribution of variants in different VGSC domains comparing painful and painless diabetic neuropathy patients. in particular, in **painful diabetic neuropathy** 9 (32.4%) variants were located in the domain linkers, 2 (5.4%) in the small loops between transmembrane segment, 11 (29.7%) in the transmembrane segments themselves, 3 (8.11%) in the voltage-sensor segment, 1 (2.7%) in in the pore-forming regions, 2 (5.4%) in the N-terminus and 1 (2.7%) in the C-terminus (Figure 32). Additionally, 5 (13.5%) variants involved β-subunits genes whereas no splicing variants were found. Conversely, in α-subunits, the variants exclusively found in patients with **painless diabetic neuropathy**, these mutations were located on regions coding for different structure of the Nav channel Protein, in particular 4 (11.76%) were located in the domain linkers, 3 (8.8%) in the small loops between transmembrane segment, 7 (20.6%) in the transmembrane segments, 4 (11.76%) in the voltage-sensor segment, 2 (5.88%) in in the pore-forming regions, 2 (5.88%) in the N-terminus and 6 (17.65%) in the C-terminus (Figure 32). Additionally, 6 (17.65%) variants involved β-subunits genes and no splicing variants were found. Considering the protein localization, PDN mostly carried variants located in the linker DII-DIII whereas PLDN in the C-terminal, although no statistical significance has been observed (Figure 32).

According to Wallis' criteria, considering the variants exclusively found in patients with **painful diabetic neuropathy,** 28 (82.3%) variants (26 unique) were class 3 and 6 (17.7%) variants (4 unique) were class 4, whereas no variants were classified as class 5. Differently, according to Waxman's criteria, 27 (79.4%) variants (26 unique) were VUS, 5 (14.7%) variants (2 unique) were pathogenic, 2 (5.9%) possibly pathogenic.

Two variants (*W1538R and L1158P*) in painful SFN were classified as pathogenic according to Waxman's classification[187]. In particular, *W1538R (SCN9A),* carried by 2 PDN patients, proved to induce gain-of-function of nociceptors at cell electrophysiology assay[162].

*L1158P (SCN11A),*carried by 3 PDN patients, conferred gain-of-function attributes to the channel, depolarized resting membrane potential of dorsal root ganglion neurons, enhanced spontaneous firing, and increased evoked firing of these neurons [42].

On the other hand, considering the variants exclusively found in patients with **painless diabetic neuropathy** 31 (91.2%) variants (30 unique) were class 3 and 3 (8.8%) variants (2 unique) were class 4, whereas no variants were classified as class 5. Differently, according to

Waxman's criteria, 28 (82.4%) are VUS, none was clearly pathogenic, 5 (14.7%) variants (3 unique) are possibly pathogenic, none was unlikely pathogenic, and only 1 (2.9%) variants could not be classified for lack of voltage clamp and patch clamp data. No significant difference was observed between PDN and PLDN according to pathogenic classes.

Moreover the compound heterzogous variant *Y158D-R814H (SCN10A)* have been classified as possibly pathogenic since it exhibited enhanced peak (peak currents 2-4-fold greater than wild-type) and late (I_{Na}-L) sodium currents[200]. In our samples the compound variants were carried by two painless diabetic neuropathy samples.

Comparative results

Considering all neuropathies irrespective of their aetiologies and phenotype, in 1015 patients we found 149 variants (120 unique) for a total of 136 mutated patients (13.4%) (Figure 33).

Considering the number of mutated patients according to aetiology and pain phenotype, we identified 11.5% of patients mutated among diabetic, 11.8% in idiopathic, 13.5% in painful and 9.7% in painless patients (Figure 33).

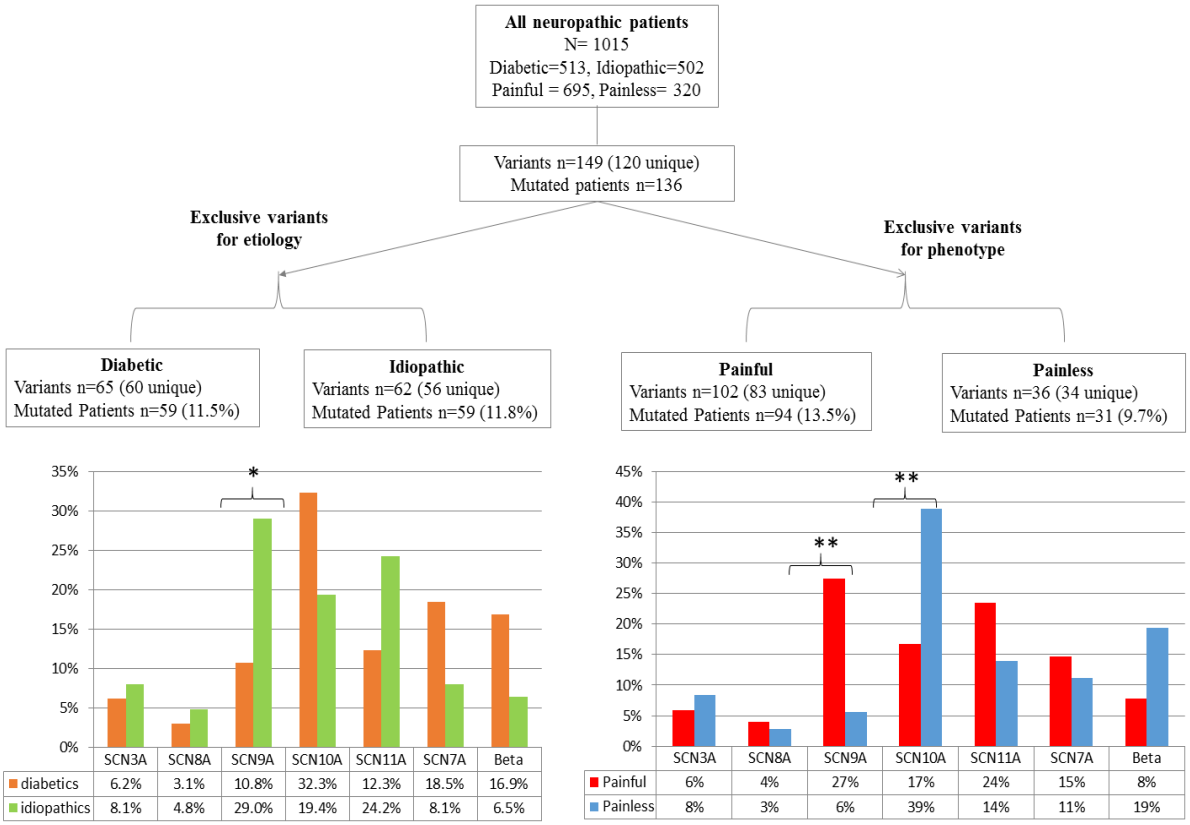

Figure 33. **Flowchart for genetic analysis of all neuropathic patients and bar plots of mutation rate among VGSCs genes.** The upper flowchart shows the number of potential pathogenic VGSCs variants for all neuropathies dividing the variants exclusively carried by diabetic or idiopathic (left panel) and the variants exclusively carried by painful or painless patients (right panel). The lower bar plots show the mutation rate among VGSCs genes according to aetiology (left panel) and to pain phenotype (right panel). *<0.05, **<0.01, p-value from Fisher exact test.

After excluding variants shared by the two different etiological cohorts, 65 variants were exclusively found in diabetic patients and 62 in idiopathic ones. Comparing diabetic versus idiopathic in relation to the distribution of the mutations in VGSCs genes, we observed a significant prevalence of *SCN9A* (p=0.013) mutations in idiopathic mutated patients whereas a non-significant predominance of *SCN10* mutations were observed in diabetic patients (Figure 33, left panel).

Additionally, after excluding variants shared by the two different pain phenotypes, 83 variants were exclusively found in painful patients and 36 in painless ones. Comparing painful versus painless patients in relation to the distribution of the mutations in VGSCs genes, we observed a highly significant prevalence of *SCN9A* (p=0.0048) mutations in painful patients and a significant predominance of *SCN10* (p=0.0099) mutations in painless patients (Figure 33, right panel).

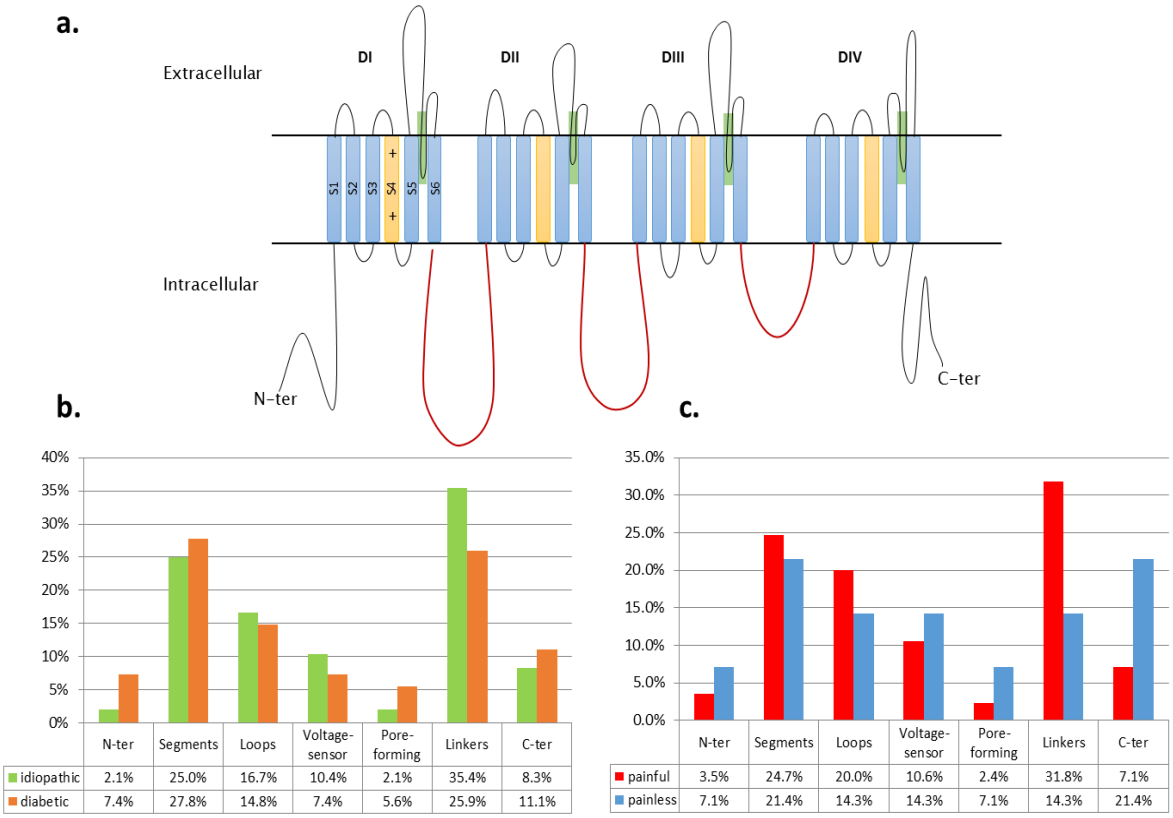

	N-ter	Segments	Loops	Voltage-sensor	Pore-forming	Linkers	C-ter
idiopathic	2.1%	25.0%	16.7%	10.4%	2.1%	35.4%	8.3%
diabetic	7.4%	27.8%	14.8%	7.4%	5.6%	25.9%	11.1%

	N-ter	Segments	Loops	Voltage-sensor	Pore-forming	Linkers	C-ter
painful	3.5%	24.7%	20.0%	10.6%	2.4%	31.8%	7.1%
painless	7.1%	21.4%	14.3%	14.3%	7.1%	14.3%	21.4%

Figure 34. **Location of variants in the topological regions of VGSCs.** a) Schematic representation of VGSCs showing the 24 trans-membrane segments contained within four regions (DI-IV). Within each region, there are six segments (S1-S6). The fourth segments, S4, within each region acts as the voltage sensor (yellow), whereas S5 and S6 come together to form the channel pore (green). N-ter, Amino-terminal region; Loop, extra-cellular and intra-cellular regions connecting adjacent segments; C-ter, Carboxyl-terminal region. b) Bar plot of mutation rate among topological regions of VGSCs according to etiology (idiopathic and diabetic); c) Bar plot of mutation rate among topological regions of VGSCs according to pain phenotype.

Referring to the corresponding topological localization on Nav protein of exclusive genetic variants, we observed a similar variant distribution between diabetic and idiopathic patients (Figure 34). Conversely, variants in the cytoplasmic linkers were the most represented in patients with painful neuropathy, while C-terminus variants were more frequent in painless neuropathies (Figure 34), although no statistical significance was observed.

Overall, we identified pathogenic variants according to Waxman's criteria only in painful patients: 8 in idiopathic SFN, 1 in diabetic patients and 1 variant in both groups. The latter, the p.Trp1538Arg in *SCN9A* gene was the most frequent pathogenic variant in our cohort and was identified in 5 idiopathic SFN and 2 diabetic neuropathy patients. This variant was first described in 2011 in a patient with unexplained chronic severe neuropathic pain[201], then in a patient with erythromelalgia phenotype[162] and recently also in a patient with painful

diabetic neuropathy[137]. Electrophysiological study performed in HEK293 cells expressing the p.Trp1538Arg mutant channel confirmed the gain-of-function effect of the mutation[162].

Other 2 pathogenic mutations already described as gain-of-function mutations[42,202] were present in more than one patients: the p.Ile228Met in *SCN9A* gene in 3 idiopathic SFN and the p.Leu1158Pro in the SCN11A gene in 3 PDN patients (Table 4).

Chrpos	Genes	ppos	cpos	Wallis	Domain	rsID	Phenotype	Freq (cohort)	Ref
3:38753831	SCN10A	Ala1304Thr	c.3910G>A	Class4	DIII:S5	rs142173735	Painful peripheral neuropathy	1 P-SFN	[41]
3:38739727	SCN10A	Gly1662Ser	c.4984G>A	Class4	DIV:Pore-forming	rs151090729	SFN	1 P-SFN	[203]
3:38950645	SCN11A	Ile381Thr	c.1142T>C	Class4	DI:S6	rs606231280	Painful peripheral neuropathy	1 P-SFN	[42]
3:38913706	SCN11A	Leu1158Pro	c.3473T>C	Class4	DIII:S4Voltage-sensor	rs141686175	Painful peripheral neuropathy	1 P-SFN	[42]
2:167137018	SCN9A	Ile720Lys	c.2159T>A	Class4	LinkerDI/DII	rs200945460	SFN	1 P-SFN	[40]
2:167162344	SCN9A	Arg185His	c.554G>A	Class4	DI:LoopS2-S3	rs73969684	SFN	1 P-SFN	[40]
2:167160752	SCN9A	Ile228Met	c.684C>G	Class4	DI:S4Voltage-sensor	rs71428908	SFN	3 P-SFN	[136,137]
2:167133767	SCN9A	Gly856Asp	c.2567G>A	Class4	DII:LoopS4-S5	rs879254102	Pain dysautonomia & acromesomelia	1 P-SFN	[170]
2:167060594	SCN9A	Trp1538Arg	c.4612T>C	Class3	DIV:LoopS1-S2	rs202084411	PDN; primary erythromelalgia; Chronic non-paroxysmal neuropathic pain	5 P-SFN 2 PDN	[137,162,201]
3:38913706	SCN11A	Leu1158Pro	c.3473T>C	Class4	DIII:S4Voltage-sensor	rs141686175	Painful peripheral neuropathy	3 PDN	[42]

Table 4. **Pathogenic variants according to Waxman's classification, associated to painful idiopathic or diabetic SFN.** chrpos, chromosome: base pair position and alleles; cpos, coding position; ppos protein position; rsID, dbSNP code; HGMD2018 annotation according to Human Genetic Mutation Database 2018; Ref., references; Freq., number of patients harbouring the variants. P-SFN: painful idiopathic SFN; PDN: painful diabetic neuropathy

Study 5: Pilot polygenic model for risk stratification on painful diabetic neuropathy

To conduct PRS analysis we considered GER sample (332 individuals) for the discovery trial and UK sample (181 individuals) for the validation trial. According to the pre-specified distinction between presence and absence of pain, 155 and 58 patients were defined as PDN (painful) and 177 and 123 as PLDN (painless) in GER and UK samples, respectively.

The following covariates were used for the statistical analysis: Age, Sex, Type of Diabetes (type 1 or type 2) and Ethnicity.

Demographic and baseline characteristics of the two cohorts are summarized in Table 5. Most of participants were Caucasian with some patients from Asia, Africa or mixed (p-value not significant).

In both cohorts, the PDN group included a significant higher number of females respect to PLDN (OR= 2.17, 1.96 and 1.94 for GER, UK, and TOTAL respectively, P≤0.05). Considering the total sample, the frequency of diabetes type 2 was significantly higher in PDN versus PLDN (OR = 1.95, P≤0.01).

In this study, we applied a polygenic model for risk stratification of PDN by combining single rare and common variants into an individual-level risk score.

We started form the complete list of 7233 variants in the 107 candidate pain-related genes (Table 8). SNPs with a call rate less than 80% and a genotype frequency significantly out of Hardy–Weinberg equilibrium with a Bonferroni corrected *p* value threshold ($p = 0.000048$) were filtered out, leaving 845 variants for the analysis.

We considered all variants without filtering for minor allele frequency, keeping 18 rare variants with MAF < 0.01, 153 low frequency variants with MAF < 0.05 and 674 common variants. Each variant was tested for association with painful diabetic neuropathy (PDN) or painless diabetic neuropathy (PLDN) trait in the discovery cohort using a logistic regression adjusting for sex, age, ethnicity and diabetes type.

Multiple PRS analyses were performed in validation cohort, with varying thresholds for the p-values (0.001, 0.05, 0.1, 0.2, 0.3, 0.4, 0.5, 1) testing all 845 SNPs. Once PRS have been calculated for all subjects in the validation (target) sample, the prediction accuracy, expressed with the Nagelkerke's R2 measure, was calculated to select the best-fit PRS. The

largest Nagelkerke's R2 value generated was 0.164 (p-value=1.8×10-5), suggesting the inclusion of 122 SNPs at the p value threshold of 0.305 into the PRS model (Table 7, Figure 35).

Characteristic	GER (discovery)		UK (validation)		TOTAL	
	Painful	**Painless**	**Painful**	**Painless**	**Painful**	**Painless**
Number of subjects, N (%)	155 (46.7%)	177 (53.3%)	58 (32.04%)	123 (67.96%)	213 (41.5%)	300 (58.5%)
Women, N(%)	54 (34.8%)‡	36 (19.8%)	26 (44.8%)*	36 (29.3%)	80 (37.6%)‡	71 (23.7%)
Diabetes type 2 (versus 1), N(%)	134 (86.5%)	139 (78.5%)	47 (81.03%)	84 (68.3%)	181 (84.98%)§	223 (74.3%)
Age, y (mean ± SD)	66.23 (±9.88)	67.5 (±10.21)	60.72 (±10.25)	61.55 (±12.93)	65.35 (±9.95)	65.08 (±11.78)
Ethnicities, N						
White	152	175	41	106	193	281
Black	0	1	0	0	0	1
Asian	1	0	15	14	16	14
North Africa	2	0	0	0	2	0
Afro-Caribbean	0	0	1	2	1	2
Mixed	0	1	1	1	1	2

Table 5. Baseline characteristics of diabetic neuropathy patients (numbers (%) or mean±SD) by Cohort. Significance of the difference with males: *p≤0.05; ‡p≤0.01 (OR= 1.96, 2.17 and 1.94 for UK, GER and TOTAL respectively); Significance of the difference with type 1 diabetes: §p≤0.01 (OR=1.95)

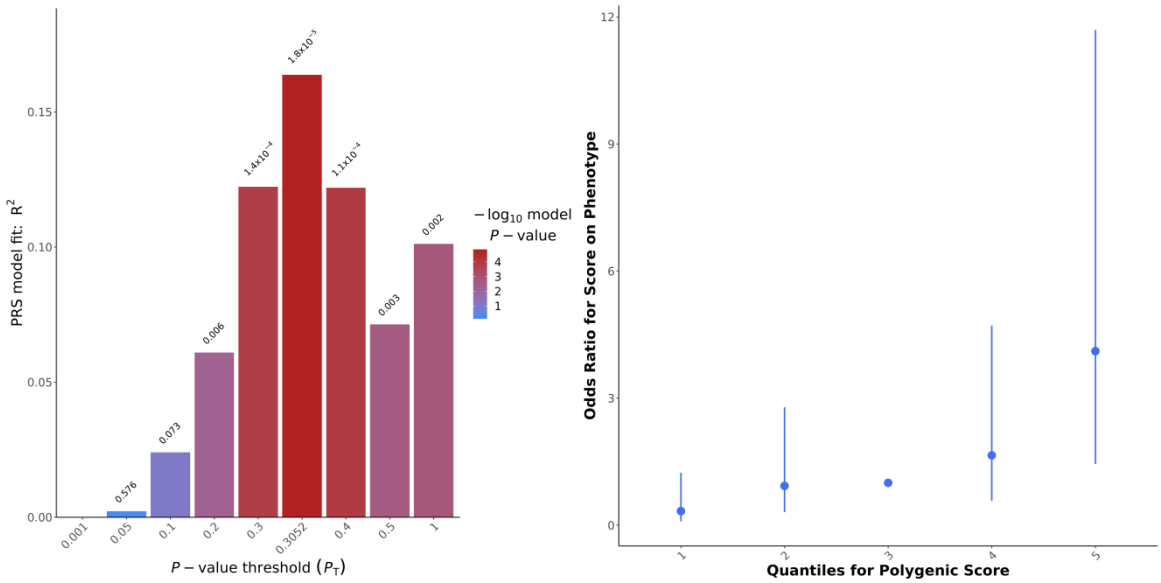

Figure 35. **Polygenic risk score analysis.** Bar plot displaying the model fit of the PRS at P-value threshold (on the left). This plot shows the predictive value in the target sample of models based on SNPs with p-values below specific thresholds in the base sample. On the right the quantile plot provides an illustration of the effect of increasing PRS on predicted risk of painful diabetic neuropathy. The results are obtained using PRsice2 software and Germany cohort (n=332) as base and UK cohort (N=181) as target.

The effect of significant non-genetic predictors (diabetes and gender) in discovery cohort, were incorporated into the predictive model together with the 122 genetic variants of PRS. Thus, obtaining a clinical polygenic risk score for each patient in target cohort.

One-way ANOVA analysis of mean PRS scores between PDN and PLDN, suggested an overall significance in PRS score because the mean PRS of the PDN samples were found to be significantly higher than that of the PLDN (0.34±0.17 versus 0.26±0.18, p = 0.004).

Predictive ability analysis of the PRS, including gender and diabetes, produced a final AUC for PDN classification with an accuracy of 60.3% (Figure 36).

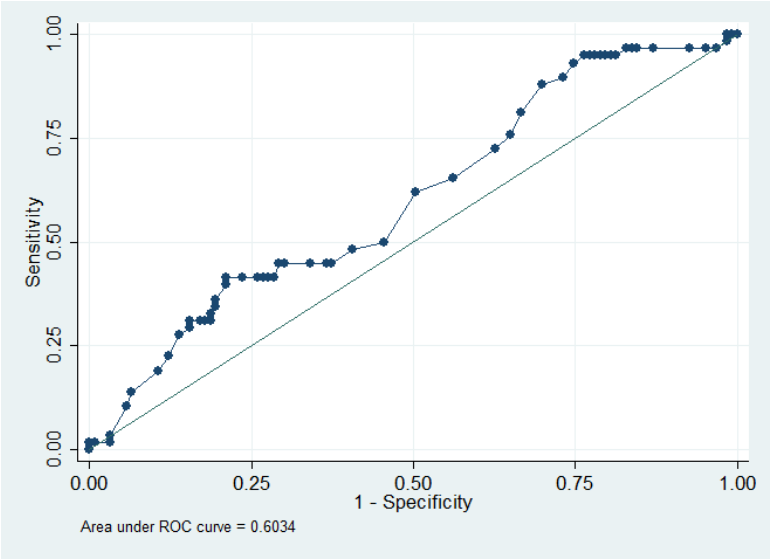

Figure 36. **ROC curve showing the discriminatory power of the PRS in predicting painful DPN occurrence.** The graph is generated by plotting the sensitivity of continuous PRS against specificity.

Samples were separately partitioned into three approximately equally sized strata (tertiles) of increasing disease risk based on PRS and including gender and diabetes. Individuals in the 3th tertile were classed as high risk whereas the samples in the 1st tertile are considered as low risk (Table 6).

	PRS (mean±STdev, N)		
Tertiles	**PDN**	**PLDN**	**TOT**
1 (low risk)	0.18± 0.10, 14	0.095 ± 0.12, 44	0.12 ± 0.12, 58
2 (median risk)	0.24 ± 0.002, 18	0.24 ± 0.003, 43	0.24 ± 0.02, 61
3 (high risk)	0.50 ± 0.11, 26	0.49 ± 0.12, 36	0.49 ± 0.12, 62

Table 6. **Tertiles.** Number of subjects and mean, standard deviation of PRS according to each tertile.

The proportion of PDN and PLDN that fells into each tertile is depicted in Figure 37. The figure shows that the proportion of PDN increases with increasing PRS.

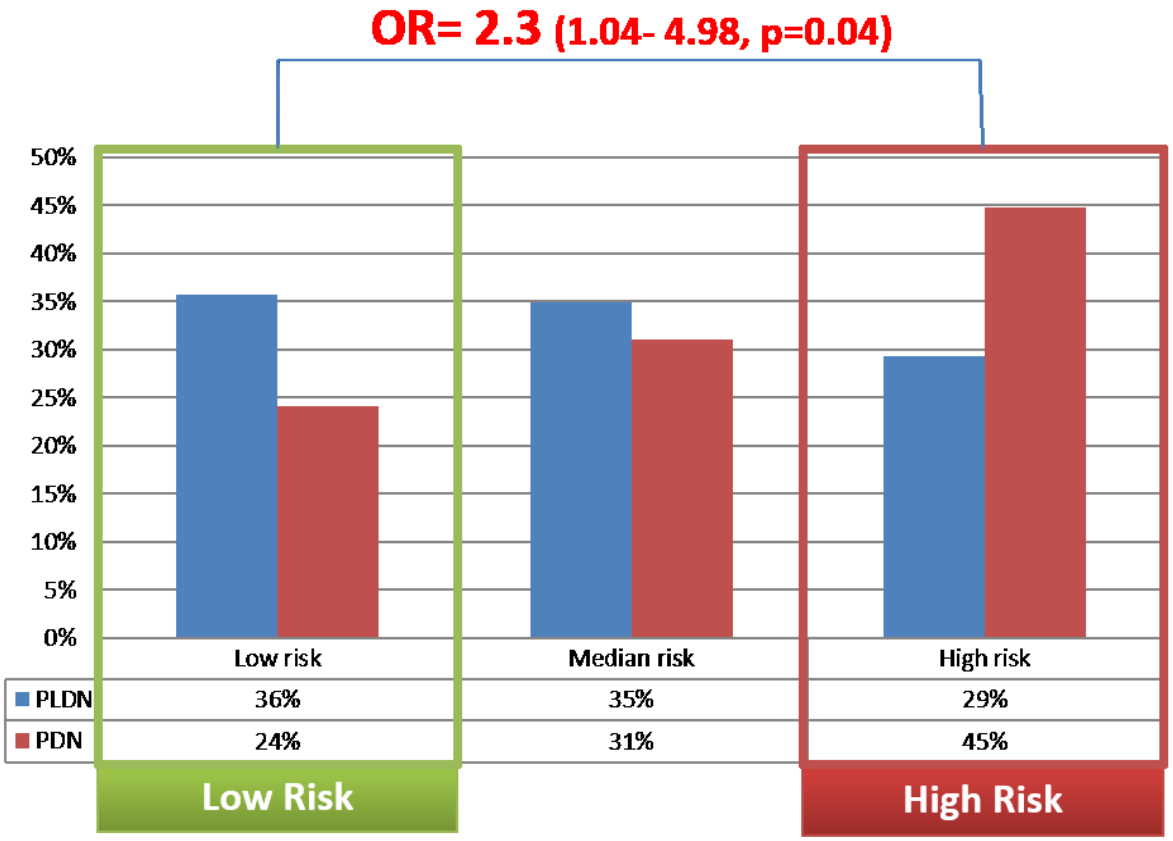

Figure 37. Proportion of PDN (painful) and PLDN (painless) in each tertile using the best predictive model. Individual probabilities were generated using PRSice-2. The polygenic risk scores (PRS) including also gender and diabetes were used to distribute individuals into tertiles. The blues bars represent the proportion of PLDN which fall into each tertile and the red bars represent the proportion of PDN. The percentages of PDN and PLDN who fall within each tertile are indicated in the Table 6. The rate of PDN increases with increasing PRS. Patients in the high risk group have a risk 2.3-fold higher of having a painful diabetic neuropathy compared to low risk group.

Logistic regression was used to compare individuals in the high-risk group (tertile 3) to individuals in the lowest risk group (tertile 1). The results showed that the odds of developing PDN were significantly increased in individuals in the highest risk group compared to individuals in the lowest risk group (OR 2.3, 95% CI 1.04- 4.98, P=0.04).

The third tertile cutoff value was considered to classify high risk patients with a sensitivity of 47.9% and a specificity of 73.1%. They still lack in sensitivity, resulting in a high proportion of individuals with PDN being misclassified as PLDN: this could mostly due to the small sample sizes, and it is expected that with increased numbers in each group the mean PRS will move towards PLDN and PDN, respectively.

Supplementary results

Table 7. List of 122 SNPs included in the best-FIT PRS.

SNP, coded as chromosome: base pair position and alleles; cpos, coding position; ppos protein position; KG AF POPMAX, maximum allele frequency of 1000genomes project; AF gnomAD; Allele frequency in gnomAD database; OR, odds ratio of logistic regression in discovery sample; P, p-value from logistic regression in discovery sample.

SNP	rsID	GENE	EFFECT	HGVS cpos	HGVS ppos	KG AF POPMAX	AF gnomAD	OR	P
11:70007484 C/G	rs2276068	ANO1	intron variant	c.1780+16C>G		0.71	0.54	1.73	0.001
3:38888764 A/G	rs62244134	SCN11A	synonymous variant	c.4797C>T	Tyr1599Tyr	0.12	0.11	0.42	0.001
11:26619872 C/T	rs7112022	ANO3	intron variant	c.1448-40T>C		0.45	0.32	0.63	0.007
11:70002184 T/TA	rs202090184	ANO1	intron variant	c.1503+91delA				1.63	0.009
8:72935039 T/C	rs10085964	TRPA1	3 prime UTR variant	c.*102G>A				0.64	0.011
2:167313451 C/T	rs11888208	SCN7A	missense variant	c.1219A>G	Ile407Val	0.00	0.00	0.54	0.012
11:70007311 A/G	rs2276066	ANO1	synonymous variant	c.1623A>G	Arg541Arg	0.78	0.66	1.54	0.015
19:42489516 A/C	rs2217342	ATP1A3	synonymous variant	c.666T>G	Thr222Thr	1.00	0.89	0.52	0.018
14:55310492 A/G	rs841	GCH1	intron variant	c.*16+227C>T		0.34	0.22	0.58	0.022
2:167137120 T/C	rs4525717	SCN9A	intron variant	,c.2108-15G>A		0.35	0.16	0.55	0.023
8:26492470 T/G	rs55906521	DPYSL2	intron variant	c.811+54G>T				0.45	0.025
1:115829313 A/G	rs6330	NGF	missense variant	c.104C>T	Ala35Val	0.46	0.37	0.70	0.030
2:167168093 C/T	rs6432901	SCN9A	synonymous variant	c.174G>A	Gln58Gln	0.76	0.58	0.71	0.033
2:234923170 G/A	rs11562948	TRPM8	intron variant	c.3265-36A>G		0.12	0.07	0.45	0.036
14:33046471 T/G	rs768787	AKAP6	intron variant	c.2469+23T>G		0.85	0.67	0.71	0.045
6:36040642 A/AT	rs61763106	MAPK14	splice region variant	c.306-5delT		0.49	0.16	1.79	0.046
9:111679964 CA/C	rs140104681	IKBKAP	intron variant	c.741-15dupT		0.16	0.09	0.61	0.050

SNP	rsID	GENE	EFFECT	HGVS cpos	HGVS ppos	KG AF POPMAX	AF gnomAD	OR	P
1:205027390 T/C	rs9787172	CNTN2	synonymous variant	c.297C>T	Asn99Asn	0.17	0.05	2.95	0.051
9:111670707 T/C	rs838824	IKBKAP	intron variant	c.1361-23A>G		0.85	0.69	1.40	0.052
20:62062883 A/G	rs73146513	KCNQ2	intron variant	c.1118+2279C>T				0.31	0.053
9:94797040 C/T	rs16908102	SPTLC1	intron variant	c.1328+52A>G				0.43	0.056
9:117853103 T/C	rs10982521	TNC	synonymous variant	c.195G>A	.,Ser65Ser	0.07	0.06	2.05	0.067
1:175365663 A/G	rs859446	TNR	intron variant	c.1240+17C>T		0.60	0.47	0.74	0.068
4:129878342 A/G	rs35006492	SCLT1	intron variant	c.1048-63C>T				0.63	0.068
11:26558873 C/T	rs375562	ANO3	intron variant	c.977-80T>C				0.57	0.070
12:121659999 A/G	rs1629287	P2RX4	intron variant	c.475+30G>A		0.44	0.36	0.74	0.070
1:205039295 C/A	rs56283998	CNTN2	intron variant	c.2431+106A>C				0.71	0.076
15:60678328 C/T	rs11858864	ANXA2	intron variant	c.44-43G>A		1.00	0.85	1.42	0.080
9:111685078 CAT/C	rs3833703	IKBKAP	intron variant	c.552+42 552+43dupAT		0.26	0.11	1.76	0.085
19:16988476 T/C	rs2258663	SIN3B	intron variant	c.3050+26T>C		0.83	0.74	1.39	0.086
1:160109788 T/C	rs41288127	ATP1A2	intron variant	c.3034+14C>T		0.13	0.13	0.67	0.087
2:234905078 T/C	rs11563208	TRPM8	synonymous variant	c.3048C>T	Ile1016Ile	0.32	0.25	0.72	0.090
11:113802601 A/G	rs1176746	HTR3B	intron variant	c.368+12A>G		0.91	0.68	1.32	0.091
6:36068041 C/T	rs2815805	MAPK14	intron variant	c.763-2307T>C		0.15	0.02	0.23	0.092
14:33291494 T/C	rs11845640	AKAP6	missense variant	c.4475C>T	Ala1492Val	0.48	0.14	0.63	0.096
16:6533549 C/A	rs7187508	RBFOX1	intron variant	c.66+166491C>A		0.79	0.52	1.32	0.100
5:75648940 AT/A	rs66963762	SV2C	intragenic variant	n.75648950delT				0.72	0.101

SNP	rsID	GENE	EFFECT	HGVS cpos	HGVS ppos	KG AF POPMAX	AF gnomAD	OR	P
12:110238481 A/G	rs1344554	TRPV4	synonymous variant	c.795C>T	His265His	0.18	0.08	2.06	0.104
2:182981968 G/A	rs1882212	PPP1R1C	synonymous variant	c.297A>G	Ala99Ala	0.60	0.23	0.73	0.107
9:94830356 A/C	rs45461899	SPTLC1	missense variant	c.452G>T	Arg151Leu	0.02	0.02	0.42	0.108
1:156836838 C/T	rs2274497	NTRK1	intron variant	c.428+68T>C				0.48	0.111
12:41463680 T/C	rs12297122	CNTN1	intron variant	c.2981-81C>T				1.63	0.111
1:50572096 A/C	rs12138061	ELAVL4	upstream gene variant	c.-3517C>A		0.35	0.22	1.36	0.116
14:52794234 T/C	rs708502	PTGER2	3 prime UTR variant	c.*62T>C				0.69	0.117
9:94877716 G/A	rs55740103	SPTLC1	upstream gene variant	c.-64T>C				1.65	0.118
8:133175736 C/T	rs2303995	KCNQ3	missense variant	c.1241A>G	Glu414Gly	0.16	0.04	0.38	0.121
3:38739494 A/G	rs116353929	SCN10A	synonymous variant	c.5217C>T	Asp1739Asp	0.03	0.03	2.15	0.121
9:117815036 A/G	rs62578424	TNC	intron variant	c.4580-4225C>T		0.13	0.11	1.48	0.123
22:22162126 G/A	rs3729910	MAPK1	synonymous variant	c.129T>C	Tyr43Tyr	0.05	0.05	0.52	0.127
9:117791617 C/T	rs12346540	TNC	intron variant	c.6169+22A>G		0.28	0.22	0.77	0.133
1:204915939 C/T	rs10157992	NFASC	intron variant	c.109+482T>C				1.32	0.133
14:70522484 G/A	rs1000521	SLC8A3	intron variant	c.1906+29T>C		0.22	0.11	0.70	0.136
1:204946764 C/T	rs6663324	NFASC	intron variant	c.1832-45T>C		0.23	0.10	0.68	0.140
6:154360508 T/G	rs6912029	OPRM1	intron variant	c.146-38G>T		0.12	0.04	0.51	0.142
2:167149700 C/T	rs41268675	SCN9A	intron variant	c.1110+41A>G		0.08	0.06	1.55	0.142
15:60643302 T/C	rs3743269	ANXA2	intron variant	c.891+90A>G				1.33	0.143
2:182850882 G/A	rs61732228	PPP1R1C	synonymous variant	c.45A>G	Val15Val	0.03	0.02	2.06	0.144

SNP	rsID	GENE	EFFECT	HGVS cpos	HGVS ppos	KG AF POPMAX	AF gnomAD	OR	P
6:73904557 T/C	rs61743058	KCNQ5	missense variant	c.2276C>T	Pro759Leu	0.05	0.04	1.65	0.150
1:204931137 G/A	rs16854813	NFASC	intron variant	c.706+4183A>G				0.68	0.150
20:62038757 T/C	rs3746364	KCNQ2	intron variant	c.1912-29G>A		0.12	0.09	0.68	0.151
10:62375033 G/A	rs1837947	ANK3	intragenic variant	n.62375033T>C				1.35	0.152
16:7657432 G/A	rs4616299	RBFOX1	intron variant	c.805+92A>G				0.80	0.161
11:118015832 A/G	rs45539032	SCN4B	synonymous variant	c.174C>T	Cys58Cys,	0.04	0.04	1.63	0.162
14:70634546 T/C	rs7161524	SLC8A3	synonymous variant	c.594G>A	Lys198Lys	0.21	0.16	0.74	0.165
9:111663754 A/G	rs2230791	IKBKAP	synonymous variant	c.1965C>T	Thr655Thr	0.18	0.07	1.56	0.165
17:64783081 G/A	rs6504459	PRKCA	missense variant	c.1702G>A	Val568Ile	1.00	0.98	0.50	0.166
10:61802561 G/T	rs2393607	ANK3	intron variant	c.13066-44C>A		0.81	0.73	0.78	0.168
2:234854552 G/A	rs17868387	TRPM8	missense variant	c.752A>G	Tyr251Cys	0.08	0.05	0.55	0.168
14:52794007 G/A	rs2229187	PTGER2	synonymous variant	c.912A>G	Leu304Leu	0.04	0.03	0.47	0.175
11:70034026 A/G	rs34064841	ANO1	synonymous variant	c.2877G>A	Pro959Pro	0.03	0.03	1.87	0.177
19:603625 C/T	rs56342526	HCN2	synonymous variant	c.714T>C	Asp238Asp	0.43	0.15	0.69	0.178
14:33014549 T/C	rs33936626	AKAP6	synonymous variant	c.690C>T	Tyr230Tyr	0.02	0.02	0.48	0.181
8:54141824 T/C	rs963549	OPRK1	3 prime UTR variant	c.*33G>A		0.53	0.17	1.42	0.182
3:38784029 T/C	rs6599250	SCN10A	intron variant	c.1868-9A>G		0.95	0.65	1.26	0.184
8:26492397 T/C	rs78121726	DPYSL2	synonymous variant	c.792C>T	Ile264Ile	0.04	0.03	0.58	0.185
1:156849775 C/T	rs12076232	NTRK1	intron variant	c.2047-16T>C		0.34	0.06	1.67	0.186
10:61843451 A/G	rs10509122	ANK3	intron variant	c.4075-76C>T				0.72	0.187

SNP	rsID	GENE	EFFECT	HGVS cpos	HGVS ppos	KG AF POPMAX	AF gnomAD	OR	P
19:613307 T/C	rs2301778	HCN2	synonymous variant	c.1644C>T	Ala548Ala,	0.34	0.29	0.79	0.187
2:166032775 C/CATT	rs34236036	SCN3A	conservative inframe deletion	c.127 129delAAT	Asn43del	0.09	0.08	1.44	0.189
14:33204825 C/T	rs41285498	AKAP6	intron variant	c.3148-39T>C		0.18	0.12	1.38	0.193
3:38805069 C/T	rs74717885	SCN10A	missense variant	c.618A>G	Ile206Met	0.16	0.03	0.47	0.195
12:41421642 G/A	rs12367345	CNTN1	intron variant	c.2711-17A>G		0.15	0.13	0.74	0.195
12:52184342 G/A	rs2241855	SCN8A	intron variant	c.4524+56A>G				1.46	0.196
1:204978643 A/C	rs78993506	NFASC	intron variant	c.3611-42C>A		0.47	0.36	1.23	0.199
5:32000397 C/T	rs115911339	PDZD2	intron variant	c.1254+20T>C		0.04	0.04	1.66	0.200
12:57958313 G/A	rs775322	KIF5A	intron variant	c.445+22A>G		0.77	0.47	1.24	0.200
12:863517 G/A	rs3858703	WNK1	intron variant	c.759+27G>A		0.88	0.68	1.26	0.204
11:69931624 A/G	rs12290914	ANO1	intron variant	c.109-2234G>A		0.29	0.11	1.33	0.206
11:57137424 T/C	rs2276038	P2RX3	missense variant	c.1148C>T	Ala383Val	0.72	0.44	1.24	0.211
1:160097315 A/C	rs2295623	ATP1A2	intron variant	c.749-27C>A		0.14	0.09	1.42	0.213
5:75427935 G/A	rs10070440	SV2C	synonymous variant	c.360G>A	Arg120Arg	0.74	0.63	1.26	0.214
16:23880477 G/A	rs7404819	PRKCB	intron variant	c.205+31750A>G		0.61	0.42	1.21	0.214
14:33291583 A/G	rs34711402	AKAP6	missense variant	c.4564G>A	Val1522Ile	0.04	0.02	1.77	0.223
14:70634200 C/T	rs34816272	SLC8A3	missense variant	c.940A>G	Arg314Gly	0.01	0.01	2.77	0.223
19:49342396 T/G	rs55966626	PLEKHA4	intron variant	c.1964+66C>A				1.34	0.223
17:64685078 A/G	rs2227857	PRKCA	synonymous variant	c.831G>A	Leu277Leu	0.37	0.32	0.82	0.228
19:16976289 C/T	rs2303091	SIN3B	synonymous variant	c.1548T>C	Ser516Ser	0.28	0.17	0.78	0.230

SNP	rsID	GENE	EFFECT	HGVS cpos	HGVS ppos	KG AF POPMAX	AF gnomAD	OR	P
6:154360797 G/A	rs1799971	OPRM1	missense variant	c.397A>G	Asn133Asp	0.42	0.19	0.73	0.230
17:75398498 T/C	rs34587622	SEPTIN9	missense variant	c.434C>T	Pro145Leu	0.12	0.08	1.39	0.232
6:73904612 A/G	rs17810318	KCNQ5	synonymous variant	c.2331G>A	Lys777Lys	0.03	0.02	0.53	0.233
16:7102036 CT/C	rs35212568	RBFOX1	intron variant	c.115-20delT		0.77	0.61	1.22	0.234
17:42987524 C/T	rs9916491	GFAP	downstream gene variant	c.*313A>G		0.26	0.27	1.24	0.236
10:61941147 G/A	rs34552044	ANK3	synonymous variant	c.2124T>C	Asp708Asp	0.04	0.03	1.54	0.249
4:129913243 T/G	rs35350849	SCLT1	intron variant	c.686+79C>A				1.59	0.256
19:41060616 G/A	rs2242131	SPTBN4	intron variant	c.5084+64A>G		0.15	0.14	0.79	0.258
6:36076280 T/C	rs6457878	MAPK14	3 prime UTR variant	c.*56C>T				0.77	0.266
5:32087253 G/A	rs157495	PDZD2	synonymous variant	c.3699A>G	Ser1233Ser	0.51	0.30	1.24	0.267
12:974308 TC/T	rs141823469	WNK1	frameshift variant	c.2175dupC	Ile726fs	0.00	0.25	0.82	0.268
5:32074509 A/G	rs2291113	PDZD2	synonymous variant	c.3297G>A	Thr1099Thr	0.22	0.08	0.69	0.269
17:42990810 A/G	rs3744468	GFAP	intron variant	c.619-12C>T		0.27	0.12	0.77	0.276
12:121671270 T/C	rs28360474	P2RX4	intron variant	c.1189-56C>T				0.63	0.277
18:55816791 A/G	rs4149601	NEDD4L	intron variant	c.49-16229G>A		0.36	0.28	0.83	0.278
16:7726757 G/A	rs2302213	RBFOX1	intron variant	c.1060-19A>G		0.16	0.13	1.28	0.279
16:24166130 C/T	rs432998	PRKCB	synonymous variant	c.1191T>C	Pro397Pro	0.50	0.34	1.21	0.279
10:61819556 A/G	rs12356776	ANK3	intron variant	c.12596-368C>T		0.04	0.03	0.58	0.280
10:62021593 C/T	rs16914671	ANK3	intron variant	c.798+24A>G		0.15	0.03	1.93	0.281
6:154439865 T/C	rs11575858	OPRM1	3 prime UTR variant	c.*9C>T		0.01	0.01	2.02	0.288

SNP	rsID	GENE	EFFECT	HGVS cpos	HGVS ppos	KG AF POPMAX	AF gnomAD	OR	P
10:118969346 C/T	rs363315	KCNK18	missense variant	c.691T>C	Ser231Pro	0.14	0.07	0.56	0.293
12:110240838 T/G	rs3825394	TRPV4	synonymous variant	c.670A>C	Arg224Arg	0.97	0.63	0.84	0.297
4:129965026 C/T	rs1450727	SCLT1	intron variant	c.161+122A>G				1.20	0.300
2:234916843 A/G	rs76495981	TRPM8	intron variant	c.3264+96G>A				1.84	0.303
14:33068608 T/C	rs17506750	AKAP6	splice region variant	c.2470-8C>T		0.09	0.06	0.73	0.305

DISCUSSION

Neuropathic pain represents a frequent feature in peripheral neuropathies, especially when small nerve fibers mediating physiological conduction of thermal and painful somatic sensations are involved. A damage or dysfunction of this group of "pain" fibers can more likely cause spontaneous or evoked pain, in keeping with the current definition of neuropathic pain a condition due to lesion or disease of the peripheral somatosensory system. SFN is typically characterized by excruciating burning sensation, paroxysmal pain, deep pain and other symptoms at feet and hand, thus the strict link between the degeneration of small fibers and the induced clinical picture makes SFN a good model for the study of neuropathic pain.

Peripheral neuropathic pain complaints encompass a variety of features. Stratification of patients according to their symptoms has represented a rational approach in order to identify different sensory profile that might be sustained by different mechanisms and might respond to different treatments[204]. However, at present, analgesic treatment for neuropathic pain remain non-specific and unrelated to underlying condition or clinical picture, with very few exceptions such as trigeminal neuralgia. Nevertheless, accurate clinical characterization of patients remains of pivotal importance for patients' subgrouping and for investigating neurobiological mechanisms and genetic architecture underlying different phenotypes such as for presence of absence of pain in patients with neuropathy.

Based on the above considerations, the assessment of a deep phenotyping of SFN patients represented a crucial step that has been pursued by implementing a neurological examination tailored on assessment of somatosensory functions and a set of validated questionnaires evaluating pain intensity and features, SFN symptoms, autonomic involvement, anxiety and mood. Integration of all data into a dedicated database represented a further essential point. It was developed and implemented in clinical practice providing a tool able to guide clinicians throughout accurate and systematic data collection. The prompt access and sharing of patients' information among physicians and researchers is one of the major strengths of this tool in the clinical setting. The capability of a customizable data extraction according to the specific requests makes it useful also in research setting, for example for a fast screening of patients suitable to access a clinical trial or for selecting cohorts of subject according to their clinical features, presence or absence of specific symptoms and signs, as well as the results of skin biopsy, neurophysiology or genetic

analysis. In this sense, a limitation of this tool is that despite being accurate, the variables included and collected in the database are predefined and might not be exhaustive to address any future application or request. However, it is a dynamic system that can be updated introducing or editing fields as necessary.

The chance to directly visualize and investigate the terminal endings of the nociceptors innervating the epidermis, through the immunohistochemical assay of skin biopsy sections, makes SFN a definite condition in which all patients have in common a reduction of IENFD. Since its introduction by McCarthy in the 90's of the last century as a tool to investigate intraepidermal nerve fibers (IENF) in sensory neuropathies[60], skin biopsy has gained increasing relevance in the diagnostic work up of patients with predominant length-dependent sensory symptoms. Skin biopsy, showing a degeneration of small sensory nerve fiber populating the epidermis at the ankle in patients complaining length dependent painful symptoms, allowed to address a definite diagnosis of neuropathic pain and is considered the "gold standard" for the diagnosis of SFN, although a true gold standard is lacking[61,62].

The retrospective analysis of skin biopsy results conducted in this thesis work, comparing the different cut-off values used over time, showed a significant improvement of the diagnostic accuracy of IENFD quantification with the introduction of the age-and-sex-adjusted normative reference values for IENFD in the 2010[62]. The comparison of the number of patients diagnosed as having a SFN, according to skin biopsy results obtained with the cut-off values in use before 2010 and after recalculating according to the last normative values, revealed a rate of 58% of false positive, namely patients wrongly addressed as having a reduced IENFD. On the other hand, only 1 patient (a woman) would see her diagnosis change from normal to reduced IENFD. Therefore, the introduction of the sex- and age-adjusted normative values significantly improved the specificity of this diagnostic tool. Interestingly, the study conducted by McArthur[192] et al. in 1998 that provided the first normative value, already assessed IENFD at different ages including subjects in different decades from 10-19 to 70-79 years. The authors did not find a significant decrement in IENFD with age except for higher values in the youngest subjects, thus they proposed a single value irrespective of age and gender. Several subsequent studies demonstrated and confirmed a progressive decline of IENFD with age and higher scores in women[53,62,205–208] also using immunofluorescence microscopy[63]. Such differences might be explained by

different counting rules as also fragments of fibers in the epidermis and not only fibers crossing the dermal-epidermal junction were initially included.

The definition of age-and-sex-adjusted normative reference values for IENF density strengthened the diagnostic reliability of skin biopsy and gave impulse to IENF investigations in a broader range of clinical conditions[34], widening the spectrum of IENFD reduction to painful and nonpainful disorders, thus introducing the concept of small fiber pathology[209]. Considering this ever-changing insight on small fibers pathology, a more comprehensive clinical assessment of patients is needed in order correctly address the diagnosis of SFN for which the reduction of IENFD at skin biopsy has to take place in presence of sensory signs or abnormal thermal threshold at QST[52].

Patients with SFN typically complain of excruciating burning sensation at hands and feet sometimes with a widespread "non-length dependent" distribution for which available analgesic treatments still remain unsatisfactory. Despite clinical trials for analgesics in neuropathic pain include a variety of clinical scales focusing on quality of life, mood disorder, interference on sleep and sensory somatic and autonomic symptoms, the average daily pain intensity on the PI-NRS remains the most relevant outcome measure whose change is often chosen as primary endpoint. In our cohort of 253 patients, we found a slightly but significantly higher average NRS of the whole day in women compared to man. On the contrary, no correlation was observed between IENFD and NRS score, confirming that the intensity of pain is unrelated to the extent of epidermal denervation[51].

The intra-day evaluation of pain features conducted on SFN patients revealed a circadian pattern of pain intensity characterized by an increase of NRS score towards the evening. A previous study investigated pain dynamics of SFN and reported only marginal and not clinically meaningful higher pain scores at night[210]. In this study we found a slight but significant increase of NRS moving from the morning or the afternoon to the evening with 20% of patients reporting an increase of more than 2 points from the morning to the evening. A change of 2 points or 30% at NRS is often considered a relevant outcome measure[211], therefore the circadian NRS variation during the daytime might represent a possible adjunctive outcome measure in clinical trials for analgesic drugs in SFN related neuropathic pain.

Clinical picture of SFN patients shows a large variability in terms of presence, distribution and intensity of sensory symptoms, pain and autonomic involvement. Some patients have

painless form, while among those complaining painful form the intensity of dolorous symptoms may significantly differ irrespectively of the underlying etiology.

A rising number of evidences has suggested an individual predisposition to pain sustained by polymorphisms in genes encoding for ion channels involved in neuronal excitability (see The genetic hypothesis for neuropathic pain). In addition, the identification of gain- and loss-of-function mutations in sodium channels genes in rare mendelian familial pain disorders, prompted the investigation for mutations in this set of ion channels also in painful neuropathy patients, leading to the identification of gain-of-function variants in *SCN9A*, *SCN10A* and *SCN11A* genes encoding for the NaV1.7, NaV1.8 and NaV1.9 alpha subunit of sodium channels and defining the new entity of channelopathy-related painful neuropathy (see Inherited pain disorders).

This work of thesis started from a similar approach. The candidate-gene analysis conducted on patients recruited in the context of the multicenter PROPANE study aimed to investigate the presence of rare genetic variants in sodium channels preferentially expressed in the peripheral nervous system in SFN patients according to the etiology and presence or absence of pain.

In our cohort of 1015 SFN patients we found 149 variants in sodium channels genes (nearly 80% in *SCN9A*, *SCN10A* and *SCN11A*) in a total of 136 mutated patients (13.4%). A recent study investigating the frequency of variants in in *SCN9A*, *SCN10A* and *SCN11A* genes in a large cohort of 1139 SFN patients reported a similar global rate of variants (11,6%)[168].

Examining our population, as illustrated in the

Comparative results, we found a similar rate of mutated patients when comparing different groups according to the aetiology (about 11.5%) and a slight prevalence in painful compared to painless phenotype (13.5% and 9.7%, respectively). Therefore, the global rate of genetic variants in VGSCs genes seems to be an independent variant and does not suggest any significant correlation with a specific aetiology or phenotype.

Analysing the distribution of variants among the different VGSCs genes, we observed a significant higher frequency of variants in *SCN9A* gene in idiopathic compared to diabetic patients, whereas diabetic patients showed a higher, though not significant, *SCN10A* variants frequency. In addition, we observed a significant prevalence of *SCN9A* variants in painful and

SCN10A variants in painless patients. No statistically significant differences in topological distribution of variants within the different domains of VGSCs have been observed.

Most of the available studies focused on the identification of rare or low frequency variants in sodium channels analysing cohorts only composed by painful neuropathy patients. Two recent studies investigated sodium channels genes variants in painful and painless neuropathy patients, one focusing on *SCN9A* in a cohort of 189 diabetic neuropathy patients[137], the other including 457 patients having either idiopathic or diabetic neuropathy for *SCN9A*, *SCN10A* and *SCN11A* sequencing[212].

Considering the *SCN9A* gene, both studies reported variants in patients with painful phenotype. However, the first study reported no variants in the painless group, whereas the latter showed no difference in terms of variants rate between painful and painless patients. In our study we found *SCN9A* variants in both phenotypes, yet their frequency was higher in painful cohort.

Such discrepancies in variants frequencies might be related to inclusion criteria or platforms used for sequencing; in addition, different strategies in variant filtering and classification likely represent a further influencing factor. One limitation of our study might be represented by the low number of painless idiopathic neuropathy patients included, mainly due to the fact that patients having minor complaints may not come to clinical attention especially in the absence of other comorbidities.

The overall results from our study and the literature do not allow defining the rare or low frequency VGSCs variants rate alone as an optimal clue for phenotype classification. Furthermore, the demonstration of the pathogenic role of the identified variants remains challenging and the fact that a variant is rare does not make it necessarily pathogenic. The Waxman's criteria[187] have proposed a pathogenic classification tailored for *SCN9A*, *SCN10A* and *SCN11A*, introducing cell electrophysiology among criteria, taking advantage of the opportunity of evaluating the effect of genetic variants on channel kinetics and cellular excitability. At present, cell electrophysiology represents the "gold standard" for defining the pathogenicity of a VGSC gene variant in particular in sporadic cases when segregation with phenotype cannot be addressed. However, looking at the identified variants, including also those considered pathogenic according to Waxman's criteria, most were present as a single variant in individual patient. These results, together with a number of observations[187], raised some concerns about the ability of single rare variants in VGSCs to predict the painful clinical

picture in a significant portion of patients. In particular, several rare *SCN9A* and *SCN10A* variants (MAF<0.01) found in patients with pain disorders do not produce any change in terms of cellular excitability; variants like Ile739Val and Arg185His in *SCN9A* gene, for which a gain-of-function effect on sodium channel was demonstrated by cell electrophysiology, seem to have a similar or even higher frequency in general population compared to SFN patients; variant-induced changes in the channel kinetics may not predict increase in excitability in DRG neurons and clinical phenotype (a good example is a gain-of-function mutation in *SCN11A* gene producing a congenital insensitivity to pain phenotype[160]); functional effect of the mutated channel may differ depending on the cell type in which it is expressed (such as in HEK293 cells or DRG neurons). All these findings suggest that many variants probably do not cause the disease themselves but rather act as risk factors.

On the basis of the above considerations, we adopted a new approach to address the risk of pain in our diabetic neuropathy cohort of 513 patients. We started from the hypothesis that all the identified variants regardless of whether they are rare or common might contribute with a small effect size to compose the clinical phenotype[189]. The analysis of covariates indicated female gender and type 2 diabetes as non-genetic predictors of painful phenotype in diabetic neuropathy, with an odd ratio around 2. This results were in line with previous results reported in the literature[100,179–181]. We combined into a polygenic risk score (PRS) the weight of each variant identified in all the 107 pain-related genes in diabetic neuropathy patients together with the non-genetic predictors, using a discovery cohort of 332 and a validation cohort of 181 patients. A total of 122 variants were obtained from discovery cohort and were used for computing PRS in the validation cohort. The analysis of PRS scores in painful and painless patients revealed a sufficient predictive ability of PRS with an AUC of 60.3%. Dividing the entire cohort into tertiles according to PRS, patients in 3rd tertile having a higher PRS had a risk 2.3-fold higher of having a painful diabetic neuropathy than those in 1st tertile having a lower PRS score.

The experience of genetic associations in common diseases has generally not supported the candidate-gene approach[188]. Furthermore, genome wide association studies (GWAS) have been successfully employed in large populations and have improved understanding of the direct association of common variants with complex traits and diseases[213]. However, the majority of these variants have small effect and limited predictive power. Hence, further models of analysis have been developed, including PRS, to aggregated the effects of variants

across the genome to estimate heritability and to predict phenotypes based on genetic profile. Studies have shown that PRS allows to achieve a substantially greater predictive power compared to a small number of genome-wide significant variants[214]. In addition, PRS can include inputs from different data set, combining data from GWAS and targeted analysis in order to provide a score encompassing the contribution of common variants with small effect and low frequency variants with a potential larger effect.

At present, only two GWAS have been conducted to investigate genetic determinants for painful diabetic neuropathy in a not well-phenotyped cohort of subject who were defined as having a painful diabetic neuropathy based on the diagnosis of diabetes and taking analgesic drugs (see Risk factors for painful diabetic neuropathy).

In our study we used all the variants identified in the targeted sequencing of 107 pain-related genes in addition to non-genetic predictors to address PRS in a cohort of 513 patients including discovery (base) and validation (target) cohorts. In general, it might be considered a small sample since GWAS studies usually include thousands of subjects. The deep phenotyping of patients that aimed at identifying a homogeneous cohort of patients was crucial for the increasing of the statistical power by narrowing the clinical variability of the cohort. In addition, we focused the analysis only at a small targeted genomic region (107 genes) which represents a strength as well as a weak of the study. On one hand it contributes to increase the statistical power requiring a smaller sample, on the other hand variants in genomic regions or genes not included in the targeted sequencing, that might have a significant effect on the phenotype, would be missed.

In conclusion, we propose a pilot model combining weighted risk of clinical and genetic variables into a polygenic risk score that was able to discriminate with sufficient accuracy painful from painless patients in a training setting. This study represents the first application of a polygenic risk score for addressing the risk of pain in diabetic neuropathy, pioneering in this clinical context the use of a tool which is best applied to common and complex diseases. Future studies, combining input data from GWAS, copy number variation and targeted genotyping in wider, independent and deep-phenotyped cohorts might improve the predictive power of PRS and reveal new insight into molecular mechanisms underlying neuropathic pain.

Table 8. List of the 107 sequenced genes.

gene	Human name	Reference sequence GRCh37	Subgroup
ANO1	Anoctamin 1, calcium activated chloride channel	NM_018043	Ion channel
ANO3	Anoctamin 3	NM_031418	Ion channel
ASIC3	Acid-sensing (proton-gated) ion channel 3	NM_020321	Ion channel
CACNA1H	Calcium channel, voltage-dependent, T type, alpha 1H subunit	NM_021098	Ion channel
CACNG2	Calcium channel, voltage-dependent, gamma subunit 2	NM_006078	Ion channel
HCN1	Hyperpolarization activated cyclic nucleotide-gated potassium channel 1	NM_021072	Ion channel
HCN2	Hyperpolarization activated cyclic nucleotide-gated potassium channel 2	NM_001194	Ion channel
KCNA2	Potassium voltage-gated channel, shaker-related subfamily, member 2	NM_001204269	Ion channel
KCNA4	Potassium voltage-gated channel, shaker-related subfamily, member 4	NM_002233	Ion channel
KCNK18	Potassium channel, subfamily K, member 18	NM_181840	Ion channel
KCNN1	Potassium intermediate/small conductance calcium-activated channel, subfamily N, member 1	NM_002248	Ion channel
KCNQ2	Potassium voltage-gated channel, KQT-like subfamily, member 2	NM_172107	Ion channel
KCNQ3	Potassium voltage-gated channel, KQT-like subfamily, member 3	NM_004519	Ion channel
KCNQ5	Potassium voltage-gated channel, KQT-like subfamily, member 5	NM_001160133	Ion channel
KCNS1	Potassium voltage-gated channel, delayed-rectifier, subfamily S, member 1	NM_002251	Ion channel
TRPA1	Transient receptor potential cation channel, subfamily A,	NM_007332	Ion channel

gene	Human name	Reference sequence GRCh37	Subgroup
	member 1		
TRPM8	Transient receptor potential cation channel, subfamily M, member 8	NM_024080	Ion channel
TRPV1	Transient receptor potential cation channel, subfamily V, member 1	NM_080706	Ion channel
TRPV3	Transient receptor potential cation channel, subfamily V, member 3	NM_145068	Ion channel
TRPV4	Transient receptor potential cation channel, subfamily V, member 4	NM_021625	Ion channel
AKAP6	A kinase (PRKA) anchor protein 6	NM_004274	Co-expression
AVIL	Advillin	NM_006576	Nav interacting partner
DRP2	Dystrophin related protein 2	NM_001939	Co-expression
ELAVL4	ELAV (embryonic lethal, abnormal vision, Drosophila)-like 4, ELAV like neuron-specific RNA binding protein 4	NM_021952	Co-expression
GCH1	GTP cyclohydrolase 1	NM_000161	Pain phenotype, receptor/channel interacting partner, etc.
GFAP	Glial fibrillary acidic protein	NM_002055	Pain phenotype, receptor/channel interacting partner, etc.
GLA	Galactosidase, alpha	NM_000169	Pain phenotype, receptor/channel interacting partner, etc.
GLO1	Glyoxalase I	NM_006708	Pain phenotype, receptor/channel interacting partner, etc.
IKBKAP	Inhibitor of kappa light polypeptide gene enhancer in B-cells, kinase complex-associated protein	NM_003640	Pain phenotype, receptor/channel interacting partner, etc.
IL6	Interleukin 6 (interferon, beta	NM_000600	Pain phenotype,

gene	Human name	Reference sequence GRCh37	Subgroup
	2)		receptor/channel interacting partner, etc.
KIF5A	Kinesin family member 5A	NM_004984	Co-expression
MPZ	Myelin protein zero	NM_000530	Co-expression
NEFM	Neurofilament, medium polypeptide	NM_005382	Co-expression
NGF	Nerve growth factor (beta polypeptide)	NM_002506	Pain phenotype, receptor/channel interacting partner, etc.
NTRK1	Neurotrophic tyrosine kinase, receptor, type 1	NM_002529	Co-expression
OPRD1	Opioid receptor, delta 1	NM_000911	Pain phenotype, receptor/channel interacting partner, etc.
OPRK1	Opioid receptor, kappa 1	NM_000912	Pain phenotype, receptor/channel interacting partner, etc.
OPRM1	Opioid receptor, mu 1	NM_001145279	Pain phenotype, receptor/channel interacting partner, etc.
PIRT	Phosphoinositide-interacting regulator of transient receptor potential channels	NM_001101387	Pain phenotype, receptor/channel interacting partner, etc.
ACTG1	Actin, gamma 1	NM_001199954	Nav interacting partner
PLEKHA4	Pleckstrin homology domain containing, family A (phosphoinositide binding specific) member 4	NM_020904	Co-expression
ANK3	Ankyrin 3, node of Ranvier (ankyrin G)	NM_020987	Nav interacting partner
ANXA2	Annexin A2	NM_001002858	Nav interacting partner
CALM1	Calmodulin 1 (phosphorylase kinase, delta)	NM_006888	Nav interacting partner
CNTN1	Contactin 1	NM_001843	Nav interacting partner

gene	Human name	Reference sequence GRCh37	Subgroup
CNTN2	Contactin 2 (axonal)	NM_005076	Nav interacting partner
DPYSL2	Dihydropyrimidinase-like 2	NM_001197293	Nav interacting partner
FGF12	Fibroblast growth factor 12	NM_021032	Nav interacting partner
FGF13	Fibroblast growth factor 13	NM_004114	Nav interacting partner
FGF14	Fibroblast growth factor 14	NM_175929	Nav interacting partner
MAP1B	Microtubule-associated protein 1B	NM_005909	Nav interacting partner
MAPK1	Mitogen-activated protein kinase 1	NM_002745	Nav interacting partner
MAPK14	Mitogen-activated protein kinase 14	NM_001315	Nav interacting partner
MAPK3	Mitogen-activated protein kinase 3	NM_001040056	Nav interacting partner
MSN	Moesin	NM_002444	Nav interacting partner
NEDD4L	Neural precursor cell expressed, developmentally down-regulated 4-like, E3 ubiquitin protein ligase	NM_001144967	Nav interacting partner
NFASC	Neurofascin	NM_001005388	Nav interacting partner
NRCAM	Neuronal cell adhesion molecule	NM_001037132	Nav interacting partner
PDZD2	PDZ domain containing 2	NM_178140	Nav interacting partner
PRKACA	Protein kinase, c-AMP-dependent, catalytic, alpha	NM_002730	Nav interacting partner
PRKCA	Protein kinase C, alpha	NM_002737	Nav interacting partner
PRKCB	Protein kinase C, beta	NM_002738	Nav interacting partner
PTGER2	Prostaglandin E receptor 2 (subtype EP2), 53kDa	NM_000956	Nav interacting partner
PTPRZ1	Protein tyrosine phosphatase, receptor-type, Z polypeptide 1	NM_002851	Nav interacting partner
SCLT1	Sodium channel and clathrin linker 1	NM_144643	Nav interacting partner
SIN3B	SIN3 transcription regulator	NM_015260	Nav interacting

gene	Human name	Reference sequence GRCh37	Subgroup
	family member B		partner
SLC8A1	Solute carrier family 8 (sodium/calcium exchanger), member 1	NM_021097	Nav interacting partner
SLC8A2	Solute carrier family 8 (sodium/calcium exchanger), member 2	NM_015063	Nav interacting partner
SLC8A3	Solute carrier family 8 (sodium/calcium exchanger), member 3	NM_183002	Nav interacting partner
SLC9A9	Solute carrier family 9, subfamily A (NHE9, cation proton antiporter 9), member 9	NM_173653	Na-channel interacting partner
SPTBN4	Spectrin, beta, non-erythrocytic 4	NM_020971	Nav interacting partner
SYN2	Synapsin II	NM_133625	Nav interacting partner
TNC	Tenascin C	NM_002160	Nav interacting partner
TNR	Tenascin R	NM_003285	Nav interacting partner
PMP2	Peripheral myelin protein 2, myelin P2 protein	NM_002677	Co-expression
PPP1R1C	Protein phosphatase 1, regulatory (inhibitor) subunit 1C	NM_001080545	Co-expression
PRX	Periaxin	NM_181882	Co-expression
RBFOX1	RNA binding protein, fox-1 homolog (C. elegans) 1	NM_145891	Nav interacting partner
SEPT9	Septin 9	NM_001113491	Pain phenotype, receptor/channel interacting partner, etc.
SPTLC1	Serine palmitoyltransferase, long chain base subunit 1	NM_006415	Pain phenotype, receptor/channel interacting partner, etc.
SV2C	Synaptic vesicle glycoprotein 2C	NM_014979	Co-expression
SYNPR	Synaptoporin	NM_001130003	Co-expression
TMEM130	Transmembrane protein 130	NM_001134450	Co-expression
TMOD2	Tropomodulin 2 (neuronal)	NM_014548	Co-expression
TUSC5	Tumor suppressor candidate 5	NM_172367	Co-expression

gene	Human name	Reference sequence GRCh37	Subgroup
VEGFA	Vascular endothelial growth factor A	NM_001025366	Pain phenotype, receptor/channel interacting partner, etc.
WNK1	WNK lysine deficient protein kinase 1	NM_001184985	Pain phenotype, receptor/channel interacting partner, etc.
ATP1A1	ATPase, Na+/K+ transporting, alpha 1 polypeptide	NM_001160233	Pain phenotype, receptor/channel interacting partner, etc.
ATP1A2	ATPase, Na+/K+ transporting, alpha 2 polypeptide	NM_000702	Pain phenotype, receptor/channel interacting partner, etc.
ATP1A3	ATPase, Na+/K+ transporting, alpha 3 polypeptide	NM_152296	Pain phenotype, receptor/channel interacting partner, etc.
ATP1B1	ATPase, Na+/K+ transporting, beta 1 polypeptide	NM_001677	Pain phenotype, receptor/channel interacting partner, etc.
HTR3B	5-hydroxytryptamine (serotonin) receptor 3B, ionotropic	NM_006028	Pain phenotype, receptor/channel interacting partner, etc.
KCNIP2	Kv channel interacting protein 2	NM_014591	Pain phenotype, receptor/channel interacting partner, etc.
P2RX2	Purinergic receptor P2X, ligand-gated ion channel, 2	NM_170682	Pain phenotype, receptor/channel interacting partner, etc.
P2RX3	Purinergic receptor P2X, ligand-gated ion channel, 3	NM_002559	Pain phenotype, receptor/channel interacting partner, etc.
P2RX4	Purinergic receptor P2X, ligand-gated ion channel, 4	NM_002560	Pain phenotype, receptor/channel interacting partner, etc.

gene	Human name	Reference sequence GRCh37	Subgroup
P2RX7	Purinergic receptor P2X, ligand-gated ion channel, 7	NM_002562	Pain phenotype, receptor/channel interacting partner, etc.
SCN3A	Sodium channel, voltage-gated, type III, alpha subunit	NM_006922	SCN genes
SCN8A	Sodium channel, voltage-gated, type VIII, alpha subunit	NM_014191	SCN genes
SCN9A	Sodium channel, voltage-gated, type IX, alpha subunit	NM_002977	SCN genes
SCN10A	Sodium channel, voltage-gated, type X, alpha subunit	NM_006514	SCN genes
SCN11A	Sodium channel, voltage-gated, type XI, alpha subunit	NM_014139/NM_199037	SCN genes
SCN7A	Sodium channel, voltage-gated, type VII, alpha subunit	NM_002976	SCN genes
SCN1B	Sodium channel, voltage-gated, type I, beta subunit	NM_001037	SCN genes
SCN2B	Sodium channel, voltage-gated, type II, beta subunit	NM_004588/NM_018400	SCN genes
SCN3B	Sodium channel, voltage-gated, type III, beta subunit	NM_001040151/NM_174934	SCN genes
SCN4B	Sodium channel, voltage-gated, type IV, beta subunit	NM_001142348	SCN genes

BIBLIOGRAPHY

1. Dyck, P. J. & Thomas, P. K. *Peripheral Neuropathy*. (Elsevier Inc., 2005).

2. Kimura, J. Peripheral Nerve Disease. *Handb. Clin. Neurophysiol. Vol. 7* (2006).

3. Kandel, E.; Schwartz, J.; Jessel, T. M. Principles of Neural Science, Fifth Edition. *McGraw-Hill* (2013).

4. Yang, F. *et al.* Genetic control of the segregation of pain-related sensory neurons innervating the cutaneous versus deep tissues. **5**, 1353–1364 (2014).

5. Zimmerman, A., Bai, L. & Ginty, D. D. The gentle touch receptors of Mammalian Skin. *Science (80-.).* **346**, 950–954 (2014).

6. Victoria E. Abraira and David D. Ginty. The Sensory Neurons of Touch. *Neuron* **79**, 1–44 (2013).

7. Björnsdotter, M., Löken, L., Olausson, H., Vallbo, Å. & Wessberg, J. Somatotopic organization of gentle touch processing in the posterior insular cortex. *J. Neurosci.* **29**, 9314–9320 (2009).

8. Bourinet, E. *et al.* Calcium-permeable ion channels in pain signaling. *Physiol. Rev.* **94**, 81–140 (2014).

9. Lallemend, F. & Ernfors, P. Molecular interactions underlying the specification of sensory neurons. *Trends Neurosci.* **35**, 373–381 (2012).

10. https://www.iasp-pain.org/terminology?navItemNumber=576#Pain.

11. Treede, R. D. *et al.* Neuropathic pain: Redefinition and a grading system for clinical and research purposes. *Neurology* **70**, 1630–1635 (2008).

12. Jensen, T. S. *et al.* A new definition of neuropathic pain. *Pain* **152**, 2204–2205 (2011).

13. Merskey, H. and Bogduk, N. Classification of Chronic Pain. 2nd Edition, IASP Task Force on Taxonom. *IASP Press. Seattle* (1994).

14. Scholz, J. *et al.* The IASP classification of chronic pain for ICD-11: Chronic neuropathic pain. *Pain* **160**, 53–59 (2019).

15. Costigan, M., Scholz, J. & Woolf, C. J. Neuropathic Pain: A Maladaptive Response of the Nervous System to Damage. *Annu Rev Neurosci.* **32**, 1–32 (2010).

16. Scholz, J. & Woolf, C. J. The neuropathic pain triad: neurons, immune cells and glia. *Nat. Neurosci.* **10**, 1361–1368 (2007).

17. Caterina, M. J. *et al.* The capsaicin receptor: a heat-activated ion channel in the pain pathway. *Nature* **389**, 816–24 (1997).

18. Manuscript, A. & Mechanisms, N. Deconstructing the Neuropathic Pain Phenotype to

Reveal Neural Mechanisms. *Neuron* **73**, 638–652 (2012).

19. Woolf, C. J. & Ma, Q. Nociceptors-Noxious Stimulus Detectors. *Neuron* **55**, 353–364 (2007).

20. Kuner, R. Central mechanisms of pathological pain. *Nat Med* **16**, 1258–1266 (2010).

21. Neumann, S., Doubell, T. P., Leslie, T. & Woolf, C. J. Inflammatory pain hypersensitivity mediated by phenotypic switch in myelinated primary sensory neurons. *Nature* **384**, 360–364 (1996).

22. Seal, R. P., Wang, X., Guan, Y., Raja, S. N. & Woodbury, C. J. Unmyelinated Low Threshold Mechanoreceptors are Required for Injury-induced Mechanical Hypersensitivity. *Nature* **462**, 651–655 (2010).

23. Woolf, C. J. Central Sensitization: Implications for the diagnosis and treatment of pain. *Pain* **152**, 1–31 (2012).

24. Finnerup, N. B. *et al.* Neuropathic pain: An updated grading system for research and clinical practice. *Pain* 1 (2016) doi:10.1097/j.pain.0000000000000492.

25. Krause, S. J. & Backonja, M.-M. Development of a neuropathic pain questionnaire. *Clin. J. Pain* **19**, 306–314 (2003).

26. Bennett, M. The LANSS Pain Scale: the Leeds assessment of neuropathic symptoms and signs. *Pain* **92**, 147–57 (2001).

27. Bouhassira, D. *et al.* Comparison of pain syndromes associated with nervous or somatic lesions and development of a new neuropathic pain diagnostic questionnaire (DN4). *Pain* **114**, 29–36 (2005).

28. Freynhagen, R., Baron, R., Gockel, U. & Tölle, T. R. painDETECT: A new screening questionnaire to identify neuropathic components in patients with back pain. *Curr. Med. Res. Opin.* **22**, 1911–1920 (2006).

29. Portenoy, R. Development and testing of a neuropathic pain screening questionnaire: ID Pain. *Curr. Med. Res. Opin.* **22**, 1555–1565 (2006).

30. Spallone, V. *et al.* Validation of DN4 as a screening tool for neuropathic pain in painful diabetic polyneuropathy. *Diabet. Med.* **29**, 578–585 (2012).

31. Grayston, R. *et al.* A systematic review and meta-analysis of the prevalence of small fiber pathology in fibromyalgia: Implications for a new paradigm in fibromyalgia etiopathogenesis. *Semin. Arthritis Rheum.* **48**, 933–940 (2019).

32. Branco, J. C. *et al.* Prevalence of Fibromyalgia: A Survey in Five European Countries. *Semin. Arthritis Rheum.* **39**, 448–453 (2010).

33. Oaklander, A. L. & Nolano, M. Scientific Advances in and Clinical Approaches to Small-Fiber Polyneuropathy A Review. **02114**, 1–12 (2019).

34. Cazzato, D. & Lauria, G. Small fibre neuropathy. *Curr. Opin. Neurol.* **30**, 490–499 (2017).

35. Terkelsen, A. J. *et al.* The diagnostic challenge of small fibre neuropathy: clinical presentations, evaluations, and causes. *Lancet Neurol.* **16**, 934–944 (2017).

36. Üçeyler, N. *et al.* Small fibre pathology in patients with fibromyalgia syndrome. *Brain* **136**, 1857–67 (2013).

37. Cazzato, D. *et al.* Small fiber neuropathy is a common feature of Ehlers-Danlos syndromes. *Neurology* **87**, 155–159 (2016).

38. Zhao, M. *et al.* Acute cold hypersensitivity characteristically induced by oxaliplatin is caused by the enhanced responsiveness of TRPA1 in mice. *Mol. Pain* **8**, 1–11 (2012).

39. Brouwer, B. A. *et al.* Painful neuropathies: The emerging role of sodium channelopathies. *J. Peripher. Nerv. Syst.* **19**, 53–65 (2014).

40. Faber, C. G. *et al.* Gain of function Na V1.7 mutations in idiopathic small fiber neuropathy. *Ann. Neurol.* **71**, 26–39 (2012).

41. Faber, C. G. *et al.* Gain-of-function Nav1.8 mutations in painful neuropathy. *Proc. Natl. Acad. Sci. U. S. A.* **109**, 19444–19449 (2012).

42. Huang, J. *et al.* Gain-of-function mutations in sodium channel NaV1.9 in painful neuropathy. *Brain* **137**, 1627–1642 (2014).

43. Martinelli-Boneschi, F. *et al. COL6A5* variants in familial neuropathic chronic itch. *Brain* aww343 (2017) doi:10.1093/brain/aww343.

44. Dütsch, M. *et al.* Small fiber dysfunction predominates in Fabry neuropathy. *J. Clin. Neurophysiol.* **19**, 575–86 (2002).

45. De Greef, B. T. A. *et al.* No fabry disease in patients presenting with isolated small fiber neuropathy. *PLoS One* **11**, 1–9 (2016).

46. Nolano, M. *et al.* Sensory deficit in Parkinson's disease: Evidence of a cutaneous denervation. *Brain* **131**, 1903–1911 (2008).

47. Kass-Iliyya, L. *et al.* Small fiber neuropathy in Parkinson's disease: A clinical, pathological and corneal confocal microscopy study. *Park. Relat. Disord.* **21**, 1454–1460 (2015).

48. Weis, J. *et al.* Small-fiber neuropathy in patients with ALS. *Neurology* **76**, 2024–2029 (2011).

49. Dalla Bella, E. *et al.* Amyotrophic lateral sclerosis causes small fiber pathology. *Eur. J. Neurol.* **23**, 416–420 (2016).

50. Sassone, J. *et al.* ALS mouse model SOD1 ^{G93A} displays early pathology of sensory small fibers associated to accumulation of a neurotoxic splice variant of peripherin. *Hum. Mol. Genet.* **25**, 1588–1599 (2016).

51. Devigili, G. *et al.* The diagnostic criteria for small fibre neuropathy: from symptoms to neuropathology. *Brain* **131**, 1912–25 (2008).

52. Devigili, G. *et al.* Diagnostic criteria for small fibre neuropathy in clinical practice and research. *Brain* (2019).

53. Bakkers, M. *et al.* Intraepidermal nerve fiber density and its application in sarcoidosis. *Neurology* **73**, 1142–1148 (2009).

54. Treister, R., O'Neil, K., Downs, H. M. & Oaklander, A. L. Validation of the composite autonomic symptom scale 31 (COMPASS-31) in patients with and without small fiber polyneuropathy. *Eur. J. Neurol.* **22**, 1124–30 (2015).

55. Dalsgaard, C. J., Rydh, M. & Haegerstrand, a. Cutaneous innervation in man visualized with protein gene product 9.5 (PGP 9.5) antibodies. *Histochemistry* **92**, 385–90 (1989).

56. Wang, L., Hilliges, M., Jernberg, T., Wiegleb-Edstrfm, D. & Johansson, O. Protein gene product 9.5-immunoreactive nerve fibres and cells in human skin. *Cell Tissue Res.* **261**, 25–33 (1990).

57. Wendelschafer-Crabb, W. R. K. and G. The innervation of human epidermis. *J. Neurol. Sci.* **115**, 184–190 (1993).

58. Hilliges, M., Wang, L. & Johansson, O. Ultrastructural evidence for nerve fibers within all vital layers of the human epidermis. *Journal of Investigative Dermatology* vol. 104 134–137 (1995).

59. Langerhans, P. Ueber die Nerven der menschlichen llaut. *Virchows Arch.* **44**, 325–338 (1868).

60. McCarthy, B. G. *et al.* Cutaneous innervation in sensory neuropathies: Evaluation by skin biopsy. *Neurology* **45**, 1848–1855 (1995).

61. Lauria, G. *et al.* European Federation of Neurological Societies/Peripheral Nerve Society Guideline on the use of skin biopsy in the diagnosis of small fiber neuropathy. Report of a joint task force of the European Fe-deration of Neurological Societies and the Peripheral Ne. *Eur. J. Neurol.* **17**, 903-e49 (2010).

62. Lauria, G. *et al.* Intraepidermal nerve fiber density at the distal leg: a worldwide normative reference study. *J. Peripher. Nerv. Syst.* **15**, 202–7 (2010).

63. Provitera, V. *et al.* A multi-center, multinational age- and gender-adjusted normative dataset for immunofluorescent intraepidermal nerve fiber density at the distal leg. *Eur. J. Neurol.* **23**, 333–338 (2016).

64. Nolano, M. *et al.* Epidermal innervation morphometry by immunofluorescence and bright-field microscopy. *J. Peripher. Nerv. Syst.* **391**, 387–391 (2015).

65. Lauria, G. *et al.* Side and time variability of intraepidermal nerve fiber density. *Neurology* (2015) doi:10.1212/WNL.0000000000001666.

66. Lauria, G. *et al.* Axonal swellings predict the degeneration of epidermal nerve fibers in painful neuropathies. *Neurology* **61**, 631–636 (2003).

67. Cheng, H. T. *et al.* Increased axonal regeneration and swellings in intraepidermal

nerve fibers characterize painful phenotypes of diabetic neuropathy. *J. Pain* **14**, 941–7 (2013).

68. Cheung, A., Podgorny, P., Martinez, J. A., Chan, C. & Toth, C. Epidermal axonal swellings in painful and painless diabetic peripheral neuropathy. *Muscle Nerve* **51**, 505–513 (2015).

69. Lauria, G. *et al.* Morphometry of dermal nerve fibers in human skin. *Neurology* **77**, 242–9 (2011).

70. Nolano, M. *et al.* Quantification of pilomotor nerves: a new tool to evaluate autonomic involvement in diabetes. *Neurology* **75**, 1089–97 (2010).

71. Gibbons, C. H., Illigens, B. M. W., Wang, N. & Freeman, R. Quantification of sweat gland innervation: a clinical-pathologic correlation. *Neurology* **72**, 1479–86 (2009).

72. Backonja, M. M. *et al.* Value of quantitative sensory testing in neurological and pain disorders: NeuPSIG consensus. *Pain* **154**, 1807–1819 (2013).

73. Rolke, R. *et al.* Quantitative sensory testing in the German Research Network on Neuropathic Pain (DFNS): Standardized protocol and reference values. *Pain* **123**, 231–243 (2006).

74. Papanas, N. & Ziegler, D. Corneal confocal microscopy: Recent progress in the evaluation of diabetic neuropathy. *J. Diabetes Investig.* **6**, 381–389 (2015).

75. Tavakoli, M. *et al.* Normative values for corneal nerve morphology assessed using corneal confocal microscopy: A multinational normative data set. *Diabetes Care* **38**, 838–843 (2015).

76. Ahmed, A. *et al.* Detection of diabetic sensorimotor polyneuropathy by corneal confocal microscopy in type 1 diabetes: A concurrent validity study. *Diabetes Care* **35**, 821–828 (2012).

77. Ziegler, D. *et al.* Early detection of nerve fiber loss by corneal confocal microscopy and skin biopsy in recently diagnosed type 2 diabetes. *Diabetes* **63**, 2454–2463 (2014).

78. Azmi, S. *et al.* Corneal confocal microscopy shows an improvement in small-fiber neuropathy in subjects with type 1 diabetes on continuous subcutaneous insulin infusion compared with multiple daily injection. *Diabetes Care* **38**, e3-4 (2015).

79. Tavakoli, M. *et al.* Corneal confocal microscopy: a novel means to detect nerve fibre damage in idiopathic small fibre neuropathy. *Exp. Neurol.* **223**, 245–50 (2010).

80. Bucher, F. *et al.* Small-Fiber Neuropathy Is Associated With Corneal Nerve and Dendritic Cell Alterations: An In Vivo Confocal Microscopy Study. *Cornea* **34**, 1114–9 (2015).

81. Gemignani, F. *et al.* Non-length-dependent small fibre neuropathy. Confocal microscopy study of the corneal innervation. *J. Neurol. Neurosurg. Psychiatry* **81**, 731–3 (2010).

82. La Cesa, S. *et al.* Skin denervation does not alter cortical potentials to surface concentric electrode stimulation: A comparison with laser evoked potentials and contact heat evoked potentials. *Eur. J. Pain (United Kingdom)* **22**, 161–169 (2018).

83. Ragé, M. *et al.* The time course of CO2 laser-evoked responses and of skin nerve fibre markers after topical capsaicin in human volunteers. *Clin. Neurophysiol.* **121**, 1256–66 (2010).

84. Di Stefano, G. *et al.* Diagnostic accuracy of laser-evoked potentials in diabetic neuropathy. *Pain* **158**, 1100–1107 (2017).

85. Lagerburg, V. *et al.* Contact heat evoked potentials: Normal values and use in small-fiber neuropathy. *Muscle Nerve* **51**, 743–749 (2015).

86. Wu, S., Wang, Y., Hsieh, P., Tseng, M. & Chiang, M. Biomarkers of neuropathic pain in skin nerve degeneration neuropathy : contact heat-evoked potentials as a physiological signature. **158**, 516–525 (2017).

87. Mouraux, A. & Iannetti, G. D. Nociceptive Laser-Evoked Brain Potentials Do Not Reflect Nociceptive-Specific Neural Activity. *J. Neurophysiol.* **101**, 3258–3269 (2009).

88. Iannetti, G. D., Hughes, N. P., Lee, M. C. & Mouraux, A. Determinants of Laser-Evoked EEG Responses: Pain Perception or Stimulus Saliency? *J. Neurophysiol.* **100**, 815–828 (2008).

89. Truini, A. *et al.* Laser-evoked potentials: Normative values. *Clin. Neurophysiol.* **116**, 821–826 (2005).

90. Illigens, B. M. W. & Gibbons, C. H. Sweat testing to evaluate autonomic function. *Clin. Auton. Res.* **19**, 79–87 (2009).

91. Thaisetthawatkul, P., Fernandes Filho, J. A. M. & Herrmann, D. N. Contribution of QSART to the diagnosis of small fiber neuropathy. *Muscle Nerve* (2013) doi:10.1002/mus.23891.

92. Finnerup, N. B. *et al.* Pharmacotherapy for neuropathic pain in adults: A systematic review and meta-analysis. *Lancet Neurol.* **14**, 162–173 (2015).

93. Adi, T. *et al.* A novel gain-of-function Na v 1.7 mutation in a carbamazepine-responsive patient with adult-onset painful peripheral neuropathy. *Mol. Pain* **14**, (2018).

94. Dosenovic, S. *et al.* Interventions for Neuropathic Pain: An Overview of Systematic Reviews. *Anesth. Analg.* **125**, 643–652 (2017).

95. De Greef, B. T. A. *et al.* Lacosamide in patients with Na v 1.7 mutations-related small fibre neuropathy: A randomized controlled trial. *Brain* **142**, 263–275 (2019).

96. ADA. Diagnosis and classification of diabetes mellitus. *Am. Diabetes care* (2015).

97. Care, D. & Suppl, S. S. 2. Classification and diagnosis of diabetes: Standards of medical care in diabetesd2019. *Diabetes Care* **42**, S13–S28 (2019).

98. Bird, S. J. & Brown, M. J. Diabetic neuropathies. *Contin. Lifelong Learn. Neurol.* **9781461465**, 647–673 (2014).

99. Shillo, P. *et al.* Painful and Painless Diabetic Neuropathies: What Is the Difference? *Curr. Diab. Rep.* **19**, 32 (2019).

100. Abbott, C. A., Malik, R. A., Van Ross, E. R. E., Kulkarni, J. & Boulton, A. J. M. Prevalence and characteristics of painful diabetic neuropathy in a large community-based diabetic population in the U.K. *Diabetes Care* **34**, 2220–2224 (2011).

101. International Diabetes Federation. *Eighth edition 2017*. *IDF Diabetes Atlas, 8th edition* (2017). doi:http://dx.doi. org/10.1016/S0140-6736(16)31679-8.

102. Themistocleous, A. C. *et al.* The Pain in Neuropathy Study (PiNS): A cross-sectional observational study determining the somatosensory phenotype of painful and painless diabetic neuropathy. *Pain* **157**, 1132–1145 (2016).

103. Feldman, E. L., Nave, K. A., Jensen, T. S. & Bennett, D. L. H. New Horizons in Diabetic Neuropathy: Mechanisms, Bioenergetics, and Pain. *Neuron* (2017) doi:10.1016/j.neuron.2017.02.005.

104. Isomaa, B. *et al.* The metabolic syndrome influences the risk of chronic complications in patients with type II diabetes. *Diabetologia* (2001) doi:10.1007/s001250100615.

105. Callaghan, B. C., Little, A. A., Feldman, E. L. & Hughes, R. A. Enhanced glucose control for preventing and treating diabetic neuropathy. *Cochrane Database Syst. Rev.* (2012) doi:10.1002/14651858.CD007543.pub2.

106. Padilla, A., Descorbeth, M., Almeyda, A. L., Payne, K. & De Leon, M. Hyperglycemia magnifies Schwann cell dysfunction and cell death triggered by PA-induced lipotoxicity. *Brain Res.* (2011) doi:10.1016/j.brainres.2010.11.013.

107. Vincent, A. M., Callaghan, B. C., Smith, A. L. & Feldman, E. L. Diabetic neuropathy: cellular mechanisms as therapeutic targets. *Nat. Rev. Neurol.* **7**, 573–583 (2011).

108. Sugimoto, K., Murakawa, Y., Zhang, W., Xu, G. & Sima, A. A. F. Insulin receptor in rat peripheral nerve: Its localization and alternatively spliced isoforms. *Diabetes. Metab. Res. Rev.* (2000) doi:10.1002/1520-7560(200009/10)16:5<354::AID-DMRR149>3.0.CO;2-H.

109. Guo, G., Kan, M., Martinez, J. A. & Zochodne, D. W. Local insulin and the rapid regrowth of diabetic epidermal axons. *Neurobiol. Dis.* (2011) doi:10.1016/j.nbd.2011.04.012.

110. Kim, B., McLean, L. L., Philip, S. S. & Feldman, E. L. Hyperinsulinemia induces insulin resistance in dorsal root ganglion neurons. *Endocrinology* (2011) doi:10.1210/en.2011-0029.

111. Schepers, R. J. & Ringkamp, M. Thermoreceptors and thermosensitive afferents. *Neurosci. Biobehav. Rev.* **34**, 177–84 (2010).

112. McKemy, D. D. The molecular and cellular basis of cold sensation. *ACS Chem. Neurosci.*

4, 238–247 (2013).

113. Gu, A. D. *et al.* Heat-Evoked Activation of the Ion Channel , TRPV4. **22**, 6408–6414 (2002).

114. Dhaka, A., Viswanath, V. & Patapoutian, A. Trp Ion Channels and Temperature Sensation. *Annu. Rev. Neurosci.* **29**, 135–161 (2006).

115. Irani, S. R. *et al.* Antibodies to Kv1 potassium channel-complex proteins leucine-rich, glioma inactivated 1 protein and contactin-associated protein-2 in limbic encephalitis, Morvan's syndrome and acquired neuromyotonia. *Brain* (2010) doi:10.1093/brain/awq213.

116. Tsantoulas, C. & McMahon, S. B. Opening paths to novel analgesics: The role of potassium channels in chronic pain. *Trends Neurosci.* **37**, 146–158 (2014).

117. Noel, J. *et al.* The mechano-activated K+ channels TRAAK and TREK-1 control both warm and cold perception. *EMBO J.* **28**, 1308–1318 (2009).

118. Mis, M. A. *et al.* Resilience to Pain: A Peripheral Component Identified Using Induced Pluripotent Stem Cells and Dynamic Clamp. *J. Neurosci.* **39**, 382–392 (2019).

119. Lee, Y., Lee, C.-H. & Oh, U. Painful channels in sensory neurons. *Mol. Cells* **20**, 315–324 (2005).

120. Gee, N. S. *et al.* The novel anticonvulsant drug, gabapentin (neurontin), binds to the α2δlta subunit of a calcium channel. *J. Biol. Chem.* **271**, 5768–5776 (1996).

121. Cruccu, G. & Truini, A. A review of Neuropathic Pain: From Guidelines to Clinical Practice. *Pain Ther.* **6**, 35–42 (2017).

122. Matsubara, T. *et al.* Thin-fibre receptors expressing acid-sensing ion channel 3 contribute to muscular mechanical hypersensitivity after exercise. *Eur. J. Pain* 1–13 (2019) doi:10.1002/ejp.1454.

123. Immke, D. C. & McCleskey, E. W. Lactate enhances the acid-sensing Na+ channel on ischemia-sensing neurons. *Nat. Neurosci.* **4**, 869–870 (2001).

124. Tsuda, M. *et al.* P2X4 receptors induced in spinal microglia gate tactile allodynia after nerve injury. *Nature* (2003) doi:10.1038/nature01786.

125. Burnstock, G. *Purinergic Mechanisms and Pain*. *Advances in Pharmacology* vol. 75 (Elsevier Inc., 2016).

126. Momin, A., Cadiou, H., Mason, A. & Mcnaughton, P. A. Role of the hyperpolarization-activated current I h in somatosensory neurons. *J. Physiol.* (2008) doi:10.1113/jphysiol.2008.163154.

127. Emery, E. C., Young, G. T., Berrocoso, E. M., Chen, L. & McNaughton, P. A. HCN2 ion channels play a central role in inflammatory and neuropathic pain. *Science (80-.).* **333**, 1462–1466 (2011).

128. Catterall, W. A. Voltage-Gated Sodium Channels: Structure, Function, and

Pathophysiology. *Encycl. Biol. Chem. Second Ed.* **11**, 564–569 (2013).

129. Lai, H. C. & Jan, L. Y. The distribution and targeting of neuronal voltage-gated ion channels. *Nat. Rev. Neurosci.* **7**, 548–562 (2006).

130. Bennett, D. L., Clark, A. J., Huang, J., Waxman, S. G. & Dib-Hajj, S. D. The Role of Voltage-Gated Sodium Channels in Pain Signaling. *Physiol. Rev.* **99**, 1079–1151 (2019).

131. Black, J. A., Nikolajsen, L., Kroner, K., Jensen, T. S. & Waxman, S. G. Multiple sodium channel isoforms and mitogen-activated protein kinases are present in painful human neuromas. *Ann. Neurol.* (2008) doi:10.1002/ana.21527.

132. Herzog, R. I., Cummins, T. R., Ghassemi, F., Dib-Hajj, S. D. & Waxman, S. G. Distinct repriming and closed-state inactivation kinetics of Nav1.6 and Nav1.7 sodium channels in mouse spinal sensory neurons. *J. Physiol.* (2003) doi:10.1113/jphysiol.2003.047357.

133. Deuis, J. R. *et al.* An animal model of oxaliplatin-induced cold allodynia reveals a crucial role for Nav1.6 in peripheral pain pathways. *Pain* (2013) doi:10.1016/j.pain.2013.05.032.

134. Tanaka, B. S. & Zhao, P. A Gain-of-Function Mutation in Nav1.6 in a Case of Trigeminal Neuralgia. *Mol. Med.* **22**, 1 (2016).

135. Bennett, D. L. H. & Woods, C. G. Painful and painless channelopathies. *Lancet Neurol.* **13**, 587–599 (2014).

136. Han, C. *et al.* Nav1.7-related small fiber neuropathy: impaired slow-inactivation and DRG neuron hyperexcitability. *Neurology* **78**, 1635–43 (2012).

137. Blesneac, I. *et al.* Rare NaV1.7 variants associated with painful diabetic peripheral neuropathy. *Pain* **159**, 469–480 (2018).

138. Han, C. *et al.* Human Na v 1.8: enhanced persistent and ramp currents contribute to distinct firing properties of human DRG neurons . *J. Neurophysiol.* **113**, 3172–3185 (2015).

139. Zimmermann, K. *et al.* Sensory neuron sodium channel Nav1.8 is essential for pain at low temperatures. *Nature* **447**, 855–8 (2007).

140. Han, C. *et al.* The Novel Activity of Carbamazepine as an Activation Modulator Extends from $Na_V1.7$ Mutations to the $Na_V1.8$-S242T Mutant Channel from a Patient with Painful Diabetic Neuropathy. *Mol. Pharmacol.* **94**, 1256–1269 (2018).

141. Alsaloum, M. *et al.* A gain-of-function sodium channel **β** 2-subunit mutation in painful diabetic neuropathy. *Mol. Pain* **15**, 174480691984980 (2019).

142. Braun, M. *et al.* Voltage-Gated Ion Channels in Human Pancreatic Beta-Cells: Electrophysiological Characterization and Role in Insulin Secretion. *Diabetes* **57**, 1618–28 (2008).

143. Zhang, Q. *et al.* Na + current properties in islet α- and β-cells reflect cell-specific Scn3a

and Scn9a expression. *J. Physiol.* **592**, 4677–4696 (2014).

144. Ernst, S. J., Aguilar-Bryan, L. & Noebels, J. L. Sodium channel β1 regulatory subunit deficiency reduces pancreatic islet glucose-stimulated insulin and glucagon secretion. *Endocrinology* **150**, 1132–1139 (2009).

145. Yang, Y. H. C., Vilin, Y. Y., Roberge, M., Kurata, H. T. & Johnson, J. D. Multiparameter screening reveals a role for Na+ channels in cytokine-induced β-cell death. *Mol. Endocrinol.* **28**, 406–417 (2014).

146. Hirade, M., Yasuda, H., Omatsu-Kanbe, M., Kikkawa, R. & Kitasato, H. Tetrodotoxin-resistant sodium channels of dorsal root ganglion neurons are readily activated in diabetic rats. *Neuroscience* **90**, 933–9 (1999).

147. Hong, S., Morrow, T. J., Paulson, P. E., Isom, L. L. & Wiley, J. W. Early painful diabetic neuropathy is associated with differential changes in tetrodotoxin-sensitive and -resistant sodium channels in dorsal root ganglion neurons in the rat. *J. Biol. Chem.* **279**, 29341–29350 (2004).

148. Bierhaus, A. *et al.* Methylglyoxal modification of Nav1.8 facilitates nociceptive neuron firing and causes hyperalgesia in diabetic neuropathy. *Nat. Med.* **18**, 926–933 (2012).

149. Hoeijmakers, J. G. J., Faber, C. G., Merkies, I. S. J. & Waxman, S. G. Channelopathies, painful neuropathy, and diabetes: Which way does the causal arrow point? *Trends Mol. Med.* **20**, 544–550 (2014).

150. Costigan, M. *et al.* Multiple chronic pain states are associated with a common amino acid-changing allele in KCNS1. *Brain* **133**, 2519–27 (2010).

151. Tegeder, I. *et al.* GTP cyclohydrolase and tetrahydrobiopterin regulate pain sensitivity and persistence. *Nat. Med.* **12**, 1269–1277 (2006).

152. Young, E. E., Lariviere, W. R. & Belfer, I. Genetic basis of pain variability: recent advances. *J. Med. Genet.* **49**, 1–9 (2012).

153. Andersen, S. & Skorpen, F. Variation in the COMT gene: implications for pain perception and pain treatment. *Pharmacogenomics* **10**, 669–84 (2009).

154. Latremoliere, A. *et al.* Reduction of Neuropathic and Inflammatory Pain through Inhibition of the Tetrahydrobiopterin Pathway. *Neuron* **86**, 1393–1406 (2015).

155. Lötsch, J. & Geisslinger, G. Current evidence for a genetic modulation of the response to analgesics. *Pain* **121**, 1–5 (2006).

156. Cox, J. J. *et al.* An SCN9A channelopathy causes congenital inability to experience pain. *Nature* **444**, 894–898 (2006).

157. Marchi, M. *et al.* A novel SCN9A splicing mutation in a compound heterozygous girl with congenital insensitivity to pain, hyposmia and hypogeusia. *J. Peripher. Nerv. Syst.* **23**, 202–206 (2018).

158. Minett, M. *et al.* Distinct Nav1.7-dependent pain sensations require different sets of

sensory and sympathetic neurons. *Nat. Commun.* **3**, 791–799 (2012).

159. Yuan, J. *et al.* Hereditary sensory and autonomic neuropathy type IID caused by an SCN9A mutation. *Neurology* **80**, 1641–1649 (2013).

160. Leipold, E. *et al.* A de novo gain-of-function mutation in SCN11A causes loss of pain perception. *Nat. Genet.* **45**, 1399–404 (2013).

161. Yang, Y. *et al.* Mutations in SCN9A, encoding a sodium channel alpha subunit, in patients with primary erythermalgia. *J. Med. Genet.* **41**, 171–174 (2004).

162. Cregg, R. *et al.* Novel mutations mapping to the fourth sodium channel domain of nav1.7 result in variable clinical manifestations of primary erythromelalgia. *NeuroMolecular Med.* **15**, 265–278 (2013).

163. Choi, J. S. *et al.* Mexiletine-responsive erythromelalgia due to a new Nav1.7 mutation showing use-dependent current fall-off. *Exp. Neurol.* **216**, 383–389 (2009).

164. Fertleman, C. R. *et al.* SCN9A Mutations in Paroxysmal Extreme Pain Disorder: Allelic Variants Underlie Distinct Channel Defects and Phenotypes. *Neuron* **52**, 767–774 (2006).

165. Fertleman, C. R. *et al.* Paroxysmal extreme pain disorder (previously familial rectal pain syndrome). *Neurology* **69**, 586–595 (2007).

166. Kremeyer, B. *et al.* A Gain-of-Function Mutation in TRPA1 Causes Familial Episodic Pain Syndrome. *Neuron* **66**, 671–680 (2010).

167. Zhang, X. Y. *et al.* Gain-of-Function mutations in SCN11A cause familial episodic pain. *Am. J. Hum. Genet.* **93**, 957–966 (2013).

168. Eijkenboom, I. *et al.* Yield of peripheral sodium channels gene screening in pure small fibre neuropathy. *J. Neurol. Neurosurg. Psychiatry* **90**, 342–352 (2019).

169. Estacion, M. *et al.* Intra- and interfamily phenotypic diversity in pain syndromes associated with a gain-of-function variant of Na V1.7. *Mol. Pain* **7**, 92 (2011).

170. Small nerve fibres, small hands and small feet: a new syndrome of pain, dysautonomia and acromesomelia in a kindred with a novel NaV1.7 mutation. - PubMed - NCBI. https://www.ncbi.nlm.nih.gov/pubmed/?term=22286749.

171. Estacion, M. *et al.* Ca2+ toxicity due to reverse Na+/Ca2+ exchange contributes to degeneration of neurites of DRG neurons induced by a neuropathy-associated Nav1.7 mutation. *J. Neurophysiol.* **114**, 1554–1564 (2015).

172. Tesfaye, S. *et al.* Vascular Risk Factors and Diabetic Neuropathy. *N. Engl. J. Med.* **352**, 341–350 (2005).

173. Green, A. Q., Krishnan, S., Finucane, F. M. & Rayman, G. Altered C-fiber function as an indicator of early peripheral neuropathy in individuals with impaired glucose tolerance. *Diabetes Care* **33**, 174–176 (2010).

174. Callaghan, B. C. *et al.* Metabolic syndrome components are associated with

symptomatic polyneuropathy independent of glycemic status. *Diabetes Care* **39**, 801–807 (2016).

175. Callaghan, B. C. *et al.* Association between metabolic syndrome components and polyneuropathy in an obese population. *JAMA Neurol.* **73**, 1468–1476 (2016).

176. O'Brien, P. D., Hinder, L. M., Callaghan, B. C. & Feldman, E. L. Neurological consequences of obesity. *Lancet Neurol.* **16**, 465–477 (2017).

177. Politi, C. *et al.* Recent advances in exploring the genetic susceptibility to diabetic neuropathy. *Diabetes Res. Clin. Pract.* **120**, 198–208 (2016).

178. Prabodha, L. B. L., Sirisena, N. D. & Dissanayake, V. H. W. Susceptible and prognostic genetic factors associated with diabetic peripheral neuropathy: A comprehensive literature review. *Int. J. Endocrinol.* **2018**, (2018).

179. Truini, A. *et al.* A cross-sectional study investigating frequency and features of definitely diagnosed diabetic painful polyneuropathy. *Pain* **159**, 2658–2666 (2018).

180. Hébert, H. L., Veluchamy, A., Torrance, N. & Smith, B. H. Risk factors for neuropathic pain in diabetes mellitus. *Pain* **158**, 560–568 (2017).

181. Raputova, J. *et al.* Sensory phenotype and risk factors for painful diabetic neuropathy: a cross sectional observational study. *Pain* 1 (2017) doi:10.1097/j.pain.0000000000001034.

182. Andersson, D. A. *et al.* Methylglyoxal Evokes Pain by Stimulating TRPA1. *PLoS One* **8**, 1–9 (2013).

183. Li, Q. S. *et al.* SCN9A variants may be implicated in neuropathic pain associated with diabetic peripheral neuropathy and pain severity. *Clin. J. Pain* **31**, 976–982 (2015).

184. Cheng, K. I., Lin, S. R., Chang, L. L., Wang, J. Y. & Lai, C. S. Association of the functional A118G polymorphism of OPRM1 in diabetic patients with foot ulcer pain. *J. Diabetes Complications* **24**, 102–108 (2010).

185. Meng, W. *et al.* A genome-wide association study suggests an association of Chr8p21.3 (GFRA2) with diabetic neuropathic pain. *Eur. J. Pain (United Kingdom)* **19**, 392–399 (2015).

186. Meng, W. *et al.* A Genome-wide Association Study Provides Evidence of Sex-specific Involvement of Chr1p35.1 (ZSCAN20-TLR12P) and Chr8p23.1 (HMGB1P46) With Diabetic Neuropathic Pain. *EBioMedicine* **2**, 1386–1393 (2015).

187. Waxman, S. G. *et al.* Sodium channel genes in pain-related disorders: phenotype–genotype associations and recommendations for clinical use. *Lancet. Neurol.* **13**, 1152–60 (2014).

188. Timpson, N. J., Greenwood, C. M. T., Soranzo, N., Lawson, D. J. & Richards, J. B. Genetic architecture: The shape of the genetic contribution to human traits and disease. *Nat. Rev. Genet.* **19**, 110–124 (2018).

189. Kaiser, J. Genetic influences on disease remain hidden. *Science (80-.).* **338**, 1016–1017 (2012).

190. Pestronk, A. *et al.* Sensory exam with a quantitative tuning fork: rapid, sensitive and predictive of SNAP amplitude. *Neurology* **62**, 461–4 (2004).

191. Vanhoutte, E. K. *et al.* Modifying the Medical Research Council grading system through Rasch analyses. *Brain* **135**, 1639–1649 (2012).

192. McArthur, J. C., Stocks, E. A., Hauer, P., Cornblath, D. R. & Griffin, J. W. Epidermal Nerve Fiber Density. *Arch. Neurol.* **55**, 1513 (1998).

193. Bolger, A. M., Lohse, M. & Usadel, B. Trimmomatic: a flexible trimmer for Illumina sequence data. *Bioinformatics* **30**, 2114–20 (2014).

194. Li, H. & Durbin, R. Fast and accurate long-read alignment with Burrows-Wheeler transform. *Bioinformatics* **26**, 589–95 (2010).

195. McKenna, A. *et al.* The Genome Analysis Toolkit: A MapReduce framework for analyzing next-generation DNA sequencing data. *Genome Res.* **20**, 1297–1303 (2010).

196. Wallis, Y. *et al.* Practice Guidelines for the Evaluation of Pathogenicity and the Reporting of Sequence Variants in Clinical Molecular Genetics. *Assoc. Clin. Genet. Sci.* 16 (2013).

197. Purcell, S. *et al.* PLINK: A tool set for whole-genome association and population-based linkage analyses. *Am. J. Hum. Genet.* **81**, 559–575 (2007).

198. Euesden, J., Lewis, C. M. & O'Reilly, P. F. PRSice: Polygenic Risk Score software. *Bioinformatics* **31**, 1466–1468 (2015).

199. Bianca T.A. de Greef1, MD, Janneke G.J. Hoeijmakers1, MD, PhD, Carla M.L. Gorissen-Brouwers1, MSc, Margot Geerts1, MSc, Catharina G. Faber1, MD, PhD, Ingemar S.J. Merkies1,2, MD, P. Associated conditions in small fiber neuropathy – A large cohort study and review of the literature. *Eur J Neurol* **38**, 42–49 (2018).

200. Savio-Galimberti, E. *et al.* SCN10A/Nav1.8 modulation of peak and late sodium currents in patients with early onset atrial fibrillation. *Cardiovasc. Res.* **104**, 355–363 (2014).

201. Dabby, R. *et al.* Chronic non-paroxysmal neuropathic pain - Novel phenotype of mutation in the sodium channel SCN9A gene. *J. Neurol. Sci.* **301**, 90–2 (2011).

202. Han, C. Nav1.7-related small fiber neuropathy. Impaired slow-inactivation and DRG neuron hyperexcitability. (2012) doi:10.1212/WNL.0b013e3182574f12.

203. Han, C. *et al.* The G1662S NaV1.8 mutation in small fibre neuropathy: impaired inactivation underlying DRG neuron hyperexcitability. *J. Neurol. Neurosurg. Psychiatry* **85**, 499–505 (2014).

204. Baron, R. *et al.* Peripheral neuropathic pain: a mechanism-related organizing principle based on sensory profiles. *Pain* **158**, 261–272 (2017).

205. Chiang, M. C. *et al.* Cutaneous innervation in chronic inflammatory demyelinating polyneuropathy. *Neurology* (2002) doi:10.1212/WNL.59.7.1094.

206. Gøransson, L. G., Mellgren, S. I., Lindal, S. & Omdal, R. The effect of age and gender on epidermal nerve fiber density. *Neurology* (2004) doi:10.1212/01.WNL.0000113732.41127.8F.

207. Umapathi, T., Tan, W. L., Tan, N. C. K. & Chan, Y. H. Determinants of epidermal nerve fiber density in normal individuals. *Muscle and Nerve* (2006) doi:10.1002/mus.20528.

208. Collongues, N. *et al.* Quantitative and qualitative normative dataset for intraepidermal nerve fibers using skin biopsy. 1–14 (2018) doi:10.1371/journal.pone.0191614.

209. Üçeyler, N. Small fiber pathology – a culprit for many painful disorders? *Pain* **157**, 1 (2015).

210. Brouwer, B. A. *et al.* The Pain Dynamics of Small Fiber Neuropathy. *J. Pain* (2019) doi:10.1016/j.jpain.2018.11.009.

211. Dworkin, R. H. *et al.* Core outcome measures for chronic pain clinical trials: IMMPACT recommendations. *Pain* **113**, 9–19 (2005).

212. Wadhawan, S. *et al.* Na V channel variants in patients with painful and nonpainful peripheral neuropathy . *Neurol. Genet.* **3**, e207 (2017).

213. Ku, C. S., Loy, E. Y., Pawitan, Y. & Chia, K. S. The pursuit of genome-wide association studies: Where are we now. *J. Hum. Genet.* **55**, 195–206 (2010).

214. Choi, S. W., Mak, T. S. H. & O'Reilly, P. F. A guide to performing Polygenic Risk Score analyses. *bioRxiv* **2**, 416545 (2018).